

Chemical Engineering Integrated Master

***Tyre reinforcements dipping process - Scale-up optimization***

**Master's Thesis**

by

Sara João Pontes Costa

Developed under the course of Dissertation and performed at

**Continental - Indústria Têxtil do Ave, S.A.**



Supervisor from FEUP: Prof. Adélio Mendes

Supervisor from Continental - ITA: Eng. Alexandre Gomes



**Chemical Engineering Department**

July 2016

*“Põe quanto és.*

*No mínimo que fazes.”*

Odes de Ricardo Reis, Fernando Pessoa

---

## Acknowledgements

As all big projects in life, this journey would not have been possible without the support, guidance, enthusiasm and perseverance of some people, to whom I must properly thank.

Professor Adélio Mendes for being a friend before a supervisor. I have to thank for all the gold advices and warnings, all the help and knowledge that was shared during this 5 years.

To Eng. Eduardo Diniz, for besides being an excellent leader with a huge devotion to this company, also having the capacity to be approachable, making this great experience possible.

To Mr. Manuel Pinheiro, for his contagious enthusiasm and for his availability to discuss and to guide about every laboratory and production details during the last months.

To Eng. Alexandre Gomes, for giving me independence to explore all my ideas, but also for support and help me to shape them, always under good humor.

To Dr. Mohammad Mahdi Abdollahzadeh, for his absolutely tireless assistance and for all the suggestions since day one.

To Eng. Carla Pires, Eng. Diana Pinto and Eng. Ana Martins for all the help, advices and lessons given, always with a good mood and with a great work spirit.

To Eng. João Baptista, Eng. Rocha, Eng. José Ricardo Osório, Eng. Rafael Castro, Eng. Joana Ferreira and Eng. Hélder Ribeiro for being so helpful and available to all my questions, as also for all the advices and suggestions made.

To Eng. Ricardo Cunha, Eng. Helena Carvalho and Eng. José Pedro Cunha for the great work environment full of enthusiasm and good humor.

To Mr. Jorge Couto, Mr. Martins, Mr. Campos, Mr. José Maria Silva, Mr. Jacinto Cruz, Mr. Ovídio Sá, Mr. Júlio Maia, Mr. Araújo, Mr. Miguel, Mr. Costa, Mr. Serra, Mr. Vasco, Mr. Francisco Araújo and Mr. Paulo Silva, for always being supportive and helpful, and for the great work ambience.

A special thanks to my colleagues, Daniel Faria and Ana Lopes, for being so friendly, understanding and patient. It was such a pleasure working with you!

To all my friends, who always color my days, for the excellent times and companionship.

My acknowledgement would never be complete without a special mention to Margarida Brito, for being so friendly, supportive, encouraging, my partner in crime, and for being an inspiration.

Last, but definitely not the least, a special thanks to the persons who always made sacrifices for me to have the education that I always desired, as with an unbounded support to everything during my life, which makes me the person I become today. To the most important persons in my life, my parents! To all my family, for all love and support. Um sincero obrigado.

---

## Abstract

The present thesis was developed at Continental - Indústria Têxtil do Ave, S.A. (C-ITA) in collaboration with the Faculty of Engineering at the University of Porto (FEUP). C-ITA belongs to Continental AG, which stands out in tyre industry, and its core-business is textile manufacturing, especially oriented to this type of industry.

Described as a simple round rubber item, tyres are a complex system made of rubber compounds and reinforcement materials, both textile and metallic. The textile reinforcements provide the shape, mechanical properties and structure required to the tyre. A good adhesion between rubber and cords is an essential requirement, carried out by the chemical treatment of the cords.

This work optimizes the industrial dipping process of the textile reinforcement studying namely the temperature distribution inside the industrial ovens, optimized adjusting the ventilation conditions; the obtained results improved the objective function by 1.28 %. The scale-down of the operating conditions observed at the industrial ovens was revisited concluding the need for its improvement. It was finally developed a CFD-based model of the industrial ovens to assist improving them; however, this model still need to be upgraded.

**Key words:** tyre; textile reinforcement; dipping process; optimization; simulation

---

## Resumo

A presente tese foi realizada na Continental - Indústria Têxtil do Ave, S.A. (C-ITA) em parceria com a Faculdade de Engenharia da Universidade do Porto (FEUP). A C-ITA pertence ao grupo Continental AG, a qual se destaca na indústria de pneus, sendo que o seu principal negócio é a fabricação de têxteis, especialmente orientada para este tipo de indústria.

Descrito como sendo um simples item de borracha redondo, os pneus são um sistema complexo constituído por compostos de borracha e de materiais de reforço, tanto têxtil como metálico. Os reforços têxteis proporcionam a forma, as propriedades mecânicas e a estrutura necessária para o pneu. Uma boa adesão entre a borracha e as cordas é um requisito essencial, levada a cabo por um tratamento químico das cordas.

Este trabalho optimizou o processo industrial de impregnação de reforços têxteis, nomeadamente a distribuição de temperatura no interior das estufas industriais, ajustando-se para isso as condições de ventilação; os resultados obtidos mostram que a função objectivo foi melhorada em 1.28 %. O scale-down das condições de operação observadas nas estufas industriais foram revistas e concluiu-se sobre a necessidade de melhoramento das mesmas. Por fim, foi desenvolvido um modelo baseado em CFD capaz de reproduzir as estufas usadas no processo industrial e de ajudar a melhorar o seu desempenho; contudo, este modelo ainda precisa de ser melhorado.

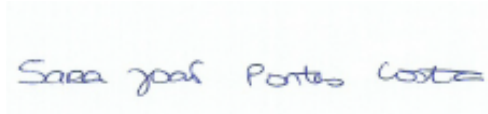
**Palavras-chave:** pneu; reforço têxtil; processo de impregnação; optimização; simulação

---



## Official Statement

I declare, under honor commitment, that the present work is original and that every non-original contribution was properly referred, by identifying its source.



Sara yael Portes Costas

# Index

<b>1</b>	<b>Introduction.....</b>	<b>1</b>
1.1	Project Presentation & Framework .....	1
1.2	Work Contributions .....	3
1.3	Thesis Organization.....	3
<b>2</b>	<b>State of the Art.....</b>	<b>4</b>
2.1	From Fibers to Textile Reinforcing Materials.....	6
2.2	Textile Terminology .....	7
2.3	Dipping Process.....	8
2.3.1	RFL-dipping solution .....	8
2.3.2	Pre-dipping solution .....	9
2.4	Production Dipping Unit (PDU) .....	9
2.4.1	Ovens.....	11
2.5	Laboratory Dipping Unit (LDU) .....	13
2.6	Physical Properties .....	14
<b>3</b>	<b>Procedure and Technical Description.....</b>	<b>16</b>
3.1	Materials .....	16
3.2	Testing Procedure .....	16
3.2.1	PDU Experiments .....	16
3.2.2	LDU Experiments .....	17
3.3	Testing Methods .....	17
3.3.1	Force-Elongation .....	18
3.3.2	Thermal Shrinkage .....	18
3.4	Data Analysis in PDU.....	19
3.5	Statistical Analysis .....	20
3.6	Simulator .....	20
3.6.1	ANSYS® Workbench .....	20
3.6.2	ANSYS® Fluent.....	20



<b>4</b>	<b>Results and Discussion .....</b>	<b>21</b>
4.1	PDU .....	21
4.2	LDU .....	28
4.2.1	Nylon A.....	29
4.2.2	Nylon B.....	30
4.2.3	Nylon C.....	32
4.2.4	Statistical Analysis .....	34
4.3	PDU and LDU .....	36
4.4	Simulation .....	38
4.4.1	Assumptions .....	39
4.4.2	Grid .....	39
4.4.3	Boundary Conditions.....	40
4.4.4	Demonstrations .....	42
<b>5</b>	<b>Conclusions .....</b>	<b>46</b>
<b>6</b>	<b>Project Assessment.....</b>	<b>47</b>
6.1	Accomplished Objectives .....	47
6.2	Limitations and Future Work .....	47
6.3	Final Assessment .....	48
<b>7</b>	<b>References .....</b>	<b>49</b>
<b>Annex 1 Production Dipping Unit.....</b>		<b>51</b>
<b>Annex 2 Product Specifications.....</b>		<b>58</b>
A.2.1	Nylons .....	58
<b>Annex 3 Data Analysis .....</b>		<b>59</b>
<b>Annex 4 Economic Analysis .....</b>		<b>60</b>
A.4.1	Natural Gas .....	60
A.4.2	Energy .....	60
<b>Annex 5 Statistical Analysis.....</b>		<b>62</b>
<b>Annex 6 Simulation.....</b>		<b>79</b>
A.6.1	Materials .....	79

A.6.1.1 What is the Boussinesq approximation? ..... 79

**A.6.2 Mathematical Modelling ..... 80**

# Index of Figures

Figure 1. Schematic representation of the reinforcing textile and its incorporation in the tyre. (Adapted from [2]) .....	2
Figure 2. Radial tyre cross section. (Adapted from [7]) .....	5
Figure 3. Tyre components. (Adapted from [7]) .....	5
Figure 4. Development stages from fiber to fabric. (Adapted from [11]) .....	6
Figure 5. Schematic representation of fiber treatments. (Adapted from [12]) .....	9
Figure 6. Schematic representation of the production dipping unit Zell. ....	10
Figure 7. Temperature cascade control block diagram. ....	12
Figure 8. Schematic representation of the Laboratory Dipping Unit (LDU). ....	13
Figure 9. Load-Elongation typical curves of various synthetic fibers. ....	18
Figure 10. Division of Zell plant into blocks.....	19
Figure 11. Results of the experimental trials performed in Nylon C at Zell unit in Oven 4. ..	23
Figure 12. Results of the experimental trials performed in Nylon C at Zell unit in Oven 5. ..	24
Figure 13. Results of the experimental trials performed in Nylon C at Zell unit in Oven 6. ..	25
Figure 14. Results of the experimental trials performed in Nylon C at Zell unit in Oven 7. ..	26
Figure 15. Load-elongation curve for Nylon A. ....	30
Figure 16. Load-elongation curve for Nylon B.....	31
Figure 17. Load-elongation curve for Nylon C. ....	33
Figure 18. Representation of the results of the thermal shrinkage tests for Nylon C experiments. ....	36
Figure 19. Representation of the compilation results of the thermal shrinkage tests for Nylon A experiments. ....	37
Figure 20. Representation of the compilation results of the thermal shrinkage tests for Nylon B experiments. ....	38
Figure 21. Geometry of the entire oven, showing a typical CFD mesh with highlighted zones and boundary conditions. ....	39
Figure 22. Contours of Static Temperature (K) inside the studied oven.....	43
Figure 23. Contours of Total Pressure (Pa) inside the studied oven.....	43

---

Figure 24. Contours of Velocity Magnitude ( $m \cdot s^{-1}$ ) inside the studied oven. ....	44
Figure 25. Contours of Velocity Magnitude ( $m \cdot s^{-1}$ ) in detail inside the studied oven. ....	45
Figure 26. Supply of greige fabric and the centre driven let-off station. ....	51
Figure 27. First fabric accumulator. ....	51
Figure 28. HMI software for a) Dip mixing and b) Fabric Treating Line [16]. ....	51
Figure 29. Dip stations. ....	52
Figure 30. Vacuum system. ....	52
Figure 31. Pull roll stands. ....	52
Figure 32. Path of the fabric between Oven 4 and Oven 5. ....	53
Figure 33. Burner with bottom and top ventilations. ....	53
Figure 34. Exhaust fan. ....	54
Figure 35. Guidance devices. ....	54
Figure 36. Fabric getting in and out of bottom of the ovens. ....	55
Figure 37. Inside view of the Oven 5 with the jet boxes and fabric on movement and one of the temperature measure device. ....	55
Figure 38. Top of the ovens, which can have a campanula or not. ....	56
Figure 39. Top of a) Ovens 1 to 4 b) Oven 5 to 7 c) and a global vision of all of them. ....	56
Figure 40. Second fabric accumulator and centre driven wind-up station. ....	57
Figure 41. Oven's section with temperature sensors position for Oven 2 and Oven 3 to 7. ...	57
Figure 42. Created tool using as example block C a) Visual Basic programming - Macros; b) tabs according with the variables presented in that block; and c) data graphically represented filtered by date and hour. ....	59

## Index of Tables

<i>Table 1. Annual production in 2015 of the different materials and the construction of the studied cords. ....</i>	<i>16</i>
<i>Table 2. Operating conditions for the different trials in different ovens for Nylon C. ....</i>	<i>22</i>
<i>Table 3. Results from the laboratory tests to Model and Trial 6 experiments. ....</i>	<i>27</i>
<i>Table 4. Results from the laboratory tests to Model and Trial 7 experiments. ....</i>	<i>27</i>
<i>Table 5. Operating conditions of the experimental trials for Nylon A. ....</i>	<i>29</i>
<i>Table 6. Laboratory results from the thermal shrinkage and shrinkage-force tests for Nylon A and the target values (<math>\mu</math> - average, <math>\sigma</math> - standard deviation). ....</i>	<i>29</i>
<i>Table 7. Operating conditions of the experimental trials for Nylon B. ....</i>	<i>30</i>
<i>Table 8. Laboratory results from the thermal shrinkage and shrinkage-force tests for Nylon B and the target values (<math>\mu</math> - average, <math>\sigma</math> - standard deviation). ....</i>	<i>31</i>
<i>Table 9. Operating conditions of the experimental trials for Nylon C. ....</i>	<i>32</i>
<i>Table 10. Laboratory results from the thermal shrinkage and shrinkage-force tests for Nylon C and the target values (<math>\mu</math> - average, <math>\sigma</math> - standard deviation). ....</i>	<i>32</i>
<i>Table 11. Statistical analysis results for laboratory experiments. ....</i>	<i>35</i>
<i>Table 12. Compilation results of the thermal shrinkage tests for Nylon C experiments. ....</i>	<i>36</i>
<i>Table 13. Compilation results of the thermal shrinkage tests for Nylon A experiments. ....</i>	<i>37</i>
<i>Table 14. Compilation results of the thermal shrinkage tests for Nylon B experiments. ....</i>	<i>37</i>
<i>Table 15. Summary of the boundary conditions. ....</i>	<i>40</i>
<i>Table 16. Summary of the fabric conditions. ....</i>	<i>41</i>
<i>Table 17. Product specifications for the studied Nylons. ....</i>	<i>58</i>
<i>Table 18. Summary table of statistical analysis for Nylon A. ....</i>	<i>62</i>
<i>Table 19. Summary table of statistical analysis for Nylon B. ....</i>	<i>67</i>
<i>Table 20. Summary table of statistical analysis for Nylon C. ....</i>	<i>72</i>
<i>Table 21. Properties of air [26]. ....</i>	<i>79</i>
<i>Table 22. Properties of Polyamide 6.6 [27, 28]. ....</i>	<i>79</i>

## Glossary and Acronyms

$C$	Courant number	
$D$	diameter	m
$dTex$	decitex	g/(10000 m)
$H_{HV}$	higher heating value	kWh·m <sup>3</sup>
$P$	pressure	Pa
Re	Reynolds number	
$S_1$	stretch level applied to the cord in the first zone	%
$S_2$	stretch level applied to the cord in the second zone	%
$S_3$	stretch level applied to the cord in the third zone	%
$t$	time	s
$T$	temperature in simulation	K
$T_1$	temperature in the first oven	°C
$T_2$	temperature in the second oven	°C
$T_3$	temperature in the third oven	°C
$T_4$	temperature in the fourth oven	°C
$V$	operation velocity	m·min <sup>-1</sup>

### Greek letters

$\mu$	average
$S$	standard deviation

### List of acronyms

AG	Automotive Group
C-ITA	Continental - Indústria Têxtil do Ave, S.A.
CFD	Computational Fluid Dynamics
$C_p$	Process Potential Index
$C_{pk}$	Process Capability Index
EPDM	Ends per Decimeter
FASE	Force at Specific Elongation
FEUP	Faculdade de Engenharia da Universidade do Porto
HHV	Higher Heating Value
LDU	Laboratory Dipping Unit
PDU	Production Dipping Unit
PID	Proportional-Integral-Derivate
RFL-dip	Resorcinol Formaldehyde Latex dip

# 1 Introduction

## 1.1 Project Presentation & Framework

*'If I had asked people what they wanted, they would have said faster horses'*, Henry Ford.

The automotive industry is very competitive and is in continuous evolution. The high standard market, with costumers demanding better energy performances and driving experiences at an affordable price, leads corporations to overcoming themselves to stay in the market.

Founded in 1871 in Hannover, Germany, Continental started out manufacturing rubber products and solid tyres for bicycles. A few years later, the company started the production of automobile pneumatic tyres, which production has been on rise since then. Currently, Continental is the market leader in the tyre industry in Germany, second place in the Europe and fourth in the world market. The Automotive and Rubber Groups at Continental comprehend five areas, Chassis & Safety, Powertrain, Interiors, Tyres and ContiTech. In 2015 the corporation employed approximately 208 000 people in 53 countries distributed by 430 locations and had two textiles reinforcement plants, one located in the USA and the other one in Lousado, Portugal [1].

Indústria Têxtil do Ave, S.A. (ITA) was founded in 1950 in Lousado, Portugal and its core-business is textile manufacturing, especially oriented towards tyre industry. Operating with a well-established knowledge and providing high-qualified textile reinforcement materials, in 1993 Continental AG decided to fully acquire ITA, becoming Continental-ITA (C-ITA) in 2015.

Antithetical to common idea, tyres are an aggregation of rubber compounds and reinforcing materials, both textile and metal. The textiles provide not only the shape and structure needed to the tyre, but also the mechanical properties when the tyre is subjected to harsh conditions during the vehicle motion. On the other hand, a good adhesion between rubber and cords are crucial and carried out by the chemical treatment, otherwise the tyre would split in parts.

Reinforcing materials manufacture is a complex process that requires parts with specific chemical and physical properties. The process starts with untreated fibers (greige fibers) that are dipped into aqueous solution, which promotes the adhesion between the cord and the rubber (chemical treatment). This process is followed by a thermal treatment, which consists in submitting these fibers into ovens with a controlled temperature, stretch and exposure time (physical treatment). This process increases the crystallinity of the fibers and then the mechanical resistance of the fabric.

To have a more precise overview on this type of industry and to smooth the understanding of the purpose of this thesis, Figure 1 pictures a basic schematic of the production process of a tyre.

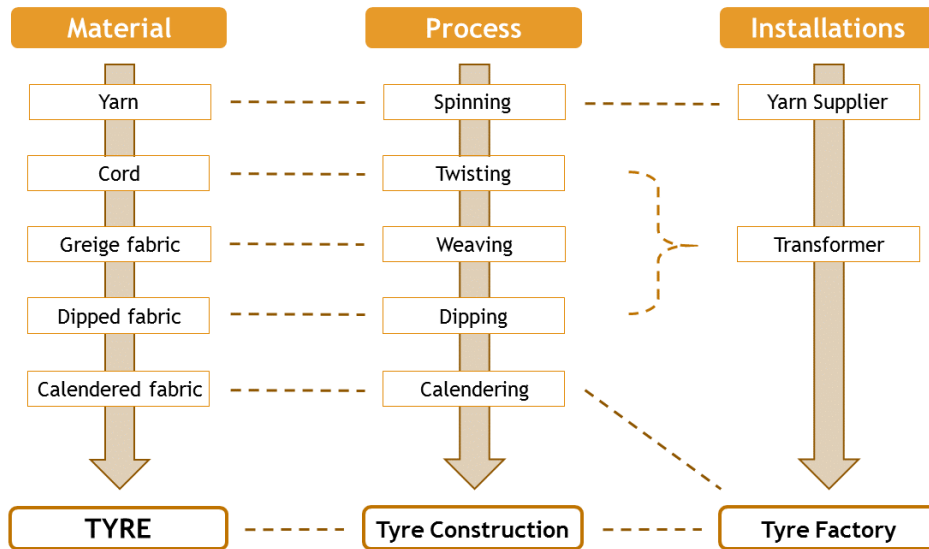


Figure 1. Schematic representation of the reinforcing textile and its incorporation in the tyre. (Adapted from [2])

This assignment optimizes the dipping process existing at C-ITA; special attention is paid to the 7 ovens composing the drying system of the plant (named *Zell*), since they are the heart of the industrial process. Although the diversity of textile materials, with different constructions and properties, this work will focus only in Nylon fabrics. For that, it was taken 3 different approaches tapering the same goal, being them the laboratory and production areas and a simulation tool:

- The laboratory approach reproduces in small scale the actual production process. Thus, it was performed a set of studies using a scale-down model described in literature [3, 4], which are implemented nowadays in the lab-dipping unit. In this thesis, it was reassessed the scale-down model to Nylon materials for checking its accuracy since the industrial plant was upgraded.
- Regarding to the production area, place where the textile reinforcement materials become complete and ready to be used in tyres, it was made a process optimization. This work focused on optimizing the temperature of the ovens and the convective phenomenon of hot air by regulating ventilations. The final objective after optimize the distribution of air inside the ovens was to reduce the operation temperature.
- Lastly, it was developed a CFD tool to simulate the thermal treatment in each oven according with the production conditions, as the temperature of the air, fabric's velocity, ventilations and exhaustion. Another interesting feature of this tool is that it allows for future works to change the design of the actual ovens to study if they have the best architecture and to study better alternatives.



Despite the fact this thesis being a kick-start and ‘unfinished’ work, it defines a reasoning research line for further studies.

## 1.2 Work Contributions

The present work was developed after deciding the textile that will be work in this project, being Nylon the chosen one.

Starting with production unit, an optimization of the process was performed in view of a better temperature distribution inside the ovens by regulating ventilation flows, followed by a reduction of operation temperature. An economic analysis was made to understand the impact caused by the made changes.

In laboratory unit, it was reviewed the practiced model for verifying its accuracy, since the industrial plant was upgraded and it was proposed changes in conditions to reach a new suitable model. A statistical treatment was performed to validate the suggested changes.

Finally, a simulation tool was also developed allowing a full view of the oven as also further works.

## 1.3 Thesis Organization

This thesis is organised in 7 main chapters, being each of them briefly described next.

Chapter 1. **Introduction** presents Continental corporation and C-ITA and gives an initial approach to tyre industry and its industrial process.

Chapter 2. **State of the Art** summarizes the actual knowledge about tyres, fibers and textile reinforcement materials, the dipping process and the existing dipping units.

Chapter 3. **Procedure and Technical Description** provides more technical information about the used materials, the adopted procedure for experiments in laboratory unit as well in production one, the software used to data and statistical analysis as also for the developed simulation tool.

Chapter 4. **Results and Discussion** is subdivided in 3 distinct parts and it refers all experimental results and its analysis/discussion.

Chapter 5. **Conclusions** point out all the prime aspects supported by this thesis.

Chapter 6. **Project Assessments** outlines the accomplished objectives and provide information and suggestions for future development.

Chapter 7. **References** is a complete list of all the references used throughout this work.

**Annexes** are the last section, where additional information is given.

## 2 State of the Art

Commonly described as round, black and expensive [5], a tyre is an advanced and complex engineering product. With a worldwide need, tyres made part of routine, from transportation to sports, being an essential element of vehicles as cars, motorbikes, planes or bikes. Although people make their choice based merely on price, a tyre is an important component that should not be underestimate, since it is must perform a variety of functions, such as being responsible for supporting the weight of the vehicle, absorbing road irregularities, providing sufficient traction for driving, braking, steering control and direction stability [5, 6].

Originating from Great Britain during the last years of the XIX century, the tyre suffers an upgrade from solid rubber tyres made by John Dunlop, which had small cross-sections and high pressure, especially for bicycle applications. In the early 1920's, larger 'balloon' tyres were introduced in the motor vehicle industry and a few years later this same tyres became tubeless. From belted bias to radial, tyres suffered an evolution through different types, being the radial ones the passenger tyre market leaders nowadays [5].

Get deep into the structure, from the inside to the outside, following the sequence of its construction and starting in carcass, **bead core** composed by steel wire embedded in rubber, is the first element, which has the capacity to ensure the tyre sits firmly on the rim; followed by **bead apex** and **bead reinforcement**, which are composed by synthetic rubber and nylon, aramid respectively, have the intention to enhance directional stability, to give steering precision and to improve comfort; **side wall**, with natural rubber in its composition, protects the casing from external damage and atmospheric conditions; **inner liner**, composed by butyl rubber, seals the air-filled inner chamber; and **textile cord ply** with rayon or polyester rubberised in its constitution, aims to control internal pressure and to maintain the tyre's shape. The parts of tread/belt assembly starts with **steel-cord for belt plies** made of high strength steel cords and with intention to enhance directional stability and shape retention, to reduce the rolling resistance as also to increase the tyre's mileage performance; followed by **jointless cap plies** that is nylon embedded in rubber and enhances high speed suitability; and **tread** with both synthetic and natural rubber in its constitution and which is sub-divided in 3 parts: **cap** provides adherence on all road surfaces, wear-resistance and directional stability, **base** reduces rolling resistance and **shoulder** forms an excellent transition between the tread and the sidewall [7]. The cross section of a radial tyre like previously described is shown in Figure 2.

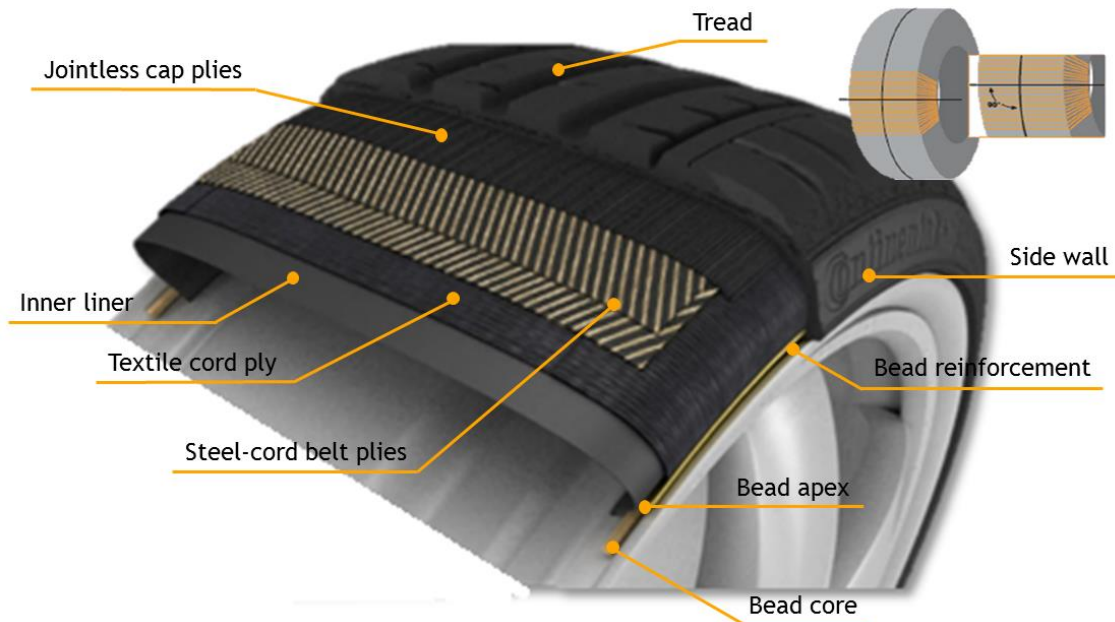


Figure 2. Radial tyre cross section. (Adapted from [7])

The components of a modern radial tyre for passenger cars contain diversified ingredients in different amounts, which vary according with the tyre’s size and type - if it is a summer or winter one [7]. Mostly composed by rubber, it also has fillers and reinforcing materials in its constitution, resulting in 20 different components. The fraction of each material group used in a typical summer tyre is presented in Figure 3. Giving special attention to reinforcing materials, it can be observed that it represents 15% of total ingredients.

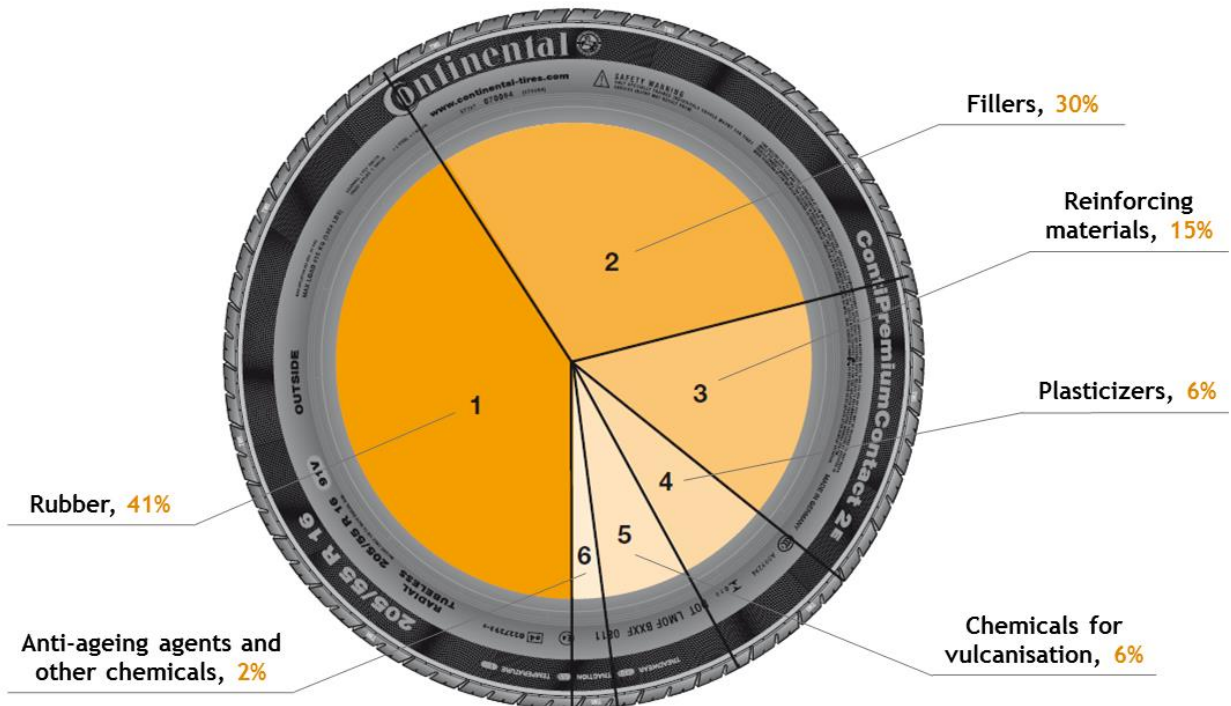


Figure 3. Tyre components. (Adapted from [7])

## 2.1 From Fibers to Textile Reinforcing Materials

Filament, yarn, cord and fabric, are the 4 levels of design which establish the life cycle of all fibers. Fibers are the groundwork of the textile reinforcing materials, being the fabrics the support of the rubber compounds in this kind of industry. They have not only to resist to all the forces that are applied to the tyre, but also have fatigue resistance, even under harsh conditions. Another essential role of this materials is being able to prevent the rubber deformation and having low heat generation, hence provide the security and stability required [5].

Starting with a pulp, it is possible to build a yarn by a process named melt spinning, which is a conventional method. The crystallinity of a spun fiber will depend on its cooling rate during spinning and the strength is improved by a process called drawing [8]. Then, it is possible to form a cord by twisting one yarn or multiple ones. A perfect twisted yarn is characterized by the individual component yarns being twisted together symmetrically [9]. Twisted yarns are initially twisted in the 'Z' direction (in the counter-clockwise direction), then those twisted yarns are twisted together but in the opposite direction, the 'S' direction (clockwise), composing the pretend greige twisted cord. The twisting process is adjusted according with the fiber and its application and it is performed not only to hold the yarn filaments together, but also to improve the mechanical properties of the material, such as the maximum tensile strength and elongation due to the distribution of tensile properties between the yarn filaments [10]. Finally, the cord can be weaved into fabric or not, according to the final purposes. This sequence of stages is shown in Figure 4.

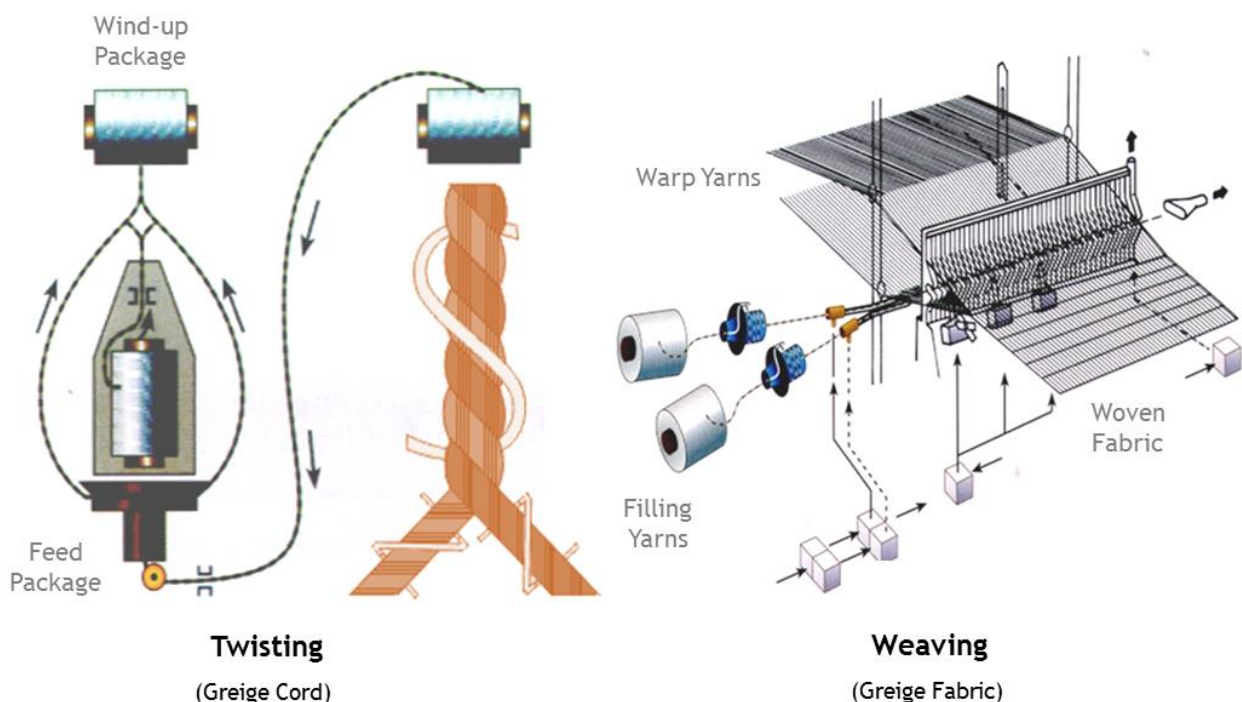


Figure 4. Development stages from fiber to fabric. (Adapted from [11])

Textile, metal and rubber compounds are examples of reinforcing materials. The difference between textile and metal are based on the material, while textile consists on textile fibers, metal are made of steel cords. Both are, nevertheless, embedded in rubber compounds at the end of the process.

C-ITA is divided into three different production sectors, being them the **fiber/twisting**, **weaving** according with the previous explanation about the development stages of fabric and **dipping area**, which will be explained in detail afterwards. The types of fibers used in this industry are limited due to the necessity of materials with sufficiently temperature-resistant to survive the vulcanization step without weakening or complete disintegration [12]. The 4 fibers used are **Aramid**, **Nylon** (usually Polyamide 6.6 - PA6.6), **Polyester** (Polyethylene Terephthalate - PET) and **Rayon** [3, 10, 12]:

- **Aramid** is a synthetic and high tenacity organic fiber, doubly stronger than Polyester or Nylon, with good dimensional stability but poor adhesion. It can be used in the carcass, belt or bead, depending on the type of tyre. It is well-known for being part of the composition of body armor vests like ‘Kevlar’.
- **Nylon**, a synthetic long chain polymer widely applied in the most diverse areas, presents good fatigue resistance in compression and good resistance to heat, strength and capability of establish bonds with rubber compounds. However, it has the disadvantage of a low melting point and a low modulus. It can be used as a cap ply in radial tyres, above or around the steel belt.
- **Polyester** is a semi-crystalline thermoplastic polymer with high tensile strength and low shrinkage, but chemically inert which drives into a hardship with rubber adhesion. It is usually used in carcass.
- **Rayon**, made from cellulose and a uniform structure, is sensitive to moisture ending on a significant loss of strength. Although being more expensive than Polyester, this fiber is heat resistant and it has good handling characteristics, justifying its use in the body ply.

This thesis will focus on Nylon fibers.

## 2.2 Textile Terminology

To use the correct nomenclature, it is important to define and understand all the designations used [13, 14]:

- **Fiber:** linear macromolecules with high strength orientated along the length of the fiber axis.
- **Filament:** smallest continuous element of a tyre cord.
- **Yarn:** a group of filaments.

- **Cord:** twisted structure of two or more yarns.
- **Greige cord:** a cord without chemical treatment.
- **Linear density:** the weight per length of the fiber. The most commonly used unit is the Decitex (dTex), which is defined according with the Equation (1).

$$dTex = \frac{10\,000 \times \text{Sample weight (g)}}{\text{Sample length (m)}} \quad (1)$$

- **Twist level:** the number of turns per unit length of a twisted yarn or cord. The twisting process is important to improve the tensile properties once the filaments get close.
- **Twist factor:** the twist is multiplied by the square root of the linear density of the yarn, which represents the mathematical correlation between twist level and dtex. In fact, same twist factor drives to same yarn properties and to equivalent helical orientation of filaments.
- **Cord construction:** represents the type of construction of the cord according with the number of yarns and how they are twisted. Taking as an example a cord construction 940x1x2, it means that each yarn has 940 dtex and the cord is made of 2 equal yarn first twisted individually and then together.
- **Fabric:** is a planner structure defined by interweave yarns or fibers, which has a substantial area in comparison to its thickness.
- **EPDM:** number of cords per fabric decimeter.

## 2.3 Dipping Process

As previously mentioned in **Section 2.1**, textile reinforcement plays a crucial role in the tyre construction. In fact, textiles do not adhere directly to rubber because of the lack of chemical affinity. ‘When using fibers in combination with rubber, good adhesion is essential especially for high safety products such as tyres.’ [12]. Thus, the fibers are commonly treated with a dip before being used in rubber compounds so the existing hurdle originated by the large difference in polarity and stiffness between fibers and rubber is overtaken [12]. Then, to form a solid interface layer at the fiber surface promoting chemical interact with the rubber compound in the calendaring and vulcanization process of the tyre, the fibers are stretched through drying process in the ovens [10].

### 2.3.1 RFL-dipping solution

Through this process named ‘Dipping’, the fiber dives into a water-based solution containing Resorcinol, Formaldehyde and rubber Latex, originate the RFL-dip solution. If the dip solution contains only latex, it would provide adhesion to the rubber matrix but not with the fiber itself making the tyre mechanically weaker. By adding resorcinol and formaldehyde, which react to form a resin, the whole dip coat acquires the essential chemical bonds between the fiber and

the rubber compound. A typical RFL-dip has solid content of around 20 % of mass fraction and a pH  $\approx$  10, once its structure when cured is a continuous resin phase and dispersed latex particles [3, 12].

### 2.3.2 Pre-dipping solution

Depending on the fiber, it can be necessary a pre-dipping before the RFL-dipping step, otherwise the fiber could not get the required adhesion to the rubber matrix. Polyester and Aramid are examples of it, as they do not contain as many reactive functional groups as Nylon or Rayon [12]. The pre-dipping solution is composed by isocyanate, which is regularly used in the industry, and by epoxy resins (polyepoxides) [15].

Figure 5 shows a schematic representation of the sequence of chemical treatments that fibers are submitted in order to get the requested adhesive properties. It is important noticing the existence of maturation and cure processes between some steps, in furtherance of the correct design and operation of the dips.

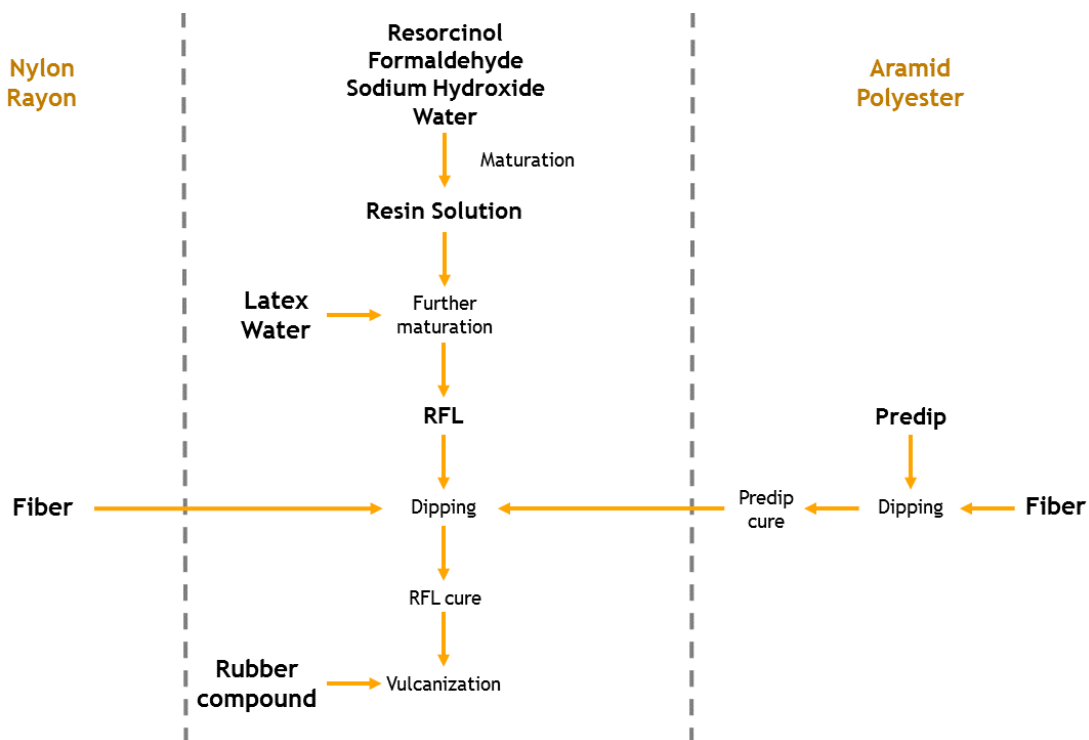


Figure 5. Schematic representation of fiber treatments. (Adapted from [12])

## 2.4 Production Dipping Unit (PDU)

Although dipping processes are well-known at textile industry and literature about it can be easy to find, the operating conditions are specific for each plant as well as for each fiber. The major parameters are the temperature, the stretch level, the exposure time and the dip solution being used. In fact, the temperature has a critical role in the process once it dehumidifies the fibers, it cures the RFL treatment into fibers when combined with the

exposure time and it provides the final thermo-mechanical properties when combined with stretch.

The machine used in production dipping process is named 'Zell' and it is a complex device, which allows controlling and managing assorted variables during the process, granting an overview of it. It has a height of approximately 36 m and its maximum velocity operation is  $110 \text{ m}\cdot\text{s}^{-1}$ . The *Zell* plant is designed in Figure 6.

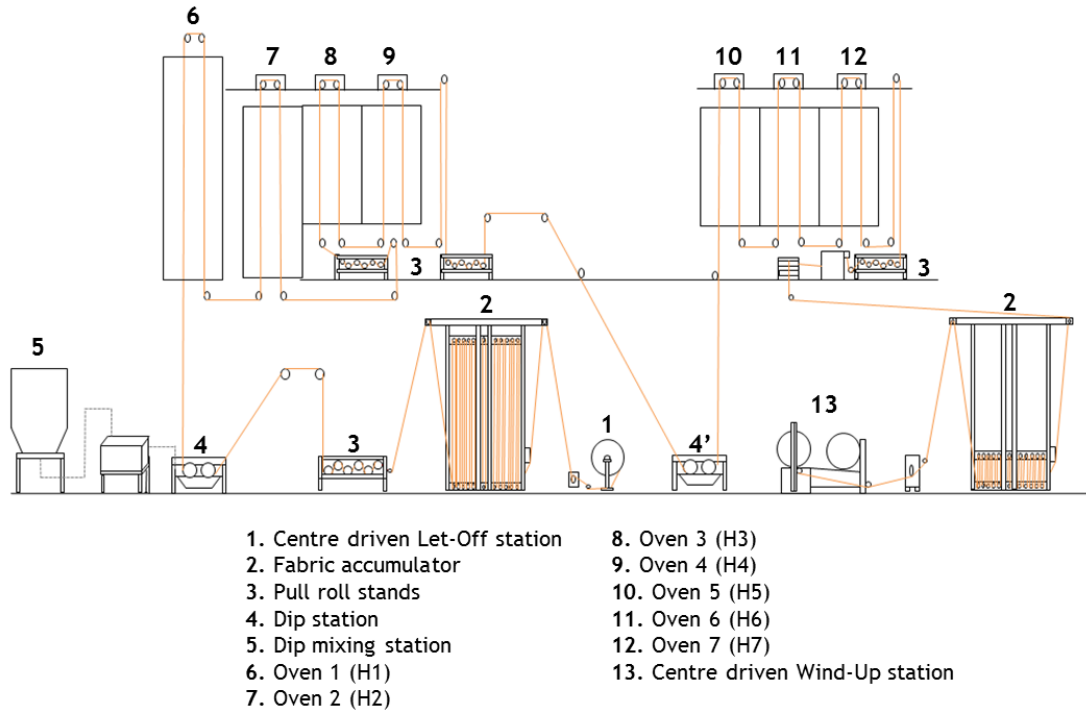


Figure 6. Schematic representation of the production dipping unit *Zell*.

Starting with greige fabric roll at **Centre driven Let-Off station (1)**, it will be ensure a correct fabric inlet under constant let off tension and at a specific velocity imposed by the a set point, which represents the velocity of the fabric at all parts of the machine [16]. Then, it goes through a **Fabric accumulator (2)**, which is important for nonstop batch changes in continuous processing ranges in order to ensure a distortion-free fabric passage [9]. Followed by a **Pull roll stands (3)**, that is used to build up the necessary tensions and to transport the fabric through the entire machine. **Dip station (4)** and **Dip mixing station (5)** are the stations that promote the chemical treatment. The dip station ensures uniform dip pick-up across the fabric width in order to reach the acquire adhesion with a minimum of this solution, while dip mixing station controls the automatic preparation of dip solutions, using a controlled software to manage all dip solutions. According to the previous explanation, some fibers need two dips (pre-dip and RFL-dip solutions), this is why two dip stations are represented (4 and 4'). The first one is associated with the pre-dip solution and the second to RFL-dip solution. In cases where only RFL-dip is applied, only dip station (4) is used, although the fabric continues the same way like if it has the pre-dip. **Oven 1 to 4 (6-9)** and **5 to 7 (10-12)** are very similar between them in



terms of design, but they have different functions during the process according with the fiber. They are composed by two sided air injection (jet lips) providing an increase of dryer efficiency and constant air velocity across the fabric width, except Oven 1 (6) that in upward way of the fabric only has one side of air injection. Finally, the **Centre driven Wind-Up station (13)** is used to wind up the dipped fabric in a uniform way and with straight edges [16].

In fact, there are some other variables that can be managed but they are not represented in above figure, such as the **Squeezing device** that will remove the surplus on the fabric, after the fabric has been dived into the dip solution; then the fabric passes through **Dewebber System** assuring an exact defined dip pick-up, where the constant aspiration can be adjusted across the entire fabric width; a **Fabric guiding** which consists on a **Centre guide**, a **Full width spreader** and a **Trio canter**, which are used to spread the fabric uniformly across the entire width at high tension to lead the fabric centre lined within the machine; and finally the **Process control**, a software based on a control system [16]. For a better understanding of this production unit, images of it are covered by the **Annex 1 Production Dipping Unit**.

#### 2.4.1 Ovens

Deepening into one of the main focus of this thesis, the ovens, it is imperative to describe them in detail for a better comprehension of the overall project.

Oven 1, which is the first and biggest one through the process - occupies 7 floors, corresponding to approximately 20 m, it has a different inside structure, as previously explained, once in upward way of the fabric it only has jet boxes by one side, opposed by the descendant way where it has jet boxes by the two sides of the fabric. This oven has two natural gas burners and at this stage its main goal is to dry the fabric.

Oven 2 has one less floor than the previous one and the fabric is ventilated by the two sides. This oven and the followings are feed by one natural gas burner. The main purpose is to cure the pre-dip or RFL solution, depending on the fiber.

Ovens 3 to 7 are similar and occupy 5 floors. Usually Ovens 3 and 4 are the ones that provide the final thermo-mechanical properties. The remaining ovens can be shut down in case they are not needed, they can be used to cure the RFL treatment and to thermo-fix the mechanical properties in those cases there are two dip treatments or they can be used only to thermo aims when there is no pre-dipped.

In fact, there is a bottom and top ventilation for each oven. Air from the exit is heated in the gas burner and fed to both ventilations, which are responsible for creating hot air streams that enable a uniform temperature inside the oven and provide a correct thermal treatment to the fabric. The outlet of this streams are the jet boxes, where the hot air is directly jetted to the fabric at high velocity. However, there is an open surface which collects the previous hot air

inside the oven and heated it again. This mechanism provides an air recycling which is hotter than the exterior air, ending up not only in natural gas saving, but also in an approach to optimize the convection streams inside the oven. In addition, there is an exhaustion system, whose main role is not only to guarantee the correct exhaustion of the vapor and but also to promote the convection streams.

Since the ovens are high and have a complex structure, it is necessary to have temperature points of control. There are 7 temperature sensors along each oven which are connected to a control system and it records the air temperature through the different positions. This control system is called *Cascade Control System*. This system is composed by two PID (Proportional-Integral-Derivative) control loops connected together and two controllers to enhance the control of a master variable (master loop) by manipulation of a slave variable (slave loop). In this particular case, the master variable is the temperature of the controller and the slave variable is the air flow rate that is feed to the gas burner. Performing slave loop control on the air flow rate, variations in gas supply can be accounted and better temperature control parameters achieved. The control system mentioned has a remote set point [17]. The block diagram that better explains this mechanism can be observed in Figure 7.

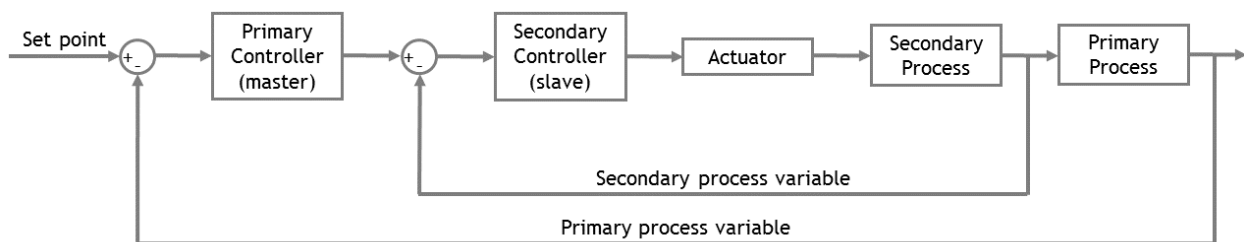


Figure 7. Temperature cascade control block diagram.

Knowing the position of the temperatures sensors (Pt100) is important since the manage of some variables, such as set point temperature, ventilations and exhaustion, are directly dependent to the results obtained from this devices. As an example, when the temperatures in the inlet and outlet of the fabric (bottom of the oven) are low, if the bottom ventilation increases, it is expected an increase of the previous mentioned temperatures; however, other zones inside the oven can also be hotter and being a problem, justifying the importance of using 7 temperature sensors. There are 2 devices on the bottom of the oven, 2 on the middle, 2 on the top and a last one is the controller for the hot air re-circulation. All of this sensors are positioned in the same side of the oven - downward way of the fabric - but positioned at different width. This type of devices has an actuation range from  $-30\text{ }^{\circ}\text{C}$  to  $+300\text{ }^{\circ}\text{C}$  and an associate error of  $\pm 0.15 + 0.002$ . To a better understanding of this sensors position, Figure 41 presented in **Annex 1 Production Dipping Unit** can show it.

## 2.5 Laboratory Dipping Unit (LDU)

Each cord has its own operation conditions in the dipping process. When a new material appears, it is needed to adjust the parameters of the process according with what it is pretended. For that, C-ITA has a laboratory machine that allows running experimental trials, since the machine operates in a similar way to PDU. LDU differs with production unit in the fact that it dips single cords and the lesser number of ovens. This equipment is able to reproduce in small scale the actual production process. Thus, it is possible to do optimization trials without compromising the production unit and avoiding high costs, since it would be very expensive to stop the production. After a full study done and reached to valid conclusions, a scale-up to the production units is done, regarding to the different features between the production and the laboratory dipping units. This adjustment is based on the temperature, ventilations and exhaustion, exposure time, stretch level and line speed, for each oven. The laboratory dipping unit (LDU) has a total of 4 ovens, it works at a maximum speed of 20 m/min and its schematic representation is presented in Figure 8.

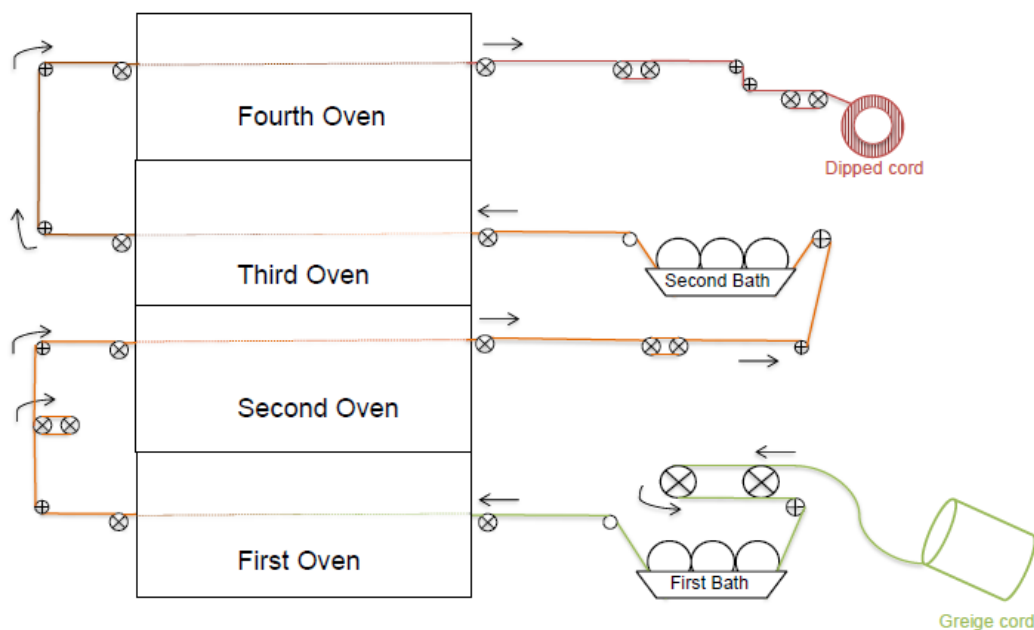


Figure 8. Schematic representation of the Laboratory Dipping Unit (LDU).

The process starts with greige cord that is subjected to a mechanical system which stabilizes and guides it through the first stretch zone and the first dip bath. Then, it passes through the first oven which is responsible for drying the cord, as well as the third one, being called the drying zones. The second oven is responsible for the stretching level, and it is called the hot stretching zone. Between the second and the third oven, it has the second bath that could be or not used according with the dip specifications already explained. The fourth oven is used to normalize the cord. At the end of the process, the dipped cord is obtained in a spool which

needs to be relaxed to reach the test conditions. The operating conditions of the process are inputted in a computer that is connected to LDU.

Although there are 4 ovens in laboratory unit compared to 7 in production one, this difference does not mean an obstacle, because the number of passages in the ovens can be changed according with the pretended exposure time and temperature in each zone.

According to Ricardo Silva's and Tiago Moura's master theses, it was concluded that when the temperature in ovens at Production Unit (PDU) is < 230 °C, in LDU corresponds to subtracting 10 °C to the temperature of the ovens, but when at PDU is upper than 230 °C, it has to reduce 15 °C. Regarding to stretch, when the 7 ovens are used in PDU, in LDU is needed to stretch 0.5 % more in the last zone. This are the settings used nowadays in the scale-down model used in LDU trials for Nylon [3, 4].

## 2.6 Physical Properties

In textile and automotive industries, it is important to define and understand different concepts, since the dipped fabric is subjected to quality control tests which have costumer's specifications that it is needed to achieve. These properties are dependent on variables such as the temperatures of the ovens (ventilations and exhaustions), exposure time and stretch level [3, 13].

- **Adhesion:** is the capability of a cord adhere to the rubber compound, after subjected to vulcanization. The range of the evaluation goes from 1 to 5 and this evaluation is based on observation of the results.
- **Breaking force (N):** force required to break the cord.
- **Dip pick up (%):** the amount of dip that a dipped cord has.
- **Elongation (%):** represents the elongation of the cord when subjected to a force.
- **Elongation at break (%):** indicates the total elongation of the cord until breaking.
- **Elongation at specific load (%):** measures the cord's length when subjected to a specific force. Some of the tests are made by using 45 N, 90 N and 135 N of driving force.
- **Force at a specific elongation (FASE) (N):** the force needed to elongate a cord a specific percentage of its initial length, commonly 2 %, 4 %, 8 % and 12 %.
- **Load (N):** the force applied to a cord.
- **Stiffness (N):** the needed force to bend a specific set of dipped cords.

Owing to the definition of thermal properties measured, it is important to have a brief description about the procedure. The samples are placed on the measuring device and subjected to a pretension, Equation (2), according to the linear density.

$$Pretension (cN) = linear\ density (dTex)(g/m) \times number\ of\ plies \times 0.05 (m \cdot cN/g) \quad (2)$$

Then, the samples are exposed to specific temperature and time, being 180 °C and 2 minutes the conditions used at C-ITA. After that, the samples cool down for 2 minutes while exposed to normal conditioning environment.

- **Thermal shrinkage (%):** measures the total shrinkage of the cord when exposed to high temperature for a certain period of time. Equation (3) defined this parameter, where  $L_0$  is the initial length of the sample and  $L_1$  the length after exposed to heat.

$$\text{Thermal Shrinkage (\%)} = \frac{\Delta L_1}{L_0} \times 100 \quad (3)$$

- **Thermal Residual Shrinkage (%):** is the remaining length after the initial shrinkage test ( $L_2$ ), while the conditioned environment and the pretension is maintained. This is obtained according with Equation (4).

$$\text{Thermal Residual Shrinkage (\%)} = \frac{\Delta L_2}{L_0} \times 100 \quad (4)$$

- **Shrinkage-force (N):** shrinkage force results from the force generated when the fiber's movement is restricted.

It is essential to highlight the special caution that trials in industry require, as changes made in order to optimize the convection streams at ovens can negatively affect the properties of the fabric and then being out of the range of customer's specifications. In fact, previous tests could be done in laboratory unit to predict the behavior of the fiber when in production, but it is important to be conscious about the complex scale-up associated to that.

## 3 Procedure and Technical Description

When it comes to a work with several tasks and a large amount of data to analyze, it is crucial to define a procedure that holds hands with a technical description in order to achieve a complete understanding on what it was done. This chapter describes the materials and methodology used during the project.

### 3.1 Materials

C-ITA has a panoply of cords originating huge amount of fabrics. To accomplish the goals of this project, it was chosen one textile material to study, Nylon. Nylon's fabrics are composed by cords that can have different construction and consequently different characteristics. Thus, it was studied 3 different cords, resulting in 3 different fabrics. The annual production of textile fibers in C-ITA and the construction of the selected cords are summarized in Table 1.

Table 1. Annual production in 2015 of the different materials and the construction of the studied cords.

Material	% Production in 2015	Construction
Aramid	0.40	-
Nylon	52.01	-
Nylon A, N <sub>A</sub>	17.20	940x1x2
Nylon B, N <sub>B</sub>	14.00	940x1x2
Nylon C, N <sub>C</sub>	3.72	1400x1x2
Polyester	42.93	-
Rayon	4.66	-

Regarding to EPDM's sequence, Nylons A and B have the same EPDM value which is lower than Nylon C. The difference between Nylon A and B is the supplier, justifying the distinct operation conditions that will be later seen. The product specifications from costumers for the studied materials are exposed in **Annex 2 Product Specifications**.

### 3.2 Testing Procedure

#### 3.2.1 PDU Experiments

As previously mentioned, the experimental tests in the production unit require special attention. It was important to start with an exhaustive study about the results obtained in PDU during the first two months of the present year for the interesting textile material. This study was based on mapping the temperature behavior allied to ventilation flows and on theoretical principles of convection air streams. After concluding the study, the approach to make experimental tests is defined. These tests were based on changing the bottom and top

ventilations to achieve the best operation conditions for a better heat distribution inside the ovens.

In fact, the actual distribution of air inside the ovens is not homogeneous. In view of homogeneity, the ventilation flows are changed, so the temperature difference decrease and approximate to the set point. When these changes are made, paying attention to the maximum and minimum temperature reached inside the oven is crucial, so that it will not have problems with the fabric as also with the final product specifications. When the temperature along the oven got out of the range defined by the set point, the hypothesis of ventilation flows is discarded, being necessary to try different settings. However, when the results are what it was expected, it is necessary to test that experimental conditions at least in 3 different days and posterior analysis to prove the material did not get compromised.

### 3.2.2 LDU Experiments

During the last years, the *Zell* unit suffered upgrades such as the improvement of the ventilations ending up in a better distribution of hot air and different operation conditions. Therefore, the model used in laboratory also need to keep up with these changes, being necessary to adjust it. In fact, it is believed that the gap between the production unit settings and the laboratory model has decreased since the actual process was upgraded. To accomplish this goal, several experiments were made to conclude about the performance of the model, according with the studied textile material.

The operation conditions of the performed experiments include the model previously proposed by Silva and Moura [3, 4], the actual production conditions used in *Zell* unit and in case of Nylon C (cf. Table 1), intermediate conditions, since the best option will probably be between the practiced model in laboratory unit and the production settings. Regarding to the dipping step, this textile material need only one dip, the RFL one. Average of 5 spools were made for each trial in view of a statistical study for further conclusions validation.

In fact, textile fibers are affected not only by temperature, but also by humidity, which justifies the laboratories at C-ITA being humidity and temperature conditioned. It is important to mention the cords before being tested were at least 24 hours in conditioning treatment, it means a conditioned room at about 23 °C and 55 % of air humidity. These conditions intend to simulate the settings that textile fabric in PDU is exposed, allowing to establish a reference between single cords and fabric.

## 3.3 Testing Methods

The tests were accomplish to dipped cord after relaxation.

### 3.3.1 Force-Elongation

Mechanical properties of the cords are often tested by force elongation tests. These tests are based on applying specific loads to fibers which are being elongated. During this elongation process, it is measured the fiber's length which increases by increasing the applied load, ending up in the required load to achieve the rupture. Plastic deformation is reached when the fiber breaks. The gradually increase of load permits to determine values at specific loads, namely at 45 N, 90 N and 135 N, and at the breaking force. Mechanical behavior of the fiber depends on parameters such as temperature, stretch level and residence time in the dipping process, presenting different curves and specific values according with each fiber. Figure 9 shows typical force-elongation curves of common synthetic fibers.

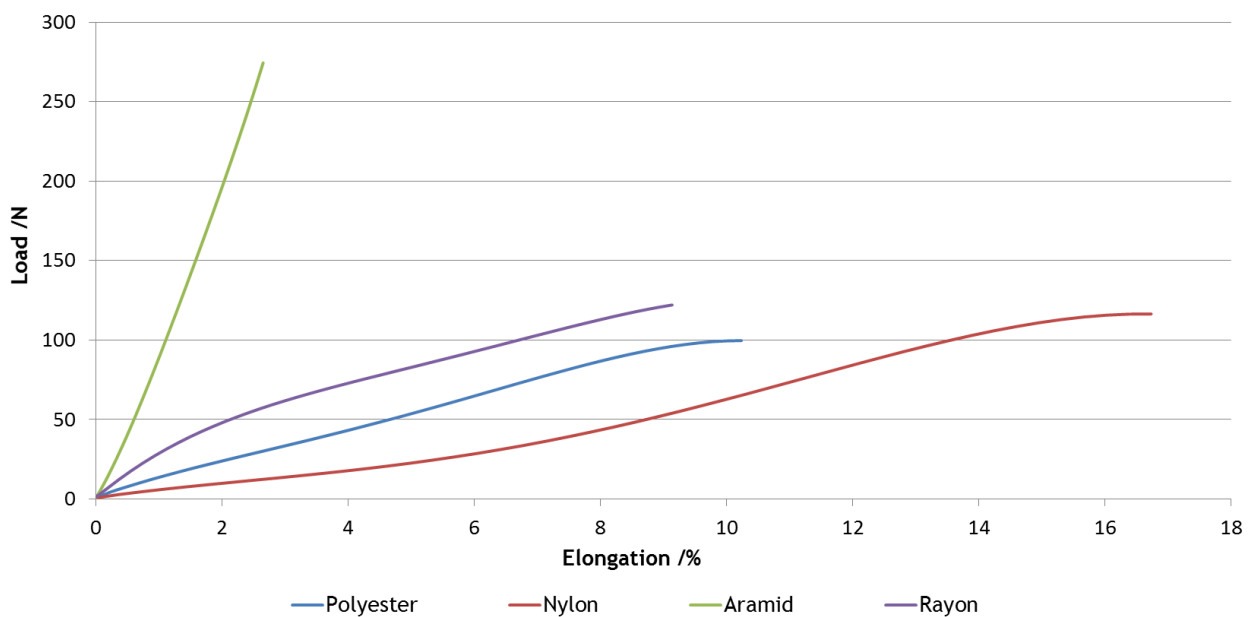


Figure 9. Load-Elongation typical curves of various synthetic fibers.

Analyzing Figure 9, it is possible to observe noticeable differences between the material's curves. The crystalline behavior of Aramid concedes a low elongation at the highest force antithetic to Nylon 6.6's behavior which has amorphous nature hence in a higher elongation.

This test method has an important purpose on tyres technology, since it reflects the cords behavior when subjected to driving forces, allowing to have prized information for the tyres design. Elongation tests were performed using a *Zwick Roell* tester. An average of 10 test runs were reported for each sample.

### 3.3.2 Thermal Shrinkage

The thermal-mechanical properties of all components of a tyre defines its performance and behavior, being an important element to resist to not all the forces that are applied to it, but also have fatigue resistance, even under harsh conditions. Most of the reinforcement textile fibers used in tyres industry tends to shrink under high temperatures, reflecting on the thermal-



mechanical properties of the cords and negatively influencing the overall performance of the tyre.

Thermal shrinkage test establish the amount of shrink of textile fibers when exposed to elevate temperatures, yielding values of shrinkage, shrink-force and residual shrinkage. The definitions and equations that better define this test are presented in **Section 2.6**.

### 3.4 Data Analysis in PDU

For assisting data analysis by *Zell* unit, which produces a huge amount of data, it was developed a visual basic application implemented in Excel, which was named *ZellAnalyzer*. This application organizes data from 5 parts of the *Zell* machine in different windows of an Excel file, eliminating meaningless information. Moreover, the developed tool allows organized the most relevant information graphically allowing a fast and accurate vision of the plant performance. In Figure 10 can be seen the division of the *Zell* plant in 5 parts.

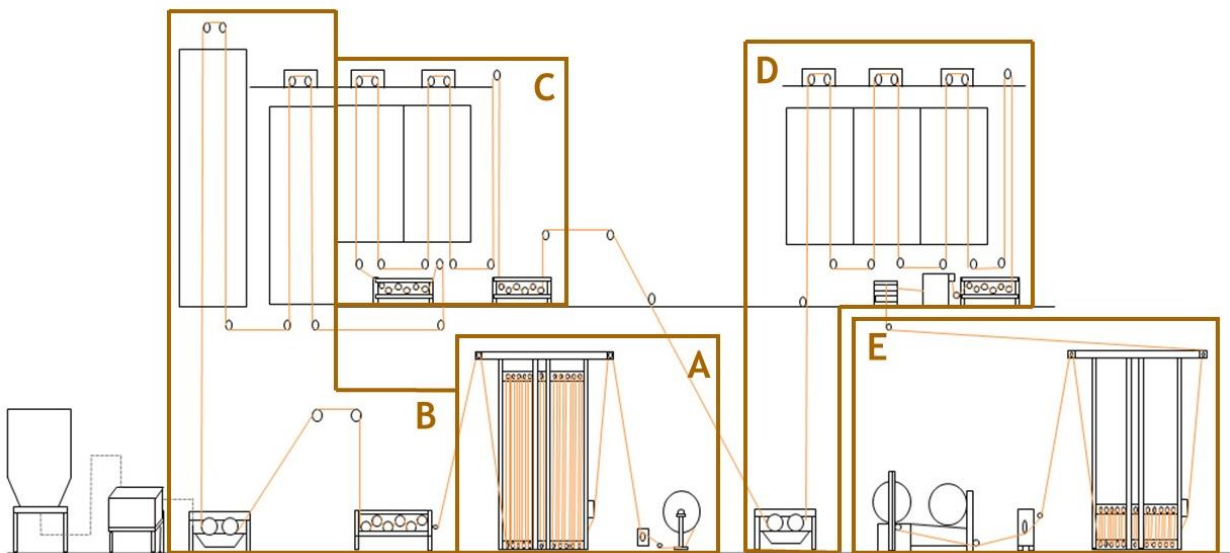


Figure 10. Division of *Zell* plant into blocks.

As it can be possible to observe in **Annex 3 Data Analysis**, which is an example of analysis of block C, the created tool enable not only a complete overlook of the process, as also a review of an exact date and hour by resorting to the available filters.

After this mechanism has been created, it was build a database with all the values provided by the software from January to February of 2016 corresponding to the selected fabric. With this data, it was possible to do a preliminary study based on mapping the behavior of temperature and ventilations flows of the chosen fabric and crossing information with quality control tests, in order to achieve a more appropriate and logical approach.

### 3.5 Statistical Analysis

The Minitab® 17 statistical software was used in view of a statistical analysis of the laboratory experimental trials and to conclude about its capability.

### 3.6 Simulator

To a better understanding about what happens on practice, it is interesting to simulate the actual conditions and it might get new conclusions about it. Although the simulation is in a budding stage, it provided the possibility to reach some interesting conclusions about the heart of the production process as also to be used in a deep way in future works. The conception of the simulator was composed by two different stages, being them the mesh and the simulation itself.

#### 3.6.1 ANSYS® Workbench

Starting with the oven design, the geometry domain was drawn in AutoCAD and the grid was generated with the software package *Meshing* included in ANSYS® version 16.0 with the view of a CFD simulation.

#### 3.6.2 ANSYS® Fluent

After the CFD grid is complete, the possibility to simulate the streams convection inside the ovens is possible, being only dependent on the boundary conditions of the case. The simulation was solved computationally using ANSYS® Fluent 16.0. ANSYS® Fluent is a well-known software for computational fluid dynamics, empowering an optimization of the product performance, since it includes well-validated physical modeling capabilities needed to model turbulence, heat transfer, flow and reactions for different industrial applications.

## 4 Results and Discussion

### 4.1 Production Dipping Unit

The *ZellAnalyzer* tool, see Section 3.4, allowed assessing the temperature homogeneity of the dipping ovens for the temperature and ventilation flows set-values used for fabrics made of Nylon C. This fabric has the highest number of thick cords among the materials studied in this thesis.

First, bottom and top ventilation flowrates were changed aiming to improve the temperature homogeneity inside the ovens, followed by a decrease of the operation temperature. The studied ovens were numbers 4 to 7 - see Figure 6. Ovens 1 and 2 were not optimized because of the different structure when compared with the rest of them and Oven 3 already had high ventilation flows, which will not enable an optimization with substantially influence in the final results. On changing the ventilation flowrates the hot-spots cannot exceed 5 °C above the set point; the ventilation flowrates should be changed systematic and smoothly. Please note that in the case Polyester fabrics the temperature set point should be changed first and only then the flowrates set points, since Polyester is very temperature sensitive and the weft of the fabric may melt inside the ovens.

After experimentally establishing the flowrate set ups that produce the best temperature homogeneity on experiments run in three different days, the temperature set up was decreased 3 °C and 5 °C to assess the best operating temperature. Samples of the produced fabric were collected and analyzed concerning customer's specifications to assess the oven operating conditions on the performance of the fabric. It was also important to underline the changes in the 4 ovens were made at the same time, the study was not made one by one, not allowing a deeper analysis.

The summary of conditions used in the 7 trials for each oven are presented in Table 2. The temperature in Ovens 4 to 7 are presented from Figure 11 to Figure 14; for each trial, it is shown the setting temperature, the average temperature and the average of maximum and the average of minimum. For a better analysis, the standard deviation of all measured temperatures was calculated and it is represented in the secondary axis.

It is fundamental making reference to the fact that although an increase or decrease on set point ventilation flows were made, that percentage of changing does not straight represent the actual increase or decrease in percentage of the air flow.

Table 2. Operating conditions for the different trials in different ovens for Nylon C.

		Temperature / °C	Exhaustion / %	Bottom ventilation / %	Top ventilation / %
Oven 4	Trial 1	235	20	65	65
	Trial 2	235	20	68	65
	Trial 3	235	20	73	63
	Trial 4	235	20	73	63
	Trial 5	235	20	73	63
	Trial 6	232	20	73	63
	Trial 7	230	20	73	63
Oven 5	Trial 1	235	10	65	75
	Trial 2	235	10	70	75
	Trial 3	235	10	75	73
	Trial 4	235	10	75	73
	Trial 5	235	10	75	73
	Trial 6	232	10	75	73
	Trial 7	230	10	75	73
Oven 6	Trial 1	235	10	60	75
	Trial 2	235	10	60	80
	Trial 3	235	10	65	75
	Trial 4	235	10	65	75
	Trial 5	235	10	65	75
	Trial 6	232	10	65	75
	Trial 7	230	10	65	75
Oven 7	Trial 1	235	15	55	80
	Trial 2	235	15	55	80
	Trial 3	235	15	63	80
	Trial 4	235	15	63	80
	Trial 5	235	15	63	80
	Trial 6	232	15	63	80
	Trial 7	230	15	63	80

Starting with an analysis to Oven 4, Trial 1 corresponds to the actual production conditions. After the ventilation optimization and the repetition of it in 3 different days, Trials 2 to 5, it is possible to notice that an increase of 8 % in bottom ventilation and a decrease of 2 % on the top one are the optimum conditions. Paying attention to both ventilations, they have the same conditions at the beginning. However, bottom one should be higher than the top one to overcome the cold air streams from the outside that get into the oven with the movement of the fabric.

When comparing with Figure 11, it can be observed that in Trial 1, for a temperature of 235 °C, the average inside the oven is around 231 °C, the average of maximum and minimum is 236 °C and 224 °C, respectively. After the ventilation optimization and its repetition in 3 different days, the average of temperature achieved was 233 °C, the average of maximum and minimum was 238 °C and 226 °C, allowing to conclude those conditions were not optimized seeing that

all measured temperatures raised 2 °C. When the first decrease of temperature (3 °C) was done - Trial 6, the measured temperatures decrease 1 °C when compared to Trial 1. When the second decrease of temperature (5 °C) was done - Trial 7, the difference is more remarkable, achieving 3 °C when compared with Trial 1.

Standard deviation can be considered low and stable during all trials, around 4 °C. In Trials 6 and 7, the temperature decrease will allow conclusions after a material analysis.

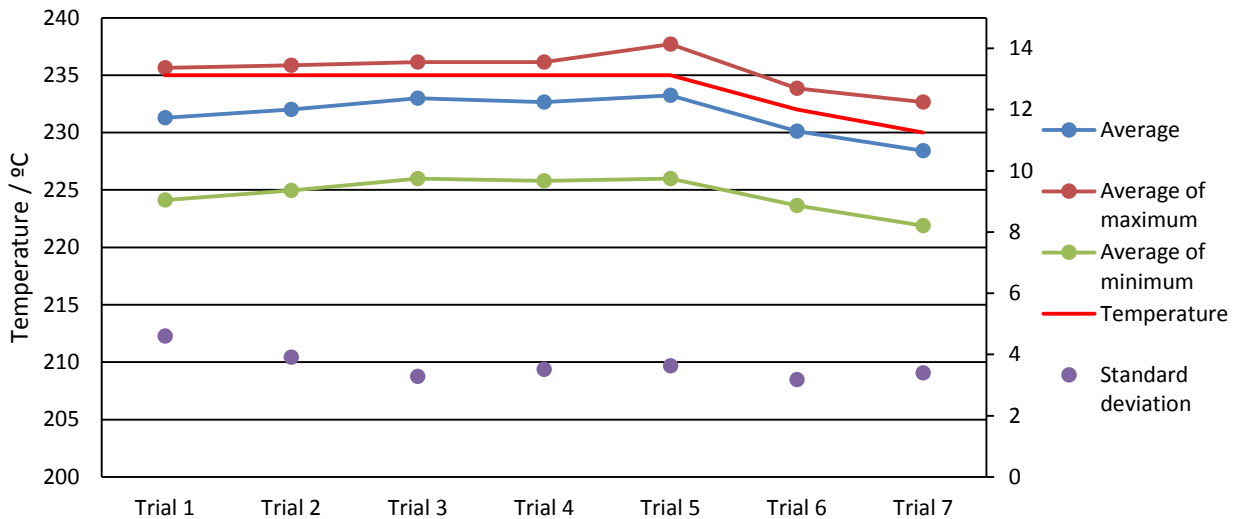


Figure 11. Results of the experimental trials performed in Nylon C at Zell unit in Oven 4.

Analyzing Oven 5, Trial 1 corresponds to production conditions currently used. The ventilation optimization trials and its repetition, corresponding to Trials 2 to 5 like in previous analysis, permitting to observe an increase of 10 % in bottom one and a decrease of 2 % on the top one are the best conditions. Like in the Oven 4, the bottom ventilation should be higher than the top one for the same reasons, what it comes against with predefined conditions.

Considering temperature distribution inside the oven, which are presented in Figure 12, it can be observed that in Trial 1, for a temperature of 235 °C, the average inside the oven is around 227 °C, the average of maximum and minimum is 235 °C and 210 °C, respectively. The gap between this values and the intended temperature are evidently higher than the Oven 4 results, which can lead to conclude the settings inadaptability. With the ventilation optimization trials and its repetition, for the same temperature, the average of temperature achieved was 233 °C, the average of maximum and minimum was 238 °C and 225 °C, allowing to conclude that although the initial gap between Oven 4 and 5 results was high, it is possible to achieve the same outcomes with manipulation of ventilations. The most significant value is the average of the coldest point inside the oven, which increased 15 °C with these adjustments. When the first decrease of temperature (3 °C) was done - Trial 6, comparing it with Trial 1 results, the average of maximum temperature was the same (235°C), the average increased 4 °C and the average of minimum increased 14 °C. When the second decrease of temperature (5 °C) was done - Trial 7,

also comparing with Trial 1 results, although the average of maximum temperature decreased 3 °C, the average and the average of minimum still increased 2 °C and 11 °C, respectively.

Regarding standard deviation, it can be observed a considerable descent, from 9 to 4 °C, which represents the temperature homogeneity inside the oven. The influence of the temperature decrease, Trials 6 and 7, will be later analyze.

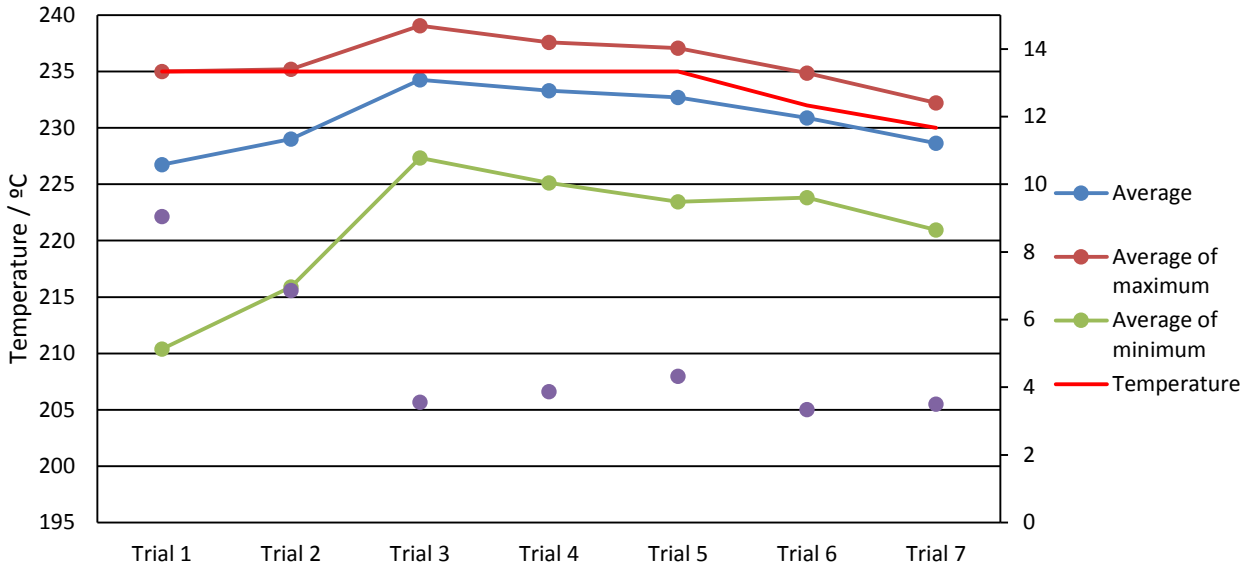


Figure 12. Results of the experimental trials performed in Nylon C at Zell unit in Oven 5.

In the Oven 6 analysis, Trial 1 also corresponds to actual production conditions. Trials 2 to 5 are the ventilation optimization and its repetition. This experiment allows to conclude that an increase of 5 % in the bottom ventilation maintaining the predefined top ventilation is the best option. One trial was made to get top ventilation higher, Trial 2, but without success. It was preferable to maintain the top ventilation and increase the bottom one. However, this set up of ventilations have a deviant behavior according with previous statements, since the top ventilation is higher than the bottom one.

Analyzing Figure 13 where is presented the temperature distribution inside the oven, it can be observed that for Trial 1, at a temperature of 235 °C, the average was 233 °C, the average of maximum and minimum was 236 °C and 226 °C, respectively. The results of the ventilation optimization trials and its repetition, for the same temperature, were slight better when comparing with Trial 1. The average of temperature achieved was 234 °C, the average of maximum and minimum was 237 °C and 229 °C, respectively. When the first decrease of temperature (3 °C) was done - Trial 6, the average of temperature was 231 °C, the average of maximum and minimum was 234 °C and 225 °C. When the second decrease of temperature (5 °C) was done - Trial 7, making comparison with Trial 1, the average of temperature decreased 5 °C, the average of maximum and minimum decreased both 4 °C.

Standard deviation was constant during all trials, rounding the 4 °C. Conclusions from the temperature decrease in Trials 6 and 7 will be reached after a material analysis.

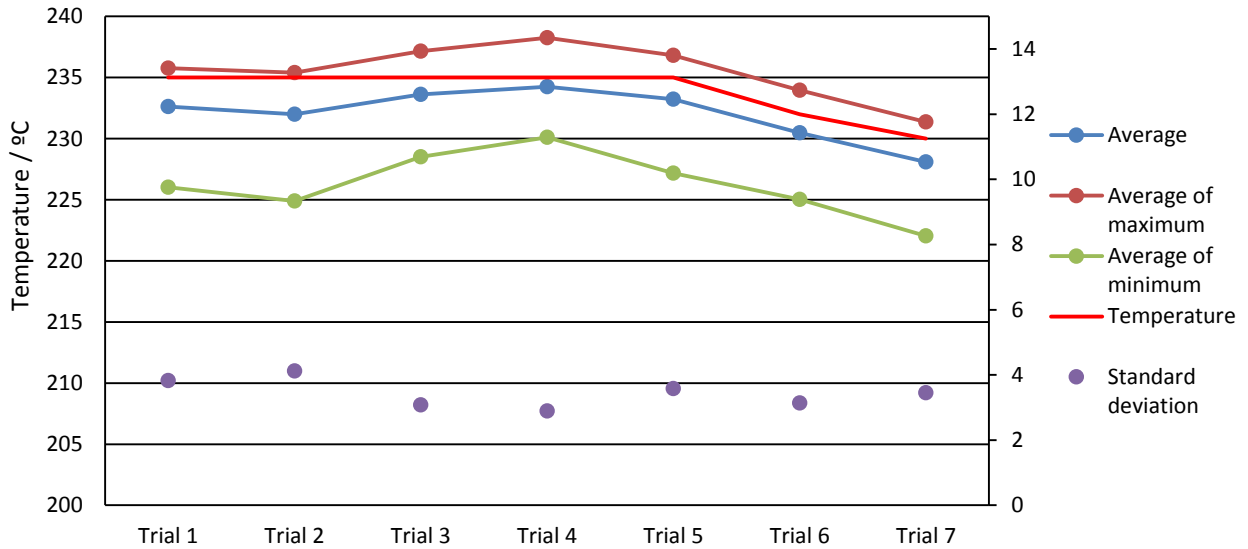


Figure 13. Results of the experimental trials performed in Nylon C at Zell unit in Oven 6.

In Oven 7, the last studied, Trials 1 and 2 correspond to the production settings. When comparing both trials there are some differences. The temperature results in Trial 2 showed higher values when compared with Trial 1, being a difference of 3 °C in the average of temperature and the average of minimum, and 0.6 °C in the average of maximum. This difference justifies the inconstant behavior of the ovens even under the same settings and the necessity to repeat the same experimental trials in different days, because the differences can be substantial. In this case, Trials 3 to 5 are the ventilation optimization and its repetition. With these experiments, it is possible to achieve the suitable conditions, increasing 8 % of the bottom ventilation maintaining the predefined top one. Once again, this set up ventilations have a deviant behavior according with previous statements, since the top ventilation is higher than the bottom one. Although the design of the ovens 4 to 7 are equal, the performance and the surrounding conditions are different between them. This fact can justify the different ventilation for the same temperature. Referencing the plant design presented in Figure 6, the oven 7 is located in the extremity of the plant, which can contribute for an oven inside cooling, since one of the oven’s side is not followed by another one. This state does not allow a temperature conduction between the oven’s walls, not contributing for the hot air streams like in the other ovens. Analyzing the Trial 1 conditions for the oven 7, it presents the highest ventilation (80 % in top ventilation) used in the trials, proving this hypothesis.

According with Figure 14 where temperature analysis is presented, for 235 °C, Trials 1 and 2 has an average of temperature of 230 °C, the average of maximum and minimum was 235 °C and 220 °C, respectively. When analyzed the results of the ventilation optimization trials and its repetition, for the same temperature, it presents better results when comparing with

Trials 1 and 2. The average of temperature achieved was 234 °C, the average of maximum and minimum was 236 °C and 228 °C, being notice the difference in the coldest point of the oven, more 8 °C than before the changes. When the first decrease of temperature (3 °C) was done - Trial 6, the average of temperature was 231 °C, the average of maximum and minimum was 232°C and 223 °C. When the second decrease of temperature (5 °C) was done - Trial 7, making comparison with Trial 1, the average decreased 1 °C, the average of maximum decrease 4 °C being justified by the set point decreased and the average of minimum increased 2 °C.

Standard deviation slight decreased during these trials, from 5 to 3 °C, representing the temperature homogeneity inside the oven. The influence of temperature drop will be further analyzed.

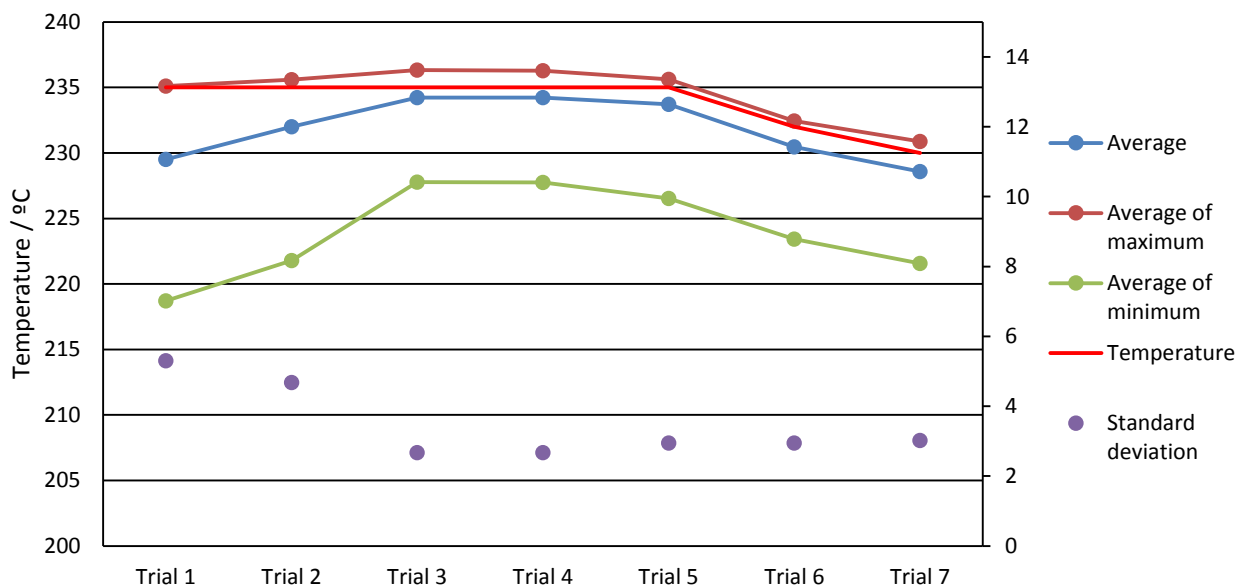


Figure 14. Results of the experimental trials performed in Nylon C at Zell unit in Oven 7.

After Trials 6 and 7 being concluded, which correspond to a decrease of temperature, it was performed tests in laboratory to ascertain if the specifications of costumers were achieved.

As a common practice, it is necessary to get a sample from the first roll of each set of a specific textile material to analyze and check if it has the correct properties before sending to the client. This process is considered a quality control system. Thus, before experimental trials being performed, this sample is always got and it becomes the *Model* trial. It is possible to notice that between Model trials there are some differences, what justifies that the production unit and the materials are not stable and have homogenous behaviors, having similar but not equal performances. At the laboratory, since the experimental trials only changes temperatures when compared with the actual settings, the tests were focused on thermal shrinkage and shrinkage-force and the results are presented in Table 3 and Table 4. Each collected sample was tested twice, the first test called 'Immediate' was performed right after the fabric sample



was collected and the second test called 'Conditioned' was performed after the 24 hours in conditioning treatment.

Table 3. Results from the laboratory tests to Model and Trial 6 experiments.

Properties	Model		Trial 6		Target
	Immediate	Conditioned	Immediate	Conditioned	Conditioned
Shrinkage 180 °C /%	6.20	4.90	6.10	4.90	4.80 ± 1
Residual Shrinkage /%	4.00	2.60	4.00	2.60	2.40 ± 1
Shrinkage Force /N	-	-	-	-	7.50 ± 2

Table 4. Results from the laboratory tests to Model and Trial 7 experiments.

Properties	Model		Trial 7		Target
	Immediate	Conditioned	Immediate	Conditioned	Conditioned
Shrinkage 180 °C /%	6.00	4.70	6.10	5.10	4.80 ± 1
Residual Shrinkage /%	3.80	2.40	-	2.90	2.40 ± 1
Shrinkage Force /N	-	7.50	-	7.42	7.50 ± 2

Analyzing the results for Trial 6 it can be observed that they are equal to the Model ones. On the other hand, the results for Trial 7 have a small difference when compared with the Model, especially the thermal and the residual shrinkage, passing from being in the target to the upper limit. In fact, being in the upper limit can be risky because it gets out of control easily, it is preferable to be on target or lightly below.

Thus, it is possible to conclude that decrease the temperature from 235 °C to 232 °C in Ovens 4 to 7 is the best option.

### Economic Analysis

The economic analysis was divided in two parts, the natural gas and the energy consumptions, not only to facilitate the analysis, but also to understand the impact caused by the changes made. All equations used are summarized in **Annex 4 Economic Analysis**.

Starting with natural gas consumption, it has an increase of 0.357 % per year justified by higher ventilation flows which demand higher heating flows and consequently consuming more natural gas. This extra consumption is reflected in approximately 140 € per year, value that is not significant when compared to the total cost of operation.

Regarding to energy consumption, it was verified a significant decrease, 12.5 % per year. In fact, according with Equation (5), which is used in fluid mechanics and it is valid for pumps and ventilators, it was believed that energy consumption will increase with the made changes, since the ventilation flows significantly increase [18].

$$P_2 = P_1 \left( \frac{N_2}{N_1} \right)^3 \quad (5)$$

Where  $P_2$  is the power requirement now,  $P_1$  is the rated power requirement,  $N_2$  is the ventilator speed now and  $N_1$  is the rated ventilator speed.

Analyzing Equation (5) is verified that for the same value of  $P_1$ , when  $N_2$  increase, the power requirement will increase significantly. This analysis do not come up with the obtained results, demanding a deeper analysis and do not consider this one.

## 4.2 Laboratory Dipping Unit

As previously explained in **Section 3.2**, the industrial machine suffered upgrades during the last years which directly affect the experiments performed in laboratory. To ascertain about the model adjustment capacity actual used in laboratory, and if not proposing a new relation between PDU and LDU, several experimental trials were performed. The operation conditions of these experimental trials include the conditions of the actual model, the actual production conditions used in *Zell* unit and in case of Nylon C, intermediate conditions, since the best option will probably be between the practiced model in laboratory unit and the production settings. For a better understanding of the nomenclature of the experimental trials, it is necessary to describe them.

- **PI Settings** - cords dipped in LDU with the laboratory conditions, corresponding to the practiced model (**Section 2.5**);
- **Study A** - cords dipped in LDU with the A operating conditions, corresponding to intermediate conditions between PDU and LDU;
- **Production Settings** - cords dipped in LDU with the operating conditions used in PDU, corresponding to the actual conditions used in PDU.

In fact, there will be one more designation on laboratory results, the *Sample*. The *Sample* is composed by cords obtained from fabric dipped in PDU from two different days. The results obtained for this samples will be the reference since they came from industrial process, and the main objective is to obtain in laboratory scale the same product that in the industrial unit.

The operating conditions of the process, such as speed, temperature and stretch level, are inputted in a software that is connected to the LDU, controlling them during the whole dipping process. Regarding to the costumer's specification, it can be found in **Annex 2 Product Specifications** the specifications required by costumers.

To conclude about which experimental trial better represents in small scale what happens in production scenario, it demands a combined analysis between the elongation and shrinkage results.

#### 4.2.1 Nylon A

To analyze this textile material, it was performed both experimental trials, the *PI Settings* and the *Production* one, to conclude about the decrease of gap between the two dipping units. The used operation conditions are presented in Table 5.

Table 5. Operating conditions of the experimental trials for Nylon A.

Name	$T_1 / ^\circ\text{C}$	$T_2 / ^\circ\text{C}$	$S_1 / \%$	$S_2 / \%$	$S_3 / \%$	$V / \text{m}\cdot\text{min}^{-1}$
<b>PI Settings</b>	135	220	2	3	0	12.9
<b>Production Settings</b>	150	235	2	3	0	12.9

The differences between the two trials are the temperature in the dry zone, equivalent to  $T_1$  and the stretching zone,  $T_2$ . The obtained results for thermal shrinkage and force-elongation are presented in Table 6 and Figure 15, respectively.

Table 6. Laboratory results from the thermal shrinkage and shrinkage-force tests for Nylon A and the target values ( $\mu$  - average,  $\sigma$  - standard deviation).

	$\mu$ Sample	$\sigma$ Sample	$\mu$ PI Settings	$\sigma$ PI Settings	$\mu$ Production Settings	$\sigma$ Production Settings	Target
<b>Shrinkage</b>							
Eff /%	4.33	0.12	5.00	0.09	4.23	0.08	$4.50 \pm 1$
Res /%	1.90	0.07	2.44	0.05	1.77	0.03	$2.00 \pm 1$
<b>Shrink-force</b>							
Eff /N	4.48	0.04	5.07	0.09	4.95	0.09	-

Analyzing the results from *Sample* and comparing with the target values it is possible to observe that it completely fits. Between the *PI Settings* and *Production Settings* trials, the *Production Settings* shows higher closeness to the desired results, since it belongs to the range of the lower bound, while the *PI Settings* belongs to the upper one, being preferably not to.

Regarding to load-elongation curves presented in Figure 15, both trials present similar curves between them and when compared to the *Sample* one, although it can be observed a deviation within curves at 12 % of elongation, it can be acceptable to conclude about the suitability to the model.

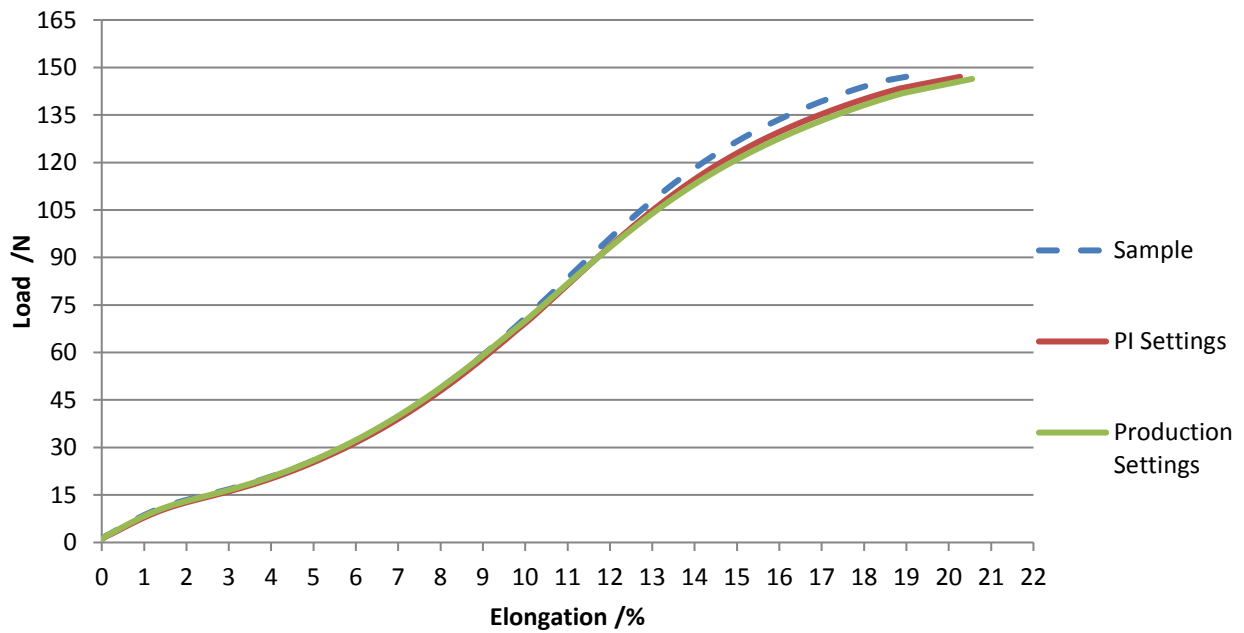


Figure 15. Load-elongation curve for Nylon A.

Therefore, it is possible to conclude that *Production Settings* trial is the best option, supporting the hypothesis that process in PDU is optimized, not being necessary an adaptability when in LDU unit withering the gap between the two units.

#### 4.2.2 Nylon B

Like previous mentioned, Nylon A and B have the same construction and EPDM, differing in the supplier. However, the trials performed were the same, the *PI Settings* and the *Production Settings*, in view of concluding about the suitability of production conditions in a smaller scale. The operation conditions are displayed in Table 7.

Table 7. Operating conditions of the experimental trials for Nylon B.

Name	$T_1 / ^\circ\text{C}$	$T_2 / ^\circ\text{C}$	$S_1 / \%$	$S_2 / \%$	$S_3 / \%$	$V / \text{m}\cdot\text{min}^{-1}$
<b>PI Settings</b>	135	227.5	2.8	3.5	0	12.9
<b>Production Settings</b>	150	242.5	2.8	3.5	0	12.9

The differences between the conditions used in the two performed trials are also the dry zone, equivalent to  $T_1$  and the stretching zone,  $T_2$ . The results for thermal shrinkage and force-elongation are presented in Table 8 and Figure 16, respectively.

Table 8. Laboratory results from the thermal shrinkage and shrinkage-force tests for Nylon B and the target values ( $\mu$  - average,  $\sigma$  - standard deviation).

	$\mu$ Sample	$\sigma$ Sample	$\mu$ PI Settings	$\sigma$ PI Settings	$\mu$ Production Settings	$\sigma$ Production Settings	Target
<b>Shrinkage</b>							
Eff /%	4.57	0.14	5.04	0.12	4.26	0.08	4.50 ± 2
Res /%	2.20	0.10	2.58	0.06	1.87	0.04	2.00 ± 2
<b>Shrink-force</b>							
Eff /N	4.61	0.10	5.22	0.09	5.11	0.08	-

Analyzing the results from *Sample* and comparing with the target values it is concluded that it completely fits. Between the *PI Settings* and *Production Settings* trials, the *Production Settings* presents higher proximity to the desired results, since it belongs to the range of the lower bound, while the *PI Settings* belongs to the upper one, like in Nylon A.

Considering the load-elongation curves showed in Figure 16, both trials present similar curves that completely cover the *Sample*, allowing to conclude about the suitability to the model.

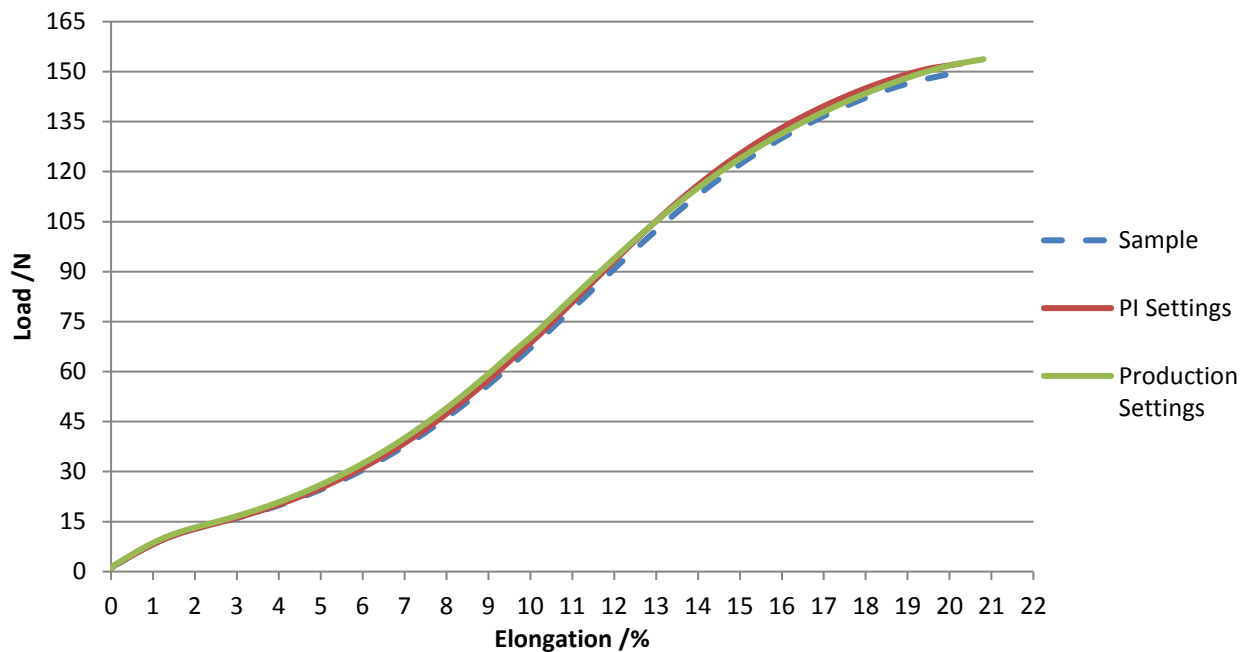


Figure 16. Load-elongation curve for Nylon B.

Thus, the *Production Settings* trial is the best approach like in Nylon A, supporting the presumption that process in PDU is optimized.

Concluding, Nylon A and Nylon B processes in PDU are optimized, allowing to use the same operation conditions in both units, obliterating the gap between them and the necessity to do a scale-up.

### 4.2.3 Nylon C

This textile material has a different construction and EDPM when compared with previous studied materials, resulting in different performed trials and results. This fabric has more cords and thick ones, becoming a stable fabric which facilitates the experiments. In fact, it does not have much space between cords, being the heat transfer different from the Nylons A and B. This state will directly interfere in the results like it will be afterwards seen. In Table 9 are presented the operating conditions used. Although this textile material only demand one dipping step, it is used the 7 ovens in PDU unit and the 4 in LDU unit.

Table 9. Operating conditions of the experimental trials for Nylon C.

Name	$T_1 / ^\circ\text{C}$	$T_2 / ^\circ\text{C}$	$T_3 / ^\circ\text{C}$	$T_4 / ^\circ\text{C}$	$S_1 / \%$	$S_2 / \%$	$S_3 / \%$	$V / \text{m}\cdot\text{min}^{-1}$
PI Settings	140	220	220	220	4.2	5.8	-2.5	10.7
Study A	150	225	225	225	4.2	5.8	-3.0	10.7
Production Settings	155	235	235	235	4.2	5.8	-3.0	10.7

It was performed 3 different trials differing in temperature and stretch. It was chosen the *PI Settings* to reproduce what it is being made in laboratory as also the conditions used in PDU before the study made described in Section 4.1. It was also considered an intermediate trial which was believed to be the best fit.

In fact the practiced model in laboratory from previous master theses suggests to reducing the same range of temperature in all ovens, even if the oven has a drying, stretching or normalizing role. In the intermediate trial, it was reduced temperature but accordingly with the gamma, since less 10 °C in 235 °C does not have the same impact than reduce 10 °C in 155 °C, plus the different goals for each oven. The results for thermal shrinkage are presented in Table 10 and force-elongation in Figure 17.

Table 10. Laboratory results from the thermal shrinkage and shrinkage-force tests for Nylon C and the target values ( $\mu$  - average,  $\sigma$  - standard deviation).

	$\mu$ Sample	$\sigma$ Sample	$\mu$ PI Settings	$\sigma$ PI Settings	$\mu$ Study A	$\sigma$ Study A	$\mu$ Production Settings	$\sigma$ Production Settings	Target
<b>Shrinkage</b>									
Eff /%	4.72	0.12	5.38	0.15	4.55	0.11	4.04	0.07	$4.80 \pm 1$
Res /%	2.31	0.10	2.88	0.09	2.56	0.07	1.58	0.03	$2.40 \pm 1$
<b>Shrink-force</b>									
Eff /N	7.07	0.13	6.91	0.06	7.68	0.05	7.81	0.08	$7.50 \pm 1$

When comparing the results from *Sample* with the target values, it is concluded that it completely fits. However, the trials *PI Settings* and *Production Settings* belong to the range of the higher and lower bounds, respectively, which is not the interest of this study. The *Study A* trial presents closeness to the desired results, like it was thought.

Regarding to the load-elongation curves in Figure 17, the *PI Settings* trial adjust correctly the *Sample* curve, contrary to the *Production Settings* curve that although to have the same curve tendency, presents a deviate. The *Study A* overlap the *Sample* curve.

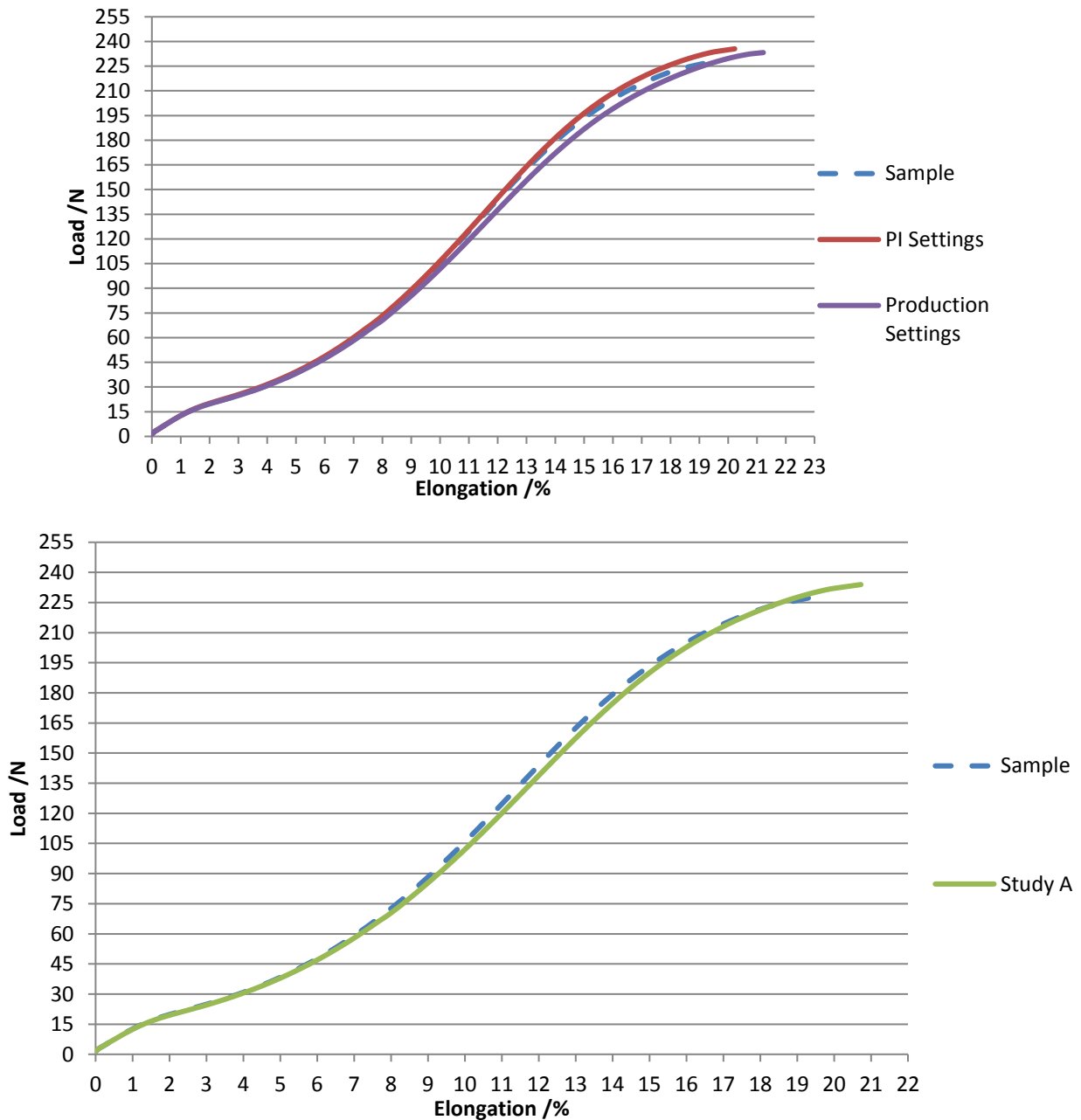


Figure 17. Load-elongation curve for Nylon C.

Therefore, it is possible to conclude that *Study A* trial is the best option, which supports the premise that production process is not optimized, which goes according with the work made and its conclusions in **Section 4.1**.

Analyzing the conclusions for the 3 studied Nylon, it is possible to observe that for Nylon C the behavior in LDU unit is different from Nylons A and B being justified by not only the process in PDU being optimized or not, but also by the construction of the fabric. From now one, when a

new material shows up to perform the scale-up or down, it must have in consideration not only the material and the dipping steps, but also the construction and characteristics of the fabric.

#### 4.2.4 Statistical Analysis

In view of statistical support, a deep analysis was made to laboratory results. The obtained values are presented in Table 11 and additional information can be find in **Annex 5 Statistical Analysis**.

Process Potential Index ( $C_p$ ) measures the potential capability of a process. The capability is defined as the ability of a process to produce product/service within defined specification limits.  $C_p$  is defined as the ratio of the allowable spread over the actual spread [19].

- $C_p < 1$ : the process is considered potentially *incapable* of meeting specification requirements
- $C_p \geq 1$ : the process has the potential to be *capable* of meeting specification requirements

Although it is considered a  $C_p \geq 2$ , a high  $C_p$  value does not guarantee that a production process will fall within specification limits, because the  $C_p$  value does not imply that the actual spread must coincide with the allowable spread.

Process Capability Index ( $C_{pk}$ ) measures the ability of a process to create product within specification limits. The  $C_{pk}$  value is an index which measures how close a process is running to its specification limits, maintaining the natural variability of the process [19].

- $C_{pk} < 1$ : the process is referred to as *incapable* of producing the product within specifications
- $C_{pk} \geq 1$ : the process is referred to as *capable* of producing the product within specifications

However, a commonly acceptable minimum value of  $C_{pk}$  is 1.33 or higher values.



Table 11. Statistical analysis results for laboratory experiments.

		Total N	C <sub>p</sub>	C <sub>p</sub> k
Nylon A	Sample			
	Shrinkage	10	1.92	1.44
	Residual	10	3.42	2.93
	Shrink-force	10	-	0.31
	PI Settings			
	Shrinkage	25	2.50	0.73
	Residual	25	4.31	1.57
	Shrink-force	25	-	3.83
	Production Settings			
	Shrinkage	25	2.72	1.67
	Residual	25	5.21	3.51
	Shrink-force	25	-	3.75
Nylon B	Sample			
	Shrinkage	10	1.96	1.83
	Residual	10	2.01	1.91
	Shrink-force	10	-	0.46
	PI Settings			
	Shrinkage	25	2.55	1.18
	Residual	25	3.11	1.52
	Shrink-force	25	-	4.06
	Production Settings			
	Shrinkage	25	4.21	3.22
	Residual	25	6.98	4.73
	Shrink-force	25	-	3.71
Nylon C	Sample			
	Shrinkage	10	1.88	1.66
	Residual	10	2.22	1.91
	Shrink-force	10	0.36	0.22
	PI Settings			
	Shrinkage	20	1.61	0.28
	Residual	20	2.49	0.80
	Shrink-force	20	5.88	2.71
	Study A			
	Shrinkage	20	1.58	1.02
	Residual	20	2.16	1.15
	Shrink-force	20	0.61	0.51
Production Settings				
Shrinkage	20	2.56	-0.22	
Residual	20	4.10	-0.72	
Shrink-force	20	4.58	3.29	

Analyzing the results presented in Table 11, it is possible to notice that for both *Sample* trials and those experiments previous concluded to be the best ones, the statistical results are also the best, respecting the required values for statistical validation above mentioned.

### 4.3 Production and Laboratory Dipping Units

To better comprehend the relation between the two dipping units, it was done a study looking through a different perspective. It was graphically represented the obtained shrinkage values according with performed temperature to conclude about a possible relation. The results obtained for Nylon C are summarized in Table 12 and presented in Figure 18.

Table 12. Compilation results of the thermal shrinkage tests for Nylon C experiments.

	LDU			PDU		Specification	
	PI Settings	Study A	Production Settings	Trial 7	Trial 6	Sample	Target
Temperature /°C	220	225	235	230	232	235	-
Shrinkage 180 °C /%	5.38	4.55	4.04	6.10	4.90	4.72	4.80

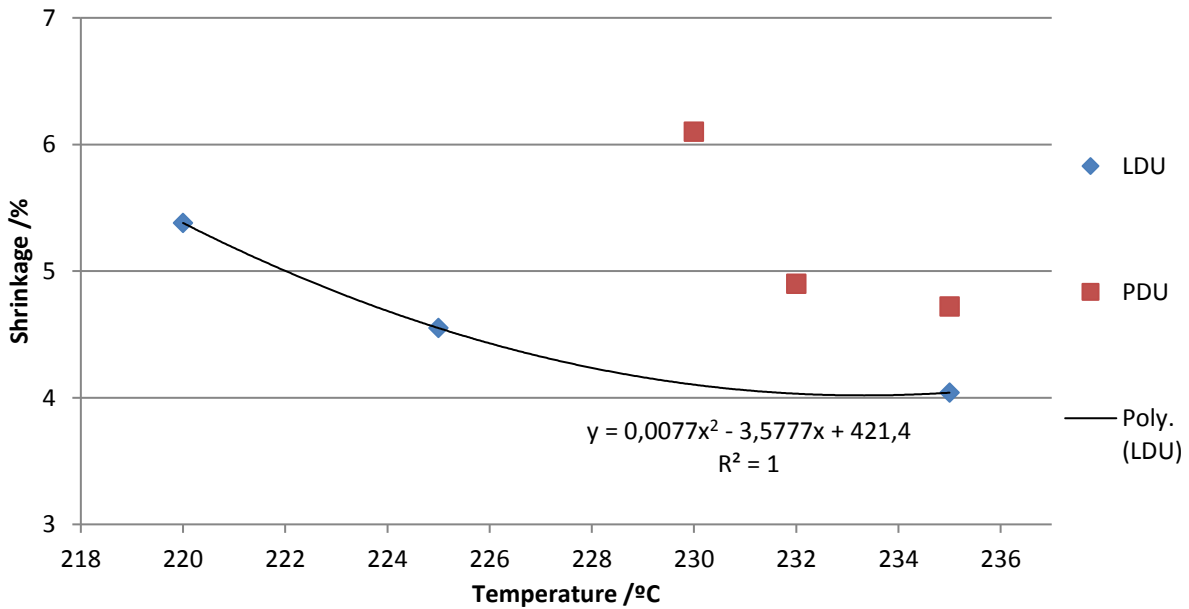


Figure 18. Representation of the results of the thermal shrinkage tests for Nylon C experiments.

In Figure 18, the LDU values represent the results of shrinkage obtained in laboratory experiments, while the PDU values represent the results of shrinkage obtained in production unit experiments. These results were previously referred. Analyzing the figure it is possible to observe that results from LDU and PDU units do not overlap even for same operation temperature, being 235 °C an example of this. The results in LDU that overlap the result in PDU at 235 °C can be find 10 °C at left horizontally, being possible to visualize the existing gap between the two units. This fact confirms the existing results deviation between the two units regarding to optimization of the industrial process and the construction of the fabric. The main goal is to get lower values of temperature to the same shrinkage, converging to results obtained from laboratory unit. However, the optimization of the industrial process follows a tendency to get results closest to the laboratory ones, but it will be difficult to overlap them because of

the construction limitation previous mentioned. Although there are only 3 points for LDU, the equation that better represents them is Equation (6) and it should help to define the temperature operation allied to the obtained performance.

$$y = 0.0077x^2 - 3.5777x + 421.4 \quad (6)$$

The same study was made for Nylon A. The results are summarized in Table 13 and represented in Figure 19.

Table 13. Compilation results of the thermal shrinkage tests for Nylon A experiments.

	LDU		PDU
	PI Settings	Production Settings	Sample
Temperature /°C	220	235	235
Shrinkage 180 °C /%	5.00	4.23	4.33

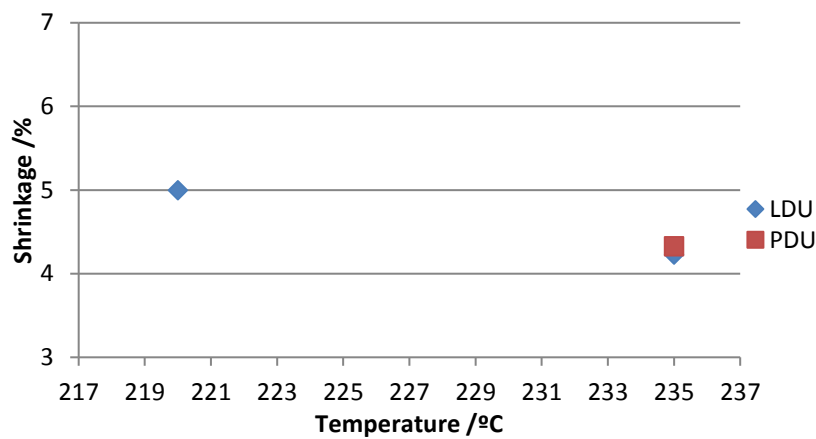


Figure 19. Representation of the compilation results of the thermal shrinkage tests for Nylon A experiments.

Previous study allowed to conclude that *Production Settings* were the best conditions to use in LDU, driving to confirm an inexistence gap between the two units. That conclusion can be confirmed by Figure 19. It can be observed that when represented Shrinkage vs Temperature, for 235 °C the results for both units overlapping, with a difference of 0.10 %, becoming clear that industrial process are optimized and the textile material has the same behavior for pilot scale as also for laboratory scale.

It was also performed the same study for Nylon B. The obtained results and its representation are presented in Table 14 and Figure 20, respectively.

Table 14. Compilation results of the thermal shrinkage tests for Nylon B experiments.

	LDU		PDU
	PI Settings	Production Settings	Sample
Temperature /°C	227.5	242.5	242.5
Shrinkage 180 °C /%	5.04	4.26	4.57

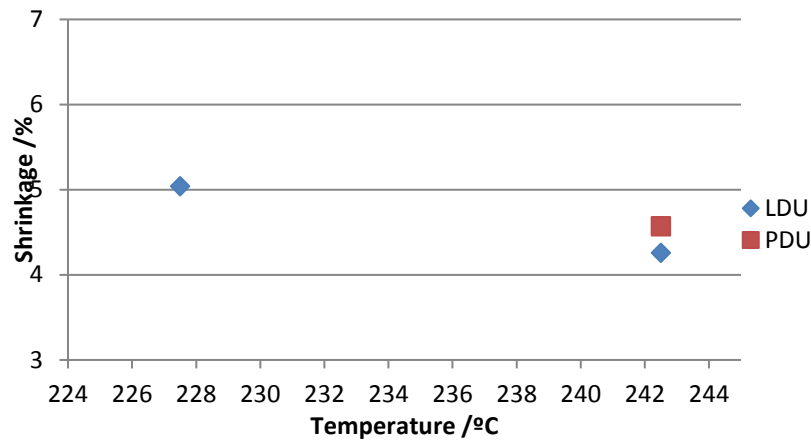


Figure 20. Representation of the compilation results of the thermal shrinkage tests for Nylon B experiments.

Analyzing Figure 20 is possible to notice that for 235 °C the results almost overlap, with a difference of 0.31 %. In fact, it can be considered that they are similar, corroborating with previous conclusions, which affirm that production process is optimized and the textile material has the same behavior for both scales.

The main objective to Nylon C is to get a graphical representation similar to Nylons A and B, where results from LDU are similar to PDU ones.

#### 4.4 CFD Simulation

Forced convection ovens are the focus of this section. They are based on hot air impingement technologies that have been used broadly in drying industry, as paper and textiles [20].

Get into the textile field, in forced convection ovens, heat is transferred to the fabric via convection, conduction and radiation, being the fraction of each transfer mode directly dependent on the temperature, velocity of the impinging air jets, type of product and oven chamber design and operation. For low air speeds, radiation is often the dominant mechanism of heat transfer, while convection is much more relevant for higher air speeds [20]. The production of fabrics with high and uniform quality as desired, it requires a good understanding of the heat transfer mechanisms. Computational Fluid Dynamics (CFD) modeling presents as an appropriate tool to better understand and solve the complexity of an infrastructure like this one [21].

In **Annex 6 Simulation** can be find additional information for better understanding this section, once it is described in detail the materials and the mathematical modelling behind these experimental trials.

Ovens are complex and puzzling devices that when extended in a simulation like this one it becomes even more difficult. Consequently, considerations must be done in order to achieve

the initial purpose. In this case, the simulation was done in 2D since the available tools do not allow to go further. However, this consideration must be taken into account during the analysis of results.

#### 4.4.1 Assumptions

Ovens are composed beyond the jet boxes by an exhaustion system and a close circuit - recirculation of hot air. In fact, the exhaustion and the recirculation of air are in a perpendicular plan to the jet boxes, which become a problem when it wants to simulate both plans in a 2D design. Thereby, the recirculation opening is not considered in the simulation. The major consequences of this are the streams balance, since it represents one less out stream, and the temperature in the zone where should be that exit stream, believed that should be lower than in the actual simulation. However, the boundary conditions for those streams, further presented, are defined by velocities and not by flows, which should not interfere the simulation. Another limitation is the jet boxes ventilation. In the actual plant, it is possible to set different flow ventilations for the bottom and the top; in this case, the same flow of ventilation is applied for both. Although this considerations, the simulation allows to get conclusions.

#### 4.4.2 Grid

The study focused on the inside part of an industrial textile oven. Figure 21 shows a schematic diagram of the oven structure. This grid was automatically generated and it is composed by a total of 185 566 cells.

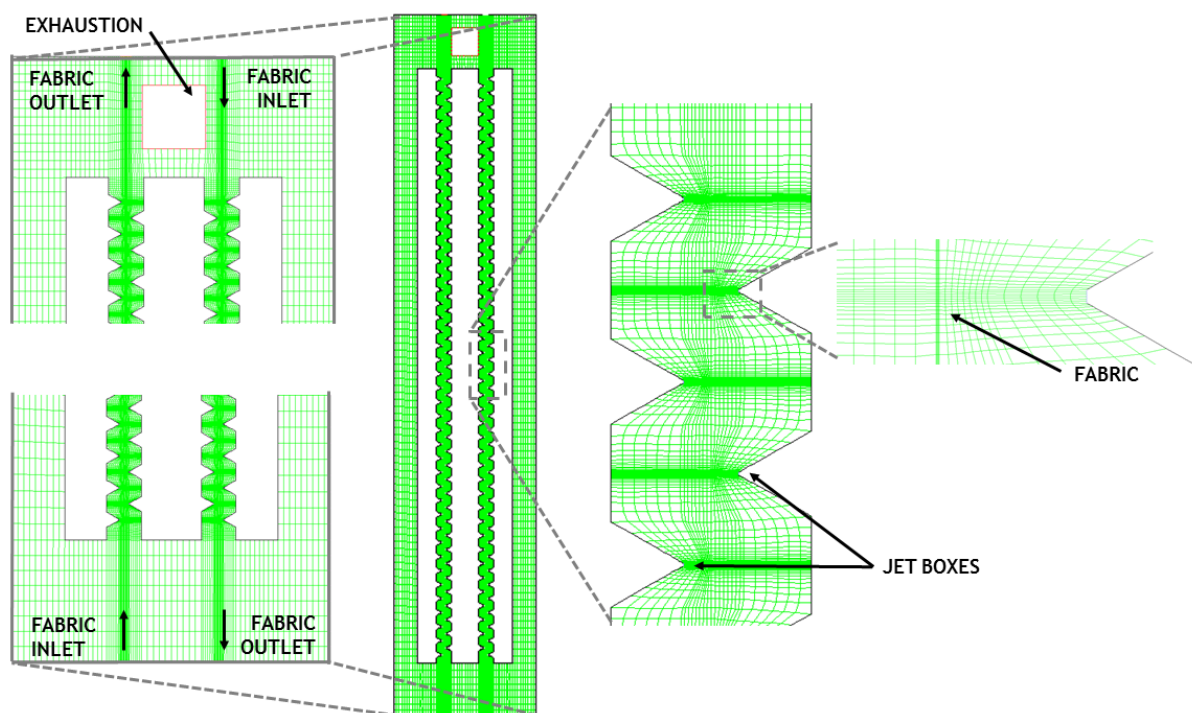


Figure 21. Geometry of the entire oven, showing a typical CFD mesh with highlighted zones and boundary conditions.

#### 4.4.3 Boundary Conditions

In order to follow the same material studied in production and laboratory units, the Nylon C was chosen to take part of this simulation, and the simulated oven was Oven 5.

Boundaries were considered for simplifying into one of two categories: flow openings and walls. The flow opening category can be subdivided in velocity inlet, pressure inlet and pressure outlet. Table 15 summarizes the boundary conditions.

- Velocity inlet: The only inlet air flow in simulation with this type is the jet boxes. The air temperature and its velocity are known from operation settings. However, the settings for the ventilations are in percentage, but once it is known the total flow, it is possible to calculate the equivalent flow for a specific percentage. In fact, the grid in those entrances is more detailed because of the needs when in simulation.
- Pressure inlet: This type is defined when the fabric get into the oven since it has two equal open area at the bottom and at the top. It is considered an ambience pressure of 101 325 Pa (1 atm).
- Pressure outlet: In this case, the behavior is the same than previous described, which means an ambience pressure of 101 325 Pa (1 atm) in the cases of exhaustion and the fabric outlet.
- Walls: This category is the most common in this under investigation system in which it is assumed a temperature in the surfaces.

For this simulation it was considered a gravitational acceleration of  $9.8 \text{ m}\cdot\text{s}^{-2}$  in all the conditions.

Table 15. Summary of the boundary conditions.

Conditions	Fabric inlet	Fabric outlet	Jet boxes	Exhaustion	Walls
Type	Pressure inlet	Pressure outlet	Velocity inlet	Pressure outlet	Walls
Temperature /K	293	293	508	423*	423*
Pressure /Pa	101 325	101 325	101 325	-	-
Gauge Pressure /Pa	0	0	0	-65**	-
Velocity /m·min <sup>-1</sup>	-	-	15**	-	-

\* It is an estimated value.

\*\* Round values to be confidential information.

It is assuming fabric inlet and outlet have constant temperature around 20 °C as also atmospheric pressure which corresponds to 101 325 Pa.

Regarding to the jet boxes, the actual velocity is confidential information, so it is assumed 15 m·min<sup>-1</sup> in this thesis, but it was used the correct value during the simulation. However, temperature and pressure have the correct values, meaning an operation temperature of 235 °C (508 K) like in production settings.

For exhaustion and walls, it was necessary to define temperature as a condition. In fact, there is any possibility to know the real values. Thus, the value presented in Table 15 is an approximation.

The gauge is frequently used to measure the pressure difference between a system and its surrounding atmosphere. The relation between this pressure and the gauge pressure can be expressed by Equation (7).

$$p_g = p_s - p_{atm} \quad (7)$$

Where  $p_g$  is the gauge pressure,  $p_s$  the system pressure and  $p_{atm}$  the atmospheric pressure. In fact, gauge pressure is the relation between the pressure and the atmospheric pressure.

For pressures above atmospheric pressure, the gauge has positive value, for pressures below it, gauge has negative value. Analyzing the gauge pressure of the exhaustion presented in Table 15, this condition has a negative value, standing for the hypothesis that the oven is under pressure.

To get the simulation complete, it was needed to design the fabric, since it has movement and it will directly interfere in the air movement inside the oven and its temperature. The fabric was considered to be a wall with a specific thickness and porosity according with the Nylon material to simulate the process as precise as possible.

In fact, the fabric inside the oven follows a path which is not in the same direction all the way. Initially the fabric goes up and then the heat treatment ends when the fabric reaches the bottom of the oven in the opposite way. Thereby, the fabric was designed to allowing set up translational velocity in different directions (up and down) according with what actual happen. The fabric conditions in simulation are presented in Table 16.

Table 16. Summary of the fabric conditions.

Conditions	Fabric
Type	Symmetry
Temperature /K	298
Pressure /Pa	101 325
Velocity /m-s	1.90*

\* Round values to be confidential information.

The velocity can get positive or negative values according with the direction of the fabric. Although the setting value for temperature was 298 K, it was just the initial estimation, because during the process the fabric will heating and adjusting this value. It was assumed that fabric was at ambience temperature, 20 °C and at atmospheric pressure, 101 325 Pa.

#### 4.4.4 Demonstrations

The simulation was executed in steady-state regime until converging and then it ran in transient mode. Transient regime is a system status which is changing from one steady-state regime to another, being dynamic. To accomplish the run calculation, a dimensionless number must be calculated, the Courant number,  $C$  described in Equation (8) in order to know the time step used in transient regime.

$$C = \frac{v_{max} \cdot \Delta t}{\Delta x} = 1 \quad (8)$$

Where  $v_{max}$  is the maximum magnitude of the velocity,  $\Delta t$  the time step and  $\Delta x$  the length interval. The time step obtained from Equation (8) was 0.0001 s. For each time step was defined a maximum of iterations, being them 100 iterations.

When a simulation like this one is executed, the intention is to run it during a long period of time and analyzing the results with a certain periodicity, observing a results evolution according with elapsed time. In fact, this simulation took too long, even in 2D, which only allowed to have results for 0.2 s, extremely short time in industry environment. One of the proposed future works is to run the simulation more time and to analyze the results evolution. Although the reduced simulation time is possible to have conclusions.

The uniformity of the temperature distribution inside the oven's chamber is one of the main goals of a correct oven design to ensure products with required properties.

Figure 22 shows the temperature distribution inside the simulated oven. Starting with the top of it, a decrease of temperature is observed surrounding the exhaustion exit. It is also noticeable the air that come inside through the fabric outlet and inlet slits go directly to the exhaustion stream, not influencing the rest of heat air streams. According with legend, the temperature in this zone is situated in a range from 20 °C (outside ambience temperature) to 192 °C. A hot stream from jet boxes is also observed by the two sides of the exhaustion with around 192 to 214 °C, temperature that air surrounding jet boxes also have. Although impinging air jets are at 235 °C (color red in scale), it is acceptable not exist any zone at that temperature, justified by the heat transfer not only to fabric but also to around air. The rest of the oven is at a temperature between 171 and 192 °C, being cooler next to walls. An interesting fact is what happen by the bottom of the oven, there is an accumulation of hot air at the same temperature than in jet boxes zone. Since the fabric gets in by the bottom, it is important to have a hotter zone to overcome the low temperature of the fabric.



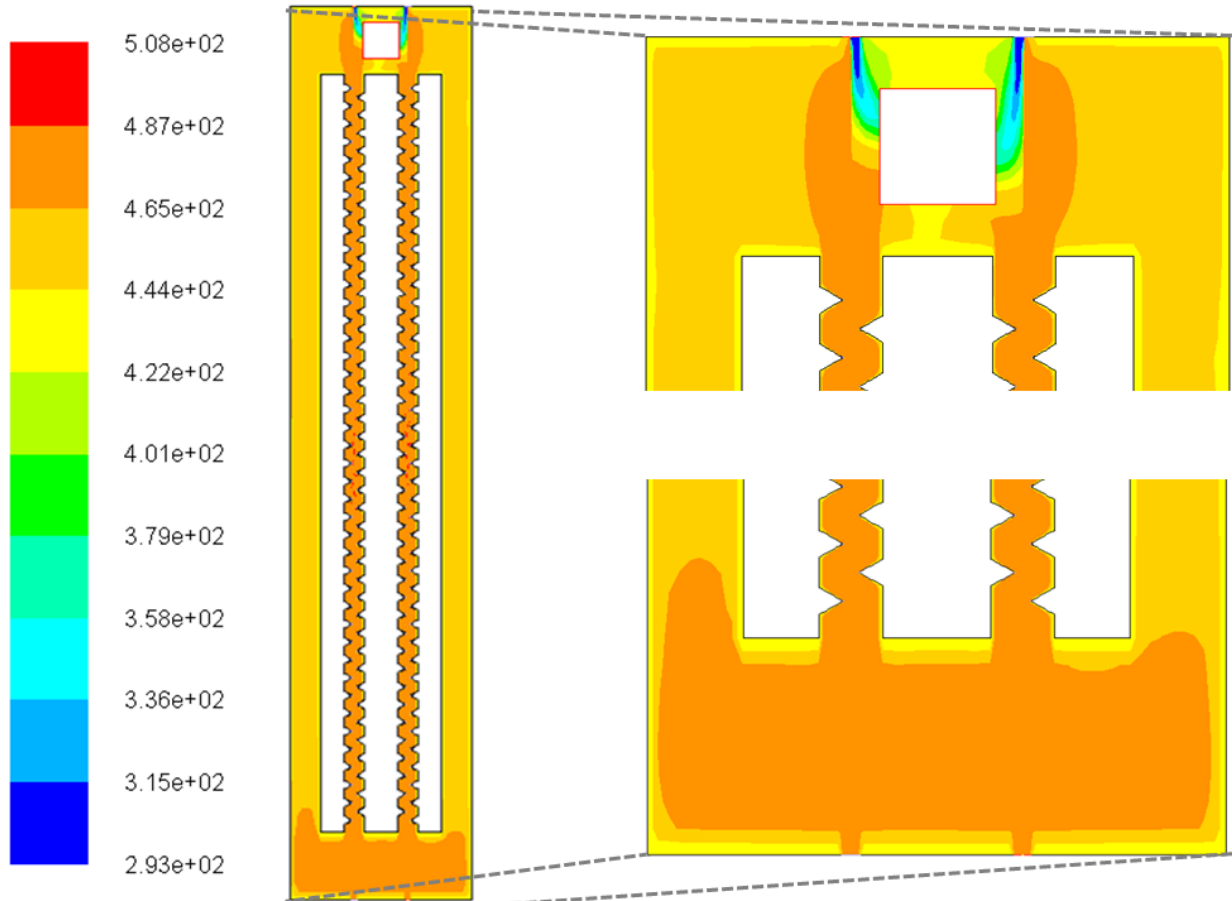


Figure 22. Contours of Static Temperature (K) inside the studied oven.

Regarding to pressure distribution inside the oven, Figure 23 is a schematic representation of it. Analyzing the legend is noticeable that all presented values are below pressure ambience,  $1 \text{ atm} \approx 10^5 \text{ Pa}$ , which shows that ovens are under pressure. In fact, it is possible to observe that exhaustion exit is lineate by red lines, color that corresponding to the higher pressure value in legend. This can be justified by the connection to exit, which is at ambience pressure. Looking to the central zone of the oven, where jet boxes are represented, it can be seen a color gradient. In the middle is where higher pressure is reached, decreasing as it goes to extremities until getting the lower pressure, which surrounds the rest of the oven. This can be justified by the way ventilation works. The two ventilators are positioned in the half height of the oven, feeding a chamber that will distribute the air for up and down in jet boxes. The air fed to the chamber has higher pressure but as it goes distributed

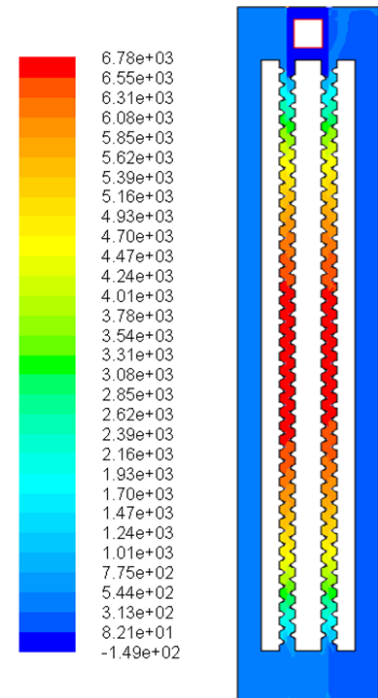


Figure 23. Contours of Total Pressure (Pa) inside the studied oven.

there is a pressure drop. The zone with red color corresponds to the location where the air is directly provided to jet boxes, although the rest of jet boxes has air with a decrease of pressure.

Temperature and pressure distribution are important to study and to get conclusions, however the velocity of the air, its preferential paths and dead zones are also relevant to completely understand what really happens inside the oven.

In Figure 24 is presented the contours of velocity magnitude of entire oven allowing to conclude the existence of dead zones in the top and the bottom, supported by the fabric inlet and outlet slits where air with velocity comes in entrained by the fabric. In dead zones the velocity gamma is low when compared to jet boxes area. Regarding to exhaustion exit, it is seen several paths in that direction, which is understandable.

The details of jet boxes are zoomed in Figure 25. It can be observed the high velocities are in the jet boxes orifices. In fact, the air gets out of the jet box with maximum velocity and until shock with fabric it suffered a decrease, building a velocity profile. In that profile is also possible to detect 'velocity waves' resulted by the bumping with fabric, dispersing to above and below the origin of the air and creating convection streams and small dead zones between jet boxes.

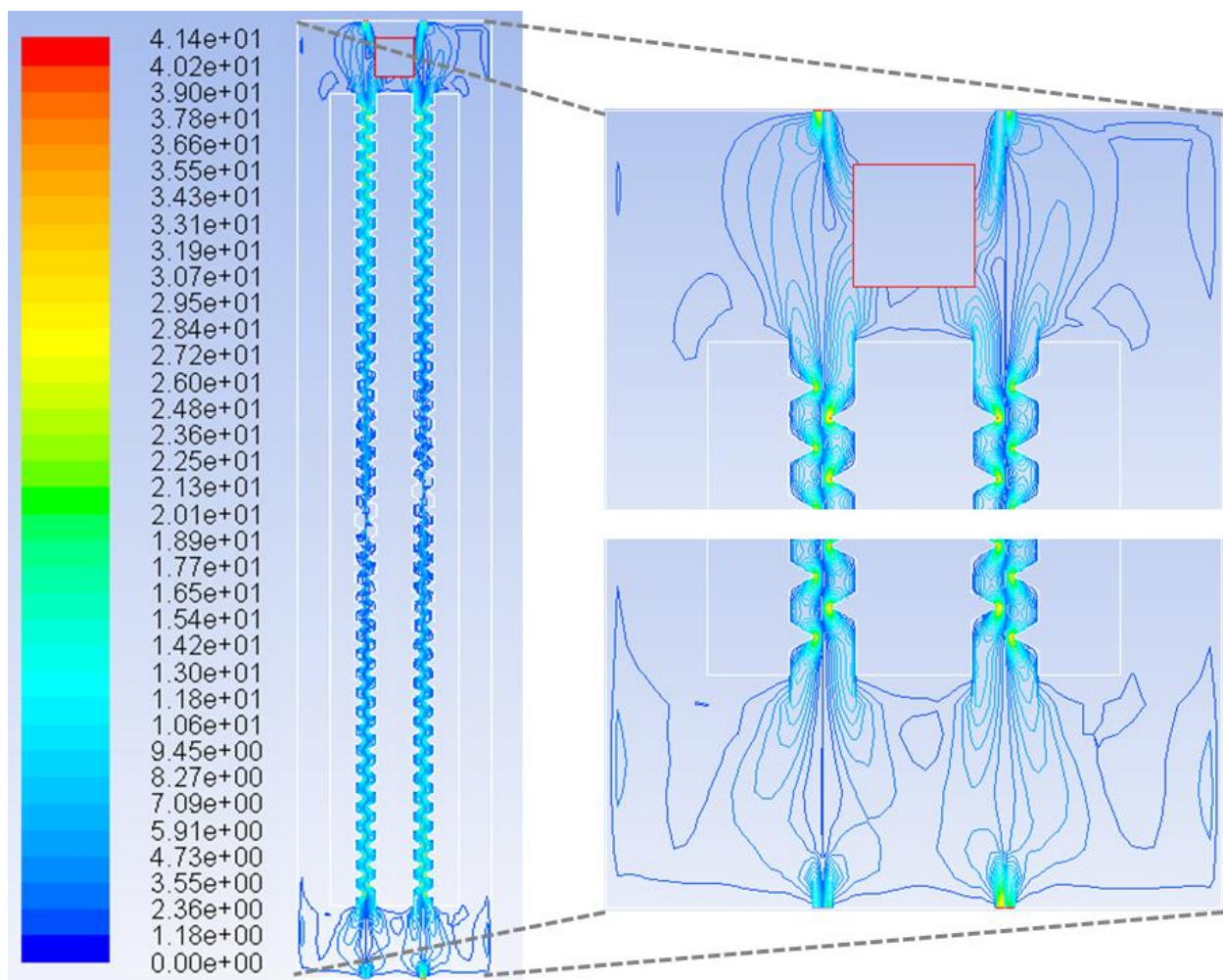


Figure 24. Contours of Velocity Magnitude ( $\text{m}\cdot\text{s}^{-1}$ ) inside the studied oven.

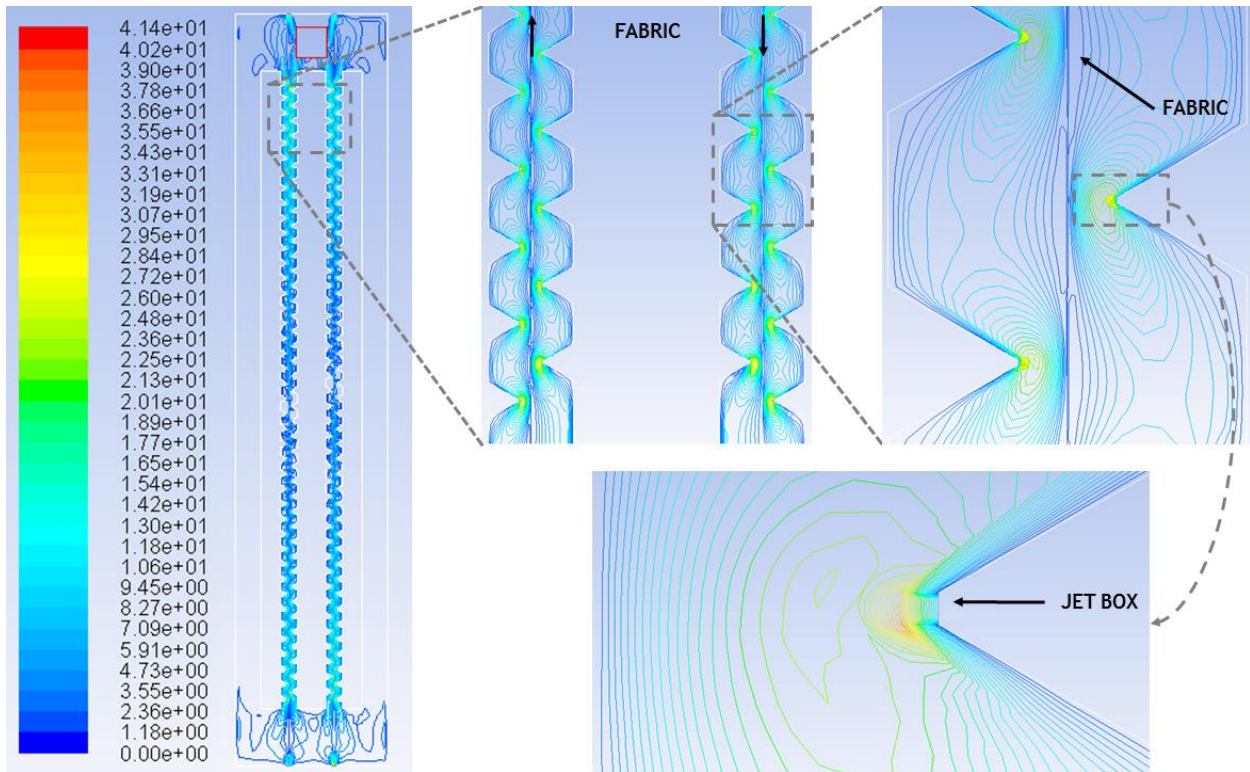


Figure 25. Contours of Velocity Magnitude ( $\text{m} \cdot \text{s}^{-1}$ ) in detail inside the studied oven.

## 5 Conclusions

The main focus of this thesis was the optimization of tyre reinforcement dipping process. Although the process is considered complex, this work studies the role of the temperature of the dipping ovens. For that, 3 different approaches were followed. This work is a great innovation from what the company did before and produced relevant results.

Starting with industrial dipping process, improvements were successfully accomplished for a Nylon material, optimizing the temperature distribution inside the ovens and reducing the operation temperature in 3 °C in 4 of the 7 used ovens. Further and deeper studies must be performed to conclude about the associated costs to this upgrading. In fact, this improvement was made for only one type of Nylon's fabric. It is believed that it is possible to optimize more materials, not only for Nylon's, but also for Aramid, Polyester and Rayon.

Regarding to laboratory work, after a set of studies being performed, it was possible to conclude about the inadapability of the actual scale-down model for at least 3 different types of Nylon's fabric. Although laboratory operation conditions were achieved to replace the previous ones, verification to all existing materials must be done.

Finally, the developed CFD tool allow to conclude about the distribution of hot air inside the ovens and to observe that same pressure varies according with a gradient. Regarding to velocity magnitude of the air, dead zones in top and bottom are observed and velocity profile at jet boxes exit, where 'velocity waves' can be seen too. Although this simulation enables an inside look of the ovens behavior, to achieve more conclusions the simulator should be improved.

## 6 Project Assessment

### 6.1 Accomplished Objectives

The main goal of this thesis was to optimize the dipping process of the tyre reinforcements. It was taken 3 different paths tapering the same goal, being them the industrial process, the laboratory area and a simulation tool.

Regarding to the industrial field, the process was optimized for one of the existing Nylon materials. In laboratory area, it was reassessed the scale-down model for three different Nylon materials, concluding its inadaptability, and it was suggested new operation conditions. The last contribution was a simulation tool development that allows understanding the hot air behavior inside the ovens of the industrial process.

### 6.2 Limitations and Future Work

Working in 3 different areas, with several and complex tasks and different work environments, made time flies. The major limitation of this work was undoubtedly the time. Five months to fully accomplish the proposed objectives was not enough. Thus, this thesis is considered to be a kick-start work for a complete and successfully improvement of all mentioned fields where several paths can be taken to achieve it.

Beginning with the industrial dipping unit, the improvement was made only for Nylon C. It is believed that more industrial production materials must be upgraded. Regarding with production unit, but not directly with the process, there is a suggestion that could positively change the radiation transfer inside the ovens. Coating the inside walls with a black paint to increase the emissivity and decrease possible losses. However, finding an ink with the necessary properties shall be a limitation.

In fact, the laboratory work allows concluding about the inadaptability of the practice model to the studied materials. In future works, it is important to verify the accuracy of the current model for the rest of the existing textile materials.

The need for more efficient ovens leading to a rising energy costs is a demanding study nowadays. This will require a deeper understanding of how to manipulate the ovens design and the operation conditions to give energy efficiency whilst maintaining the quality of the product. CFD is increasingly being used to improve the efficiency of baking processes. However, the same are not verified for textile area, which could be an interesting area for a future work. Upgrade the developed tool to 3D and running the simulation with more iteration number corresponding to a larger period of time is a suggestion of start. Another path that can be taken is acquired about the adaptability of the actual design and also the possibility of dependence

on air temperature with relation to distance beneath the jet boxes due to the strong turbulent mixing within the oven. Moreover, before using this tool for optimization, since the air flows within forced convection ovens are highly turbulent in the jet boxes region, it is important to validate CFD predictions against experimental data.

### **6.3 Final Assessment**

Challenging, enriching and rewarding since day one, that is how I describe this thesis. Having as a master thesis a theme that has a different approach than previous works, made the project even more attractive and enthusiast, even under the inherent ups and downs. At the end of this hard work months, I feel quite a sense of accomplishment. C-ITA turned out to be a great partner, providing industry guidance essential to this working experience.

## 7 References

- [1] “Continental,” 4 March 2016. [Online]. Available: [http://www.continental-corporation.com/www/portal\\_com\\_en/themes/continental/](http://www.continental-corporation.com/www/portal_com_en/themes/continental/).
- [2] E. Correia, “Dipped and greige cords load-elongation behaviour made of nylon yarn,” 2013.
- [3] R. Silva, “Scale-up from Laboratory Dipping Unit,” 2011.
- [4] T. Moura, “Scale Up from Laboratory Dipping Unit (LDU) into Production Dipping Units (PDU) of process specifications for dipping tire cord fabrics and cables,” 2012.
- [5] U. National Highway Traffic Safety Administration, “The Pneumatic Tire,” February 2006. [Online]. Available: <http://www.nhtsa.gov/Vehicle+Safety/Tires>. [Accessed 6 March 2016].
- [6] J. Y. Wong, “Mechanics of Pneumatic Tires,” in *Theory of Ground Vehicles*.
- [7] “Tyre Basics Passenger Car Tyres,” 2012. [Online]. Available: [http://www.continental-corporation.com/www/portal\\_com\\_en/themes/continental/](http://www.continental-corporation.com/www/portal_com_en/themes/continental/). [Acedido em 4 March 2016].
- [8] W. Callister and D. Rethwisch, *Materials Science and Engineering*, 2009, p. 614.
- [9] H.-K. Rouette, *Encyclopedia of Textile Finishing*, 2000, pp. 792, 2448.
- [10] R. Falcão, “Influence of conversion settings on dynamic properties of polyamide fibres for tyre cords,” 2015.
- [11] [Online]. Available: <http://www.swicofil.com/companyinfo/manualtwistdirection.html>. [Acedido em 10 February 2016].
- [12] W. B. Wennekes, “Adhesion of RFL-treated cords to rubber : new insights into interfacial phenomena,” 2008.
- [13] D. Pinto, “Hybrid Technology: A simulation model to predict optimized textile reinforcements properties,” 2013.
- [14] BISFA, “Terminology of man-made fibers,” 2009.
- [15] A. Freitas, “Correlation between the reinforcement-to-rubber,” 2012.

- [16] BENNINGER, "Tire Cord - Treatment Lines and Technology".
- [17] F. Magalhães, "Notes of Process Dynamics and Control course," 2015.
- [18] L. K. W. Nazih K. Shamas, Water Supply and Wastewater Removal, 2011.
- [19] D. Kumar, Six Sigma Best Practices: A Guide to Business Process Excellence for Diverse Industries, 2006.
- [20] Z. Khatir, J. Paton, H. Thompson, N. Kapur, V. Tropov and M. Lawes, "Computational fluid dynamics (CFD) investigation of air flow and temperature," *Applied Energy*, p. 89-96, 2012.
- [21] M. Boulet, B. Marcos, M. Dostie e C. Moresoli, "CFD modeling of heat transfer and flow field in a bakery pilot oven," *Journal of Food Engineering*, vol. 97, p. 393-402, 2010.
- [22] J. M. Campos, Notas para o Estudo da Mecânica dos Flúidos, 2012, p. 213.
- [23] Z. Khatir, H. Thompson, N. Kapur, V. Toropov e J. Paton, "Multi-objective Computational Fluid Dynamics (CFD) design," *Applied Thermal Engineering*, vol. 60, pp. 480-486, 2013.
- [24] Z. Khatir, J. Paton, H. Thompson, N. Kapur e V. Toropov, "Optimisation of the energy efficiency of bread-baking ovens," *Applied Energy*, vol. 112, p. 918-927, 2013.
- [25] ANSYS, "ANSYS Fluent Theory Guide," 2013.
- [26] T. E. ToolBox, "Air Properties," [Online]. Available: [http://www.engineeringtoolbox.com/air-properties-d\\_156.html](http://www.engineeringtoolbox.com/air-properties-d_156.html). [Acedido em 8 May 2016].
- [27] "AZO Materials," [Online]. Available: <http://www.azom.com/article.aspx?ArticleID=477>. [Acedido em 8 May 2016].
- [28] "Professional Plastics," [Online]. Available: <http://www.professionalplastics.com/>. [Acedido em 8 May 2016].
- [29] "COMSOL - Multiphysics Cyclopedia," [Online]. Available: <https://www.comsol.pt/multiphysics/boussinesq-approximation>. [Accessed 8 May 2016].
- [30] "Fluent Incorporated," [Online]. Available: <http://jullio.pe.kr/fluent6.1/help/html/ug/node512.htm> . [Accessed 3 March 2016].



## Annex 1 Production Dipping Unit



Figure 26. Supply of greige fabric and the centre driven let-off station.



Figure 27. First fabric accumulator.

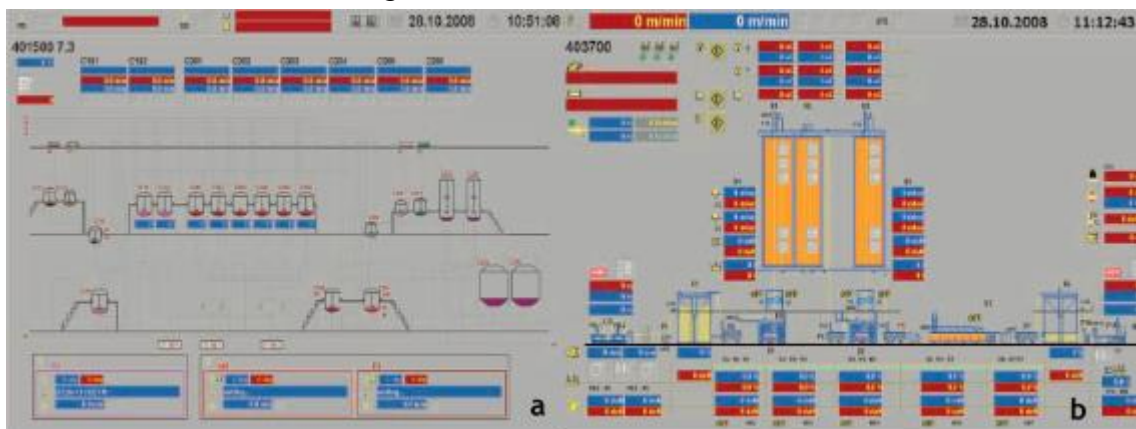


Figure 28. HMI software for a) Dip mixing and b) Fabric Treating Line [16].



Figure 29. Dip stations.



Figure 30. Vacuum system.



Figure 31. Pull roll stands.



Figure 32. Path of the fabric between Oven 4 and Oven 5.



Figure 33. Burner with bottom and top ventilations.



Figure 34. Exhaust fan.



Figure 35. Guidance devices.



Figure 36. Fabric getting in and out of bottom of the ovens.



Figure 37. Inside view of the Oven 5 with the jet boxes and fabric on movement and one of the temperature measure device.

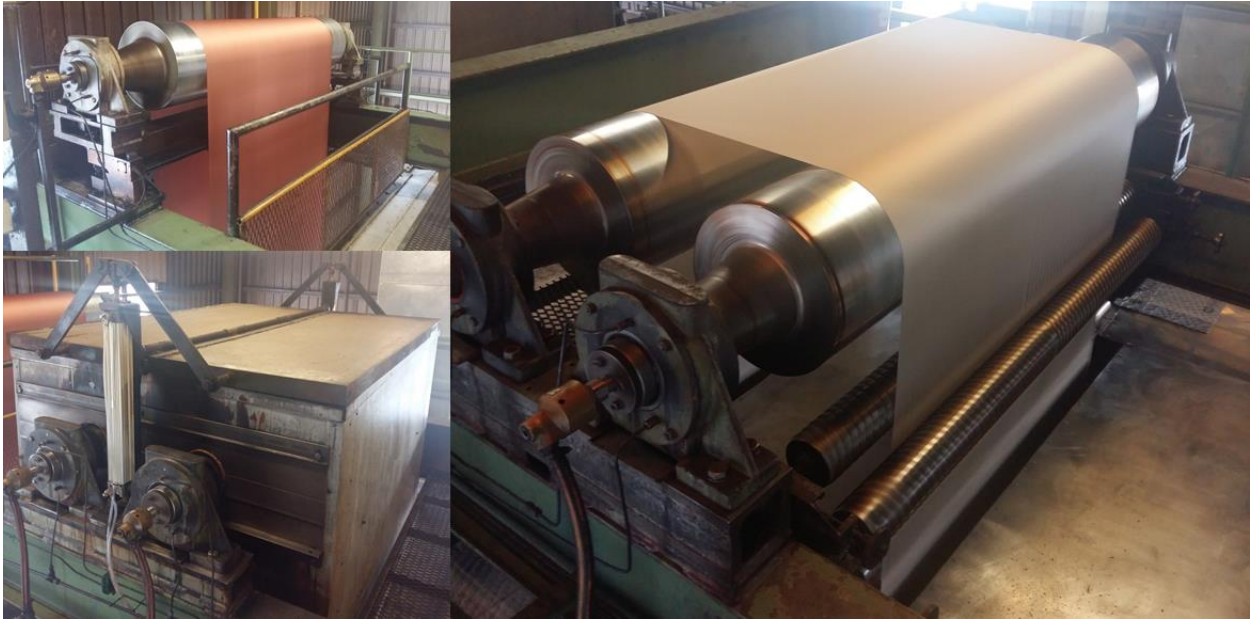


Figure 38. Top of the ovens, which can have a campanula or not.

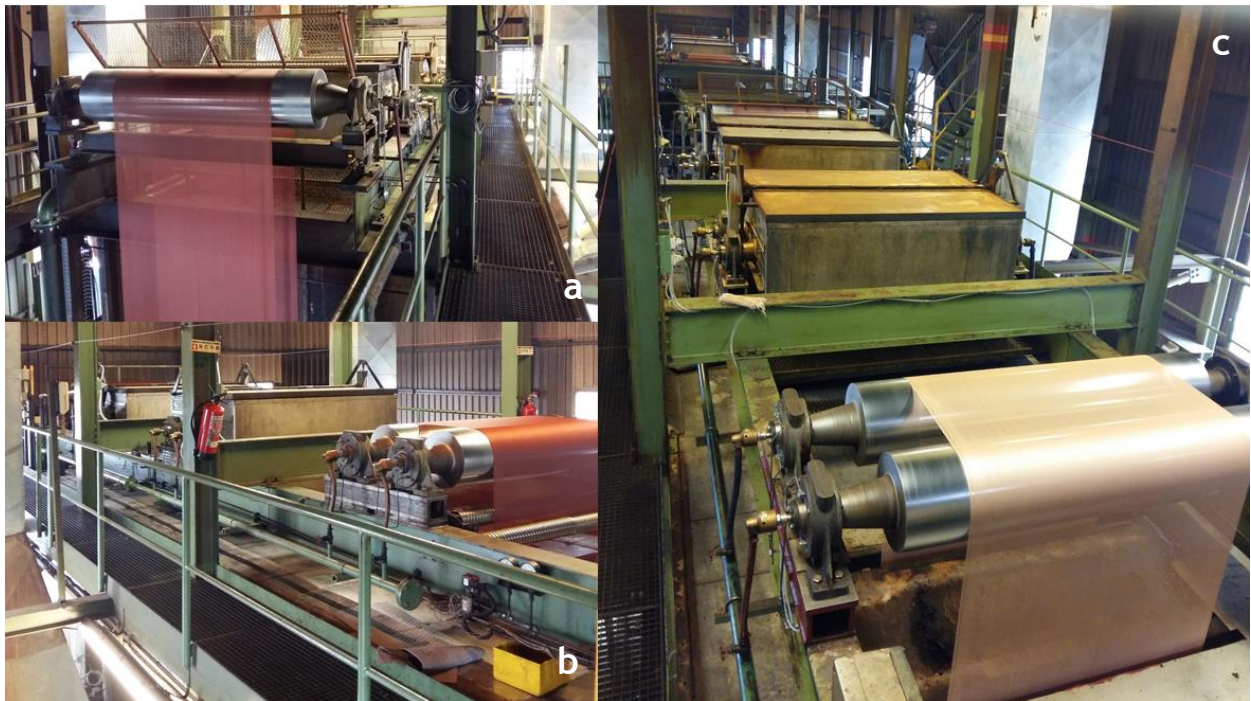


Figure 39. Top of a) Ovens 1 to 4 b) Oven 5 to 7 c) and a global vision of all of them.



Figure 40. Second fabric accumulator and centre driven wind-up station.

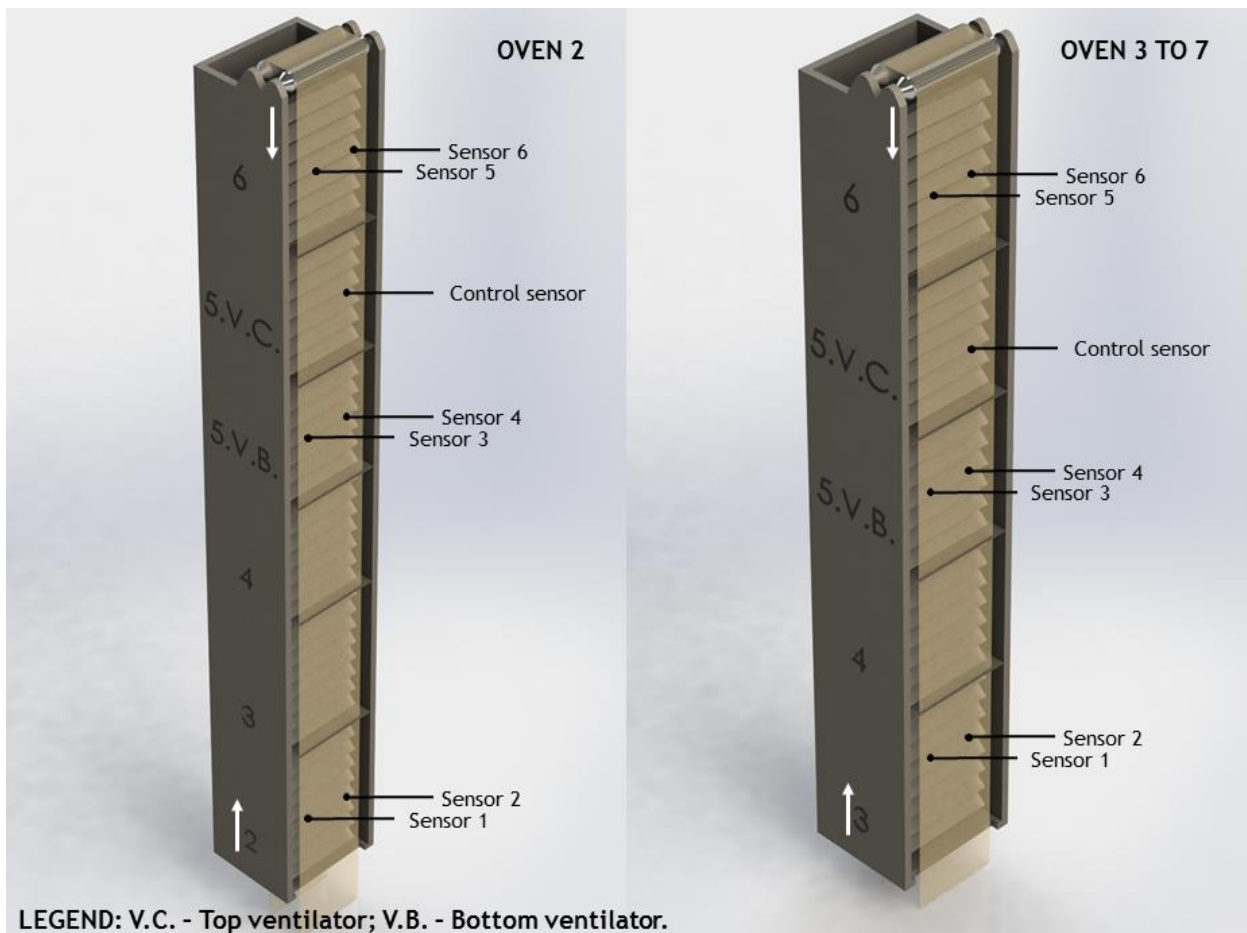


Figure 41. Oven's section with temperature sensors position for Oven 2 and Oven 3 to 7.

## Annex 2 Product Specifications

### A.2.1 Nylons

Table 17. Product specifications for the studied Nylons.

Properties	Specification Nylon A	Specification Nylon B	Specification Nylon C
Breaking Force /N	150 ± 30	150 ± 20	220 ± 40
Elong. at break /%	20 ± 5	-	20 ± 5
FASE 2% /N	12 ± 5	12 ± 5	19 ± 5
FASE 4% /N	20 ± 5	20 ± 5	30 ± 6
FASE 8% /N	45 ± 6	-	74 ± 9
FASE 12% /N	90 ± 12	-	145 ± 20
Shrinkage 180 °C /%	4.50 ± 1	4.50 ± 2	4.80 ± 1
Residual Shrinkage /%	2 ± 1	2 ± 2	2.40 ± 1
Shrinkage Force /N	-	-	7.50 ± 2



# Annex 3 Data Analysis

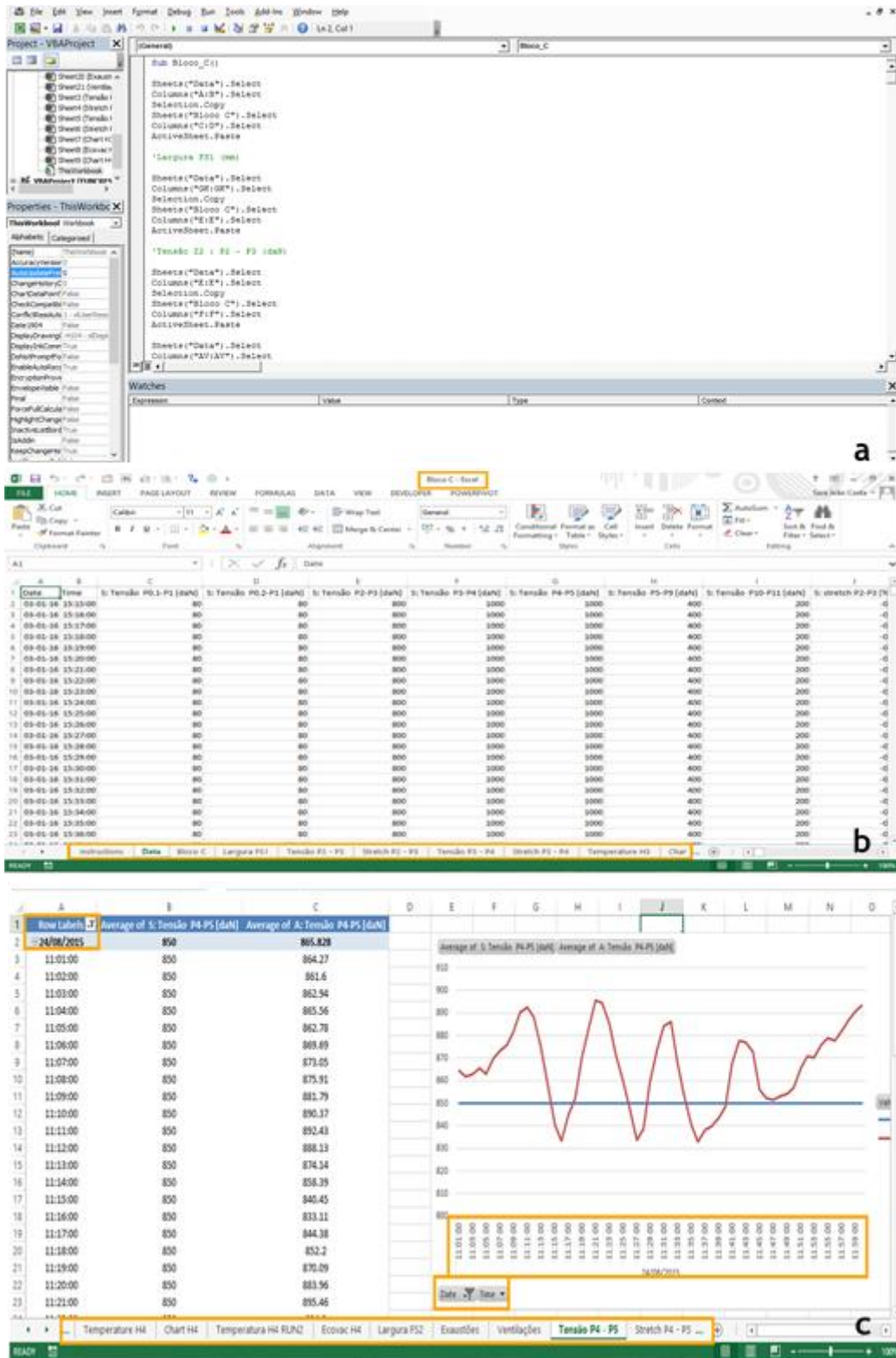


Figure 42. Created tool using as example block C a) Visual Basic programming - Macros; b) tabs according with the variables presented in that block; and c) data graphically represented filtered by date and hour.

## Annex 4 Economic Analysis

In view of economically analyze the impact of PDU changes, it was made an economic balance. The equations used for that are followed described.

### A.4.1 Natural Gas

Starting to calculate the gas consumption, the Equation (9) describes that.

$$\text{Gas consumption (m}^3\text{/h)} = \frac{\Delta \text{ Measured values (m}^3\text{)} \times 60 \text{ (min)}}{\Delta t \text{ (min)} \times fc} \quad (9)$$

Where  $\Delta \text{ Measured values}$  is the difference between the final and the initial value of natural gas presented in counter,  $\Delta t$  is the time interval between measures and  $fc$  is the correction factor.

Then, it was calculated the Specific consumption according with Equation (10).

$$\begin{aligned} \text{Specific consumption (m}^3\text{/kg)} \\ = \frac{\text{Gas consumption (m}^3\text{/h)}}{60 \times \text{Specific weight of roll (kg/m)} \times \text{Operating velocity (m/min)}} \end{aligned} \quad (10)$$

Where the *Gas consumption* is calculated in Equation (9), the *Specific weight of roll* is calculated by dividing the roll weight to the total length of that roll and the *Operating velocity* the velocity that Zell unit operates with Nylon C.

According with Equation (11) is possible to convert the Specific consumption to a different unit which will further help in calculations.

$$\text{Specific consumption (kWh/kg)} = \text{Specific consumption (m}^3\text{/kg)} \times H_{HV} \text{ (kWh. m}^3\text{)} \quad (11)$$

Where *Specific consumption* is calculated in Equation (10) and the  $H_{HV}$  is the Higher Heating Value.

Finally, it is possible to calculate the price per produced tone by Equation (12).

$$\text{€/ton} = \text{Specific consumption (kWh/kg)} \times 1000 \times \text{€/kWh} \quad (12)$$

Where *Specific consumption* (kWh/kg) is calculated in Equation (11) and €/kWh is the average of the practiced price during the last year.

### A.4.2 Energy

Starting to calculate the energy consumption, the Equation (13) describes that.

$$\text{Electricity consumption (kW)} = \frac{\Delta \text{ Measured values (kW)} \times 60 \text{ (min)}}{\Delta t \text{ (min)}} \quad (13)$$

Where  $\Delta$  *Measured values* is the difference between the final and the initial value of energy consumption presented in counter and  $\Delta t$  is the time interval between measures.

Then, it was calculated the Specific consumption according with Equation (14).

$$\begin{aligned} & \text{Specific consumption (kWh/kg)} \\ &= \frac{\text{Electricity consumption (kW)}}{60 \times \text{Specific weight of roll (kg/m)} \times \text{Operating velocity (m/min)}} \end{aligned} \quad (14)$$

Where the *Electricity consumption* is calculated in Equation (13), the *Specific weight of roll* is calculated by dividing the roll weight to the total length of that roll and the *Operating velocity* the velocity that *Zell* unit operates with Nylon C.

Finally, it is possible to calculate the price per produced tone by Equation (15).

$$\text{€/ton} = \text{Specific consumption (kWh/kg)} \times 1000 \times \text{€/kWh} \quad (15)$$

Where *Specific consumption* (kWh/kg) is calculated in Equation (14) and €/kWh is the average of the practiced price during the last year.

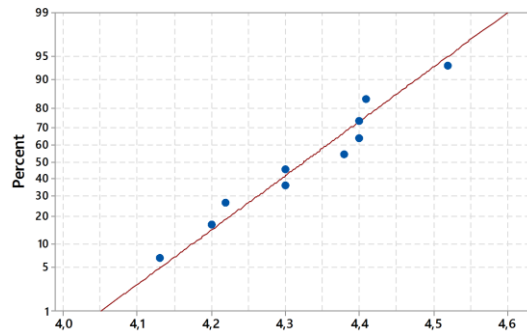
# Annex 5 Statistical Analysis

Table 18. Summary table of statistical analysis for Nylon A.

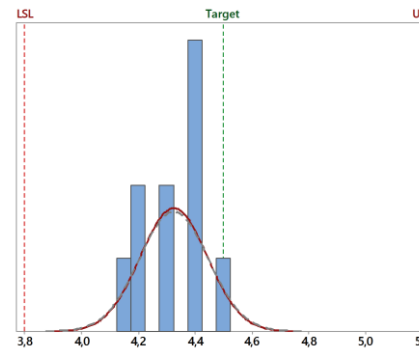
## Nylon A

Sample  
Shrinkage

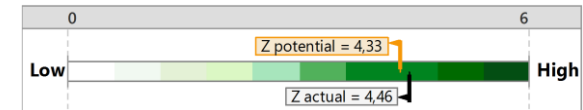
Normality Plot



Actual Capability Histogram

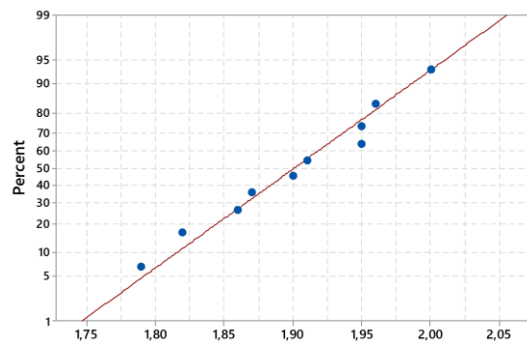


Total N 10  
C<sub>p</sub> 1.92  
C<sub>pk</sub> 1.44  
P-value 0.568

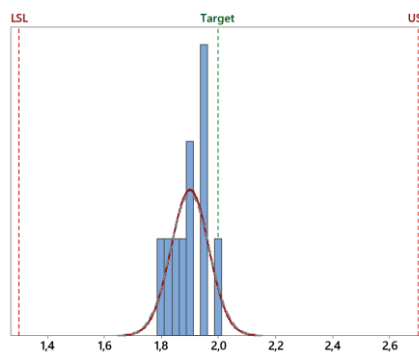


Residual

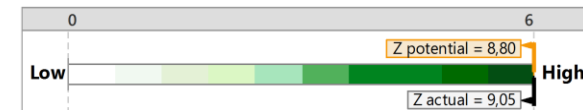
Normality Plot



Actual Capability Histogram

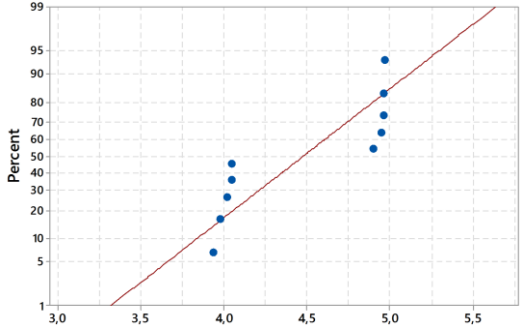


Total N 10  
C<sub>p</sub> 3.42  
C<sub>pk</sub> 2.93  
P-value 0.852

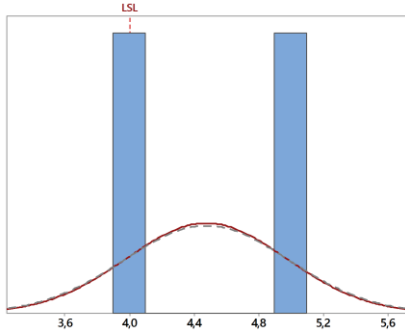


**Shrink-force**

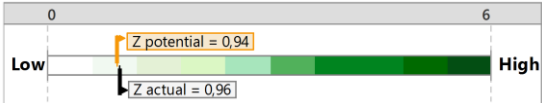
**Normality Plot**



**Actual Capability Histogram**



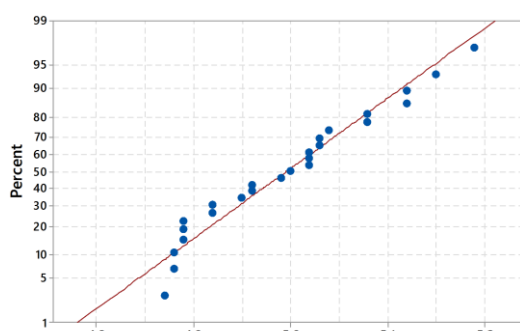
Total N 10  
 $C_p$  -  
 $C_{pk}$  0.31  
 P-value < 0.005



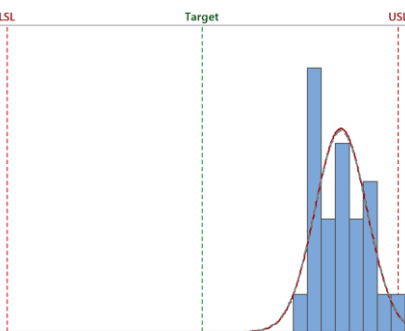
**PI Settings**

**Shrinkage**

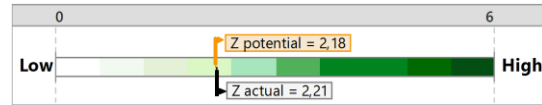
**Normality Plot**



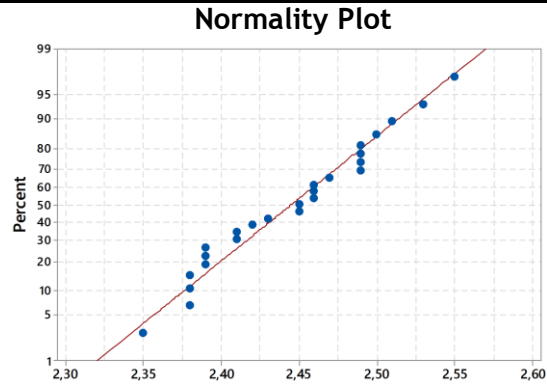
**Actual Capability Histogram**



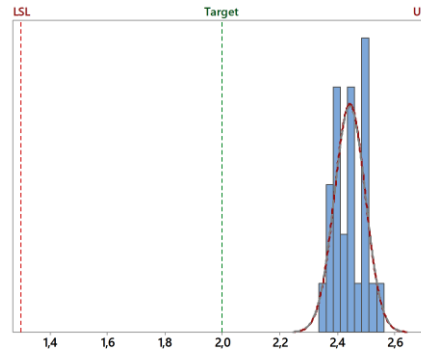
Total N 25  
 $C_p$  2.50  
 $C_{pk}$  0.73  
 P-value 0.292



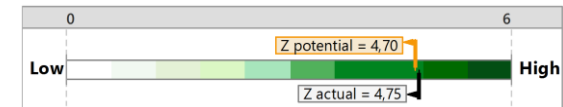
**Residual**



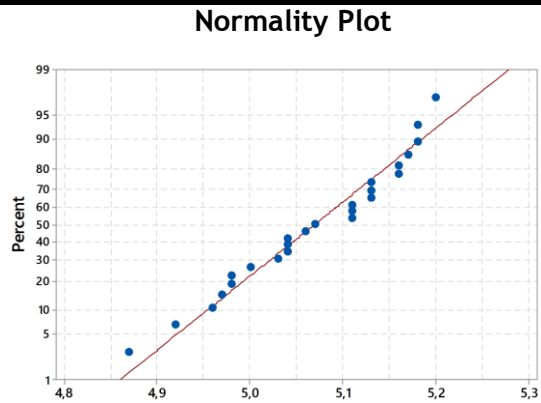
**Actual Capability Histogram**



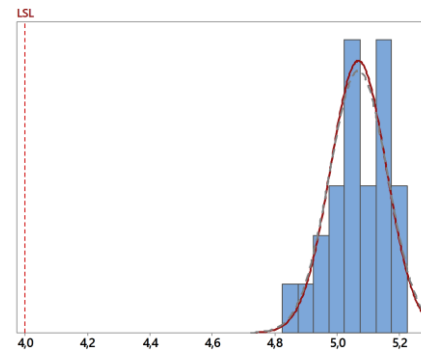
Total N 25  
 $C_p$  4.31  
 $C_{pk}$  1.57  
 P-value 0.324



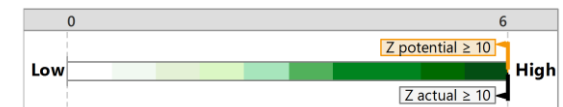
**Shrink-force**



**Actual Capability Histogram**



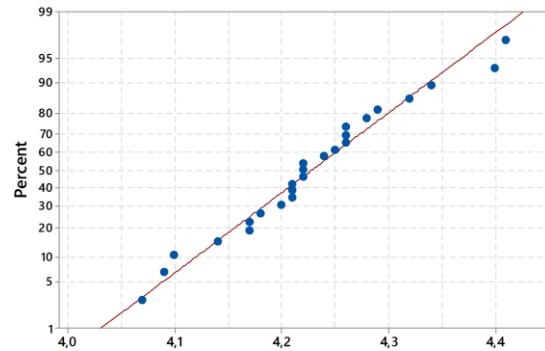
Total N 25  
 $C_p$  -  
 $C_{pk}$  3.83  
 P-value 0.325



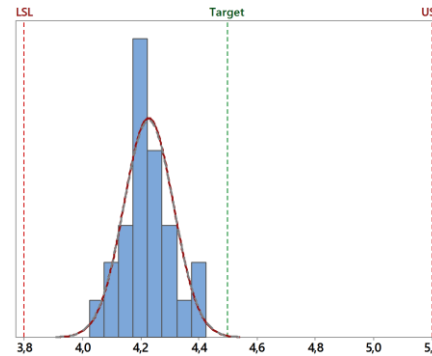
## Production Settings

### Shrinkage

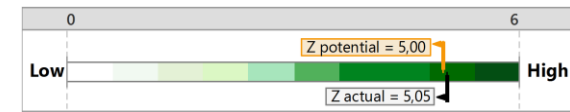
Normality Plot



Actual Capability Histogram

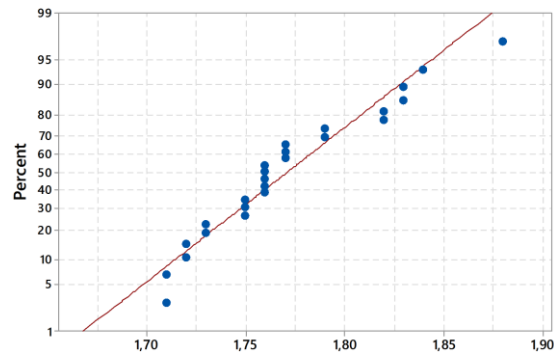


Total N 25  
 $C_p$  2.72  
 $C_{pk}$  1.67  
 P-value 0.522

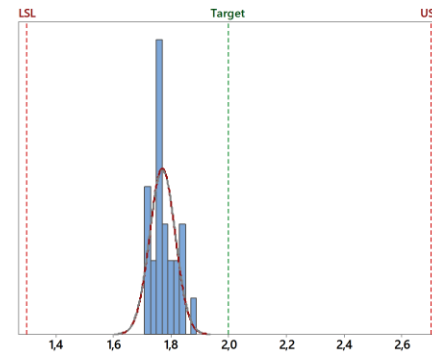


### Residual

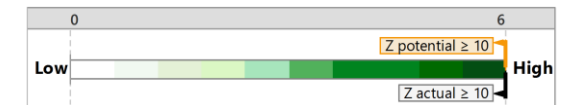
Normality Plot



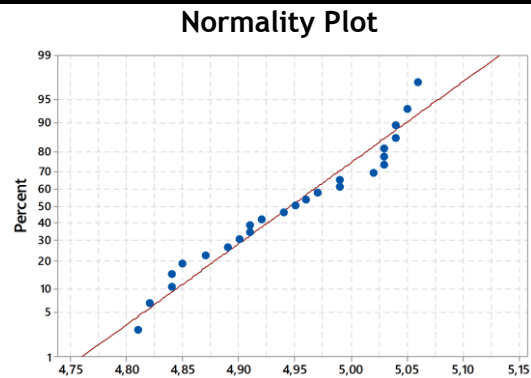
Actual Capability Histogram



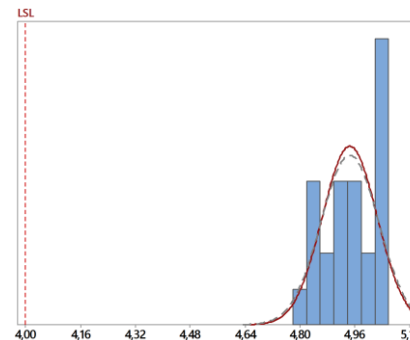
Total N 25  
 $C_p$  5.21  
 $C_{pk}$  3.51  
 P-value 0.075



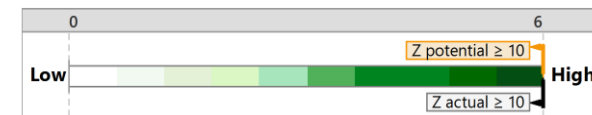
## Shrink-force



## Actual Capability Histogram



Total N	25
$C_p$	-
$C_{pk}$	3.75
P-value	0.162



Starting to analyze the results for *Sample* trial, which is the reference, it is possible to observe that the 3 presented capability graphics are in the range between the target and the lower specification limit, being what is the intended. Regarding to Process Potential Index ( $C_p$ ), Process Capability Index ( $C_{pk}$ ) and p-value, they presented values that shows that experimental trial is correctly adapted, as well the scale of how capable is the process, where shrinkage and shrink-force present high values.

On the other hand, the capability graphics for *PI Settings* trial show that results belong to the range between the target and the upper specification limit, which is not the intended. As previously said, it is preferable to be under the target than above. Considering the  $C_p$ ,  $C_{pk}$  and p-value, they also presented consistent values as also the how capable is the process graphics.

Regarding to *Production Settings* trial, which was previous concluded to be the best fit conditions, the results presented in capability graphics belong to the range between the target and the lower specification limit, like *Sample* trial. The  $C_p$ ,  $C_{pk}$  and p-value show that trial is correctly adapted, as well the scale of how capable is the process, presenting all high values of potential.

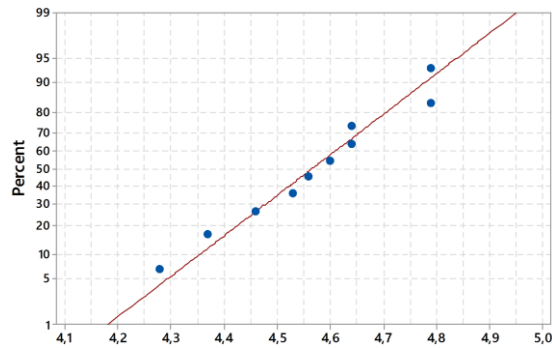


Table 19. Summary table of statistical analysis for Nylon B.

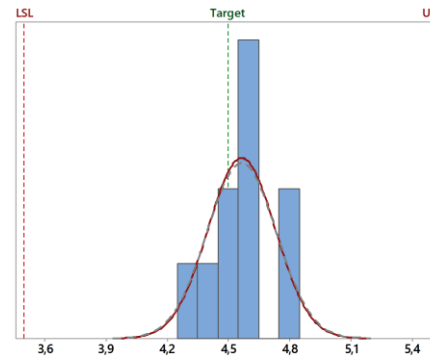
### Nylon B

#### Sample Shrinkage

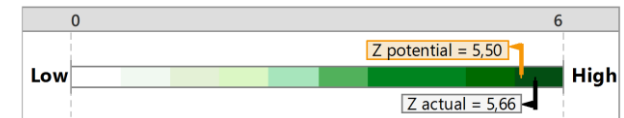
Normality Plot



Actual Capability Histogram

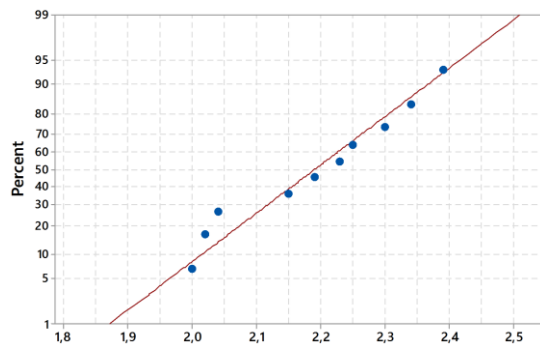


Total N 10  
 $C_p$  1.96  
 $C_{pk}$  1.83  
 P-value 0.816

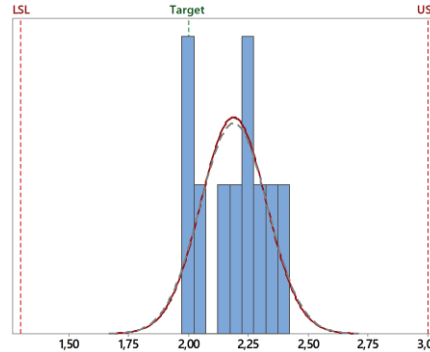


#### Residual

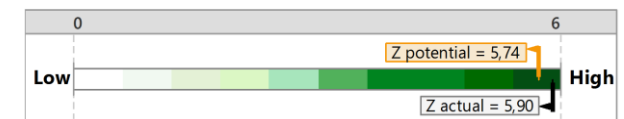
Normality Plot



Actual Capability Histogram

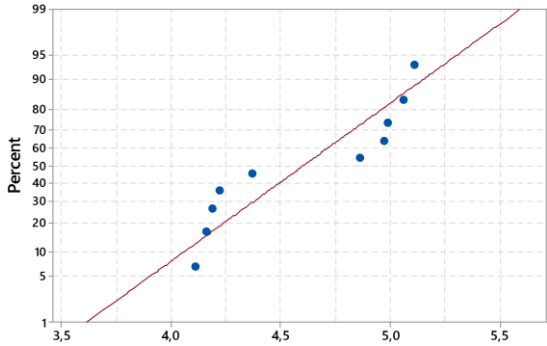


Total N 10  
 $C_p$  2.01  
 $C_{pk}$  1.91  
 P-value 0.654

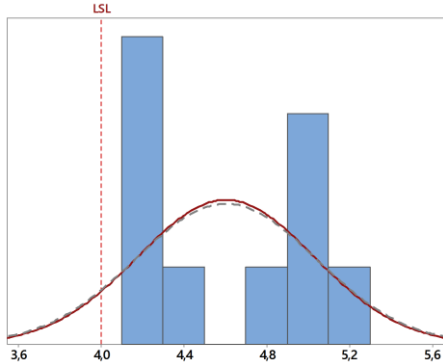


**Shrink-force**

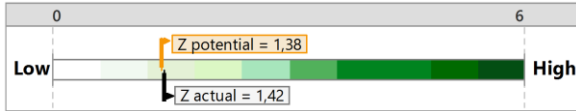
**Normality Plot**



**Actual Capability Histogram**



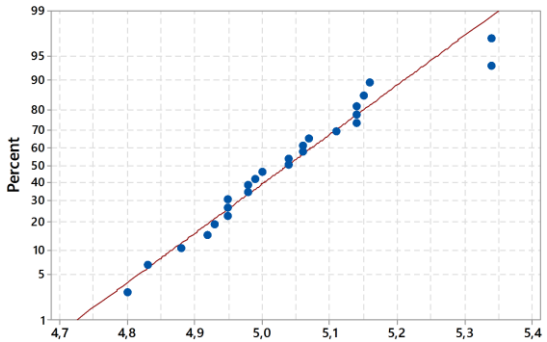
Total N 10  
 $C_p$  -  
 $C_{pk}$  0.46  
 P-value 0.023



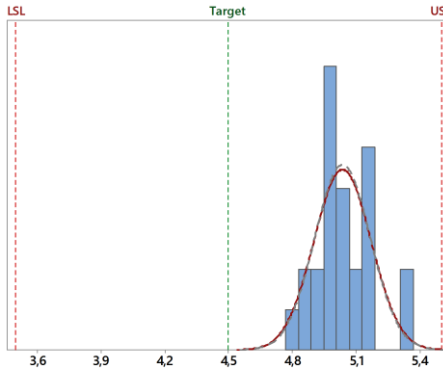
**PI Settings**

**Shrinkage**

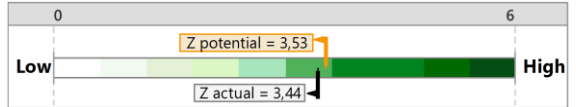
**Normality Plot**



**Actual Capability Histogram**

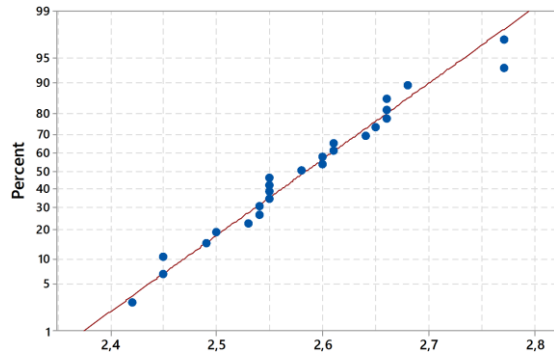


Total N 25  
 $C_p$  2.55  
 $C_{pk}$  1.18  
 P-value 0.392

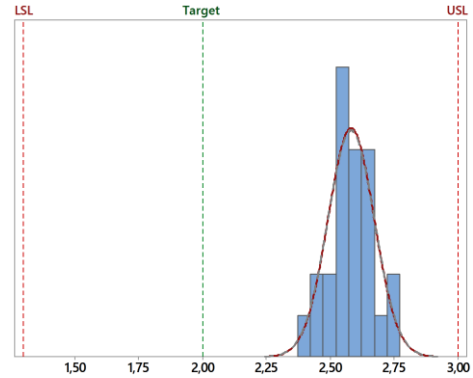


**Residual**

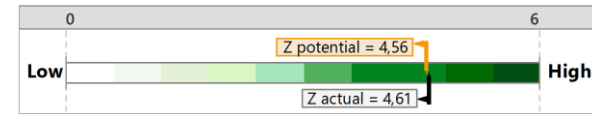
**Normality Plot**



**Actual Capability Histogram**

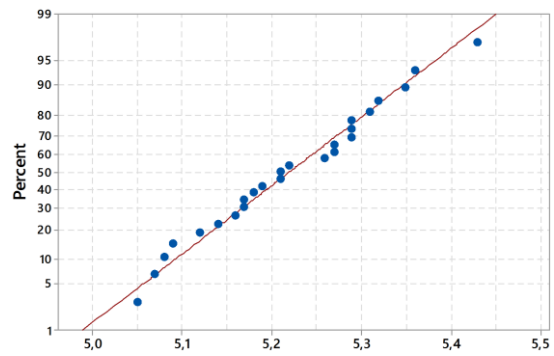


Total N 25  
 $C_p$  3.11  
 $C_{pk}$  1.52  
 P-value 0.588

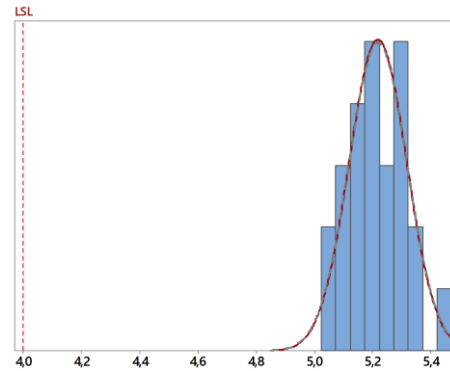


**Shrink-force**

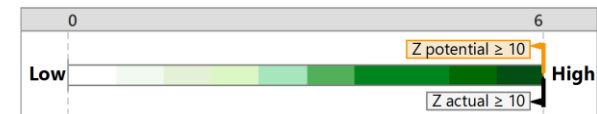
**Normality Plot**



**Actual Capability Histogram**



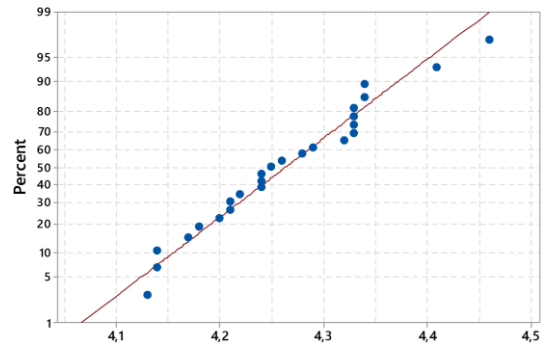
Total N 25  
 $C_p$  -  
 $C_{pk}$  4.06  
 P-value 0.864



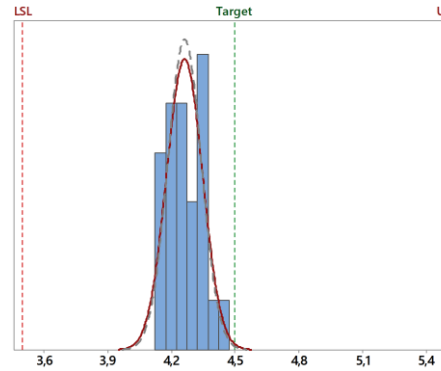
## Production Settings

### Shrinkage

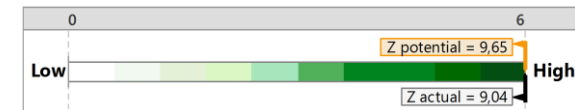
Normality Plot



Actual Capability Histogram

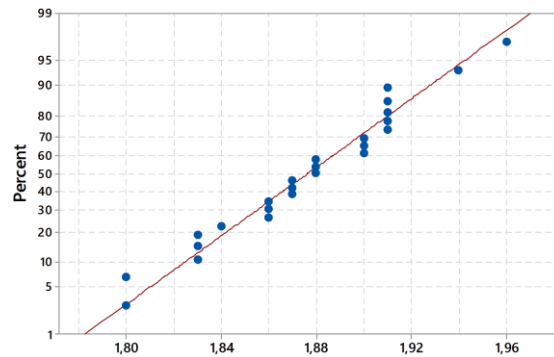


Total N 25  
 $C_p$  4.21  
 $C_{pk}$  3.22  
 P-value 0.493

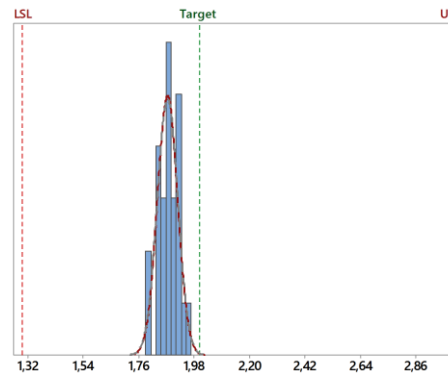


### Residual

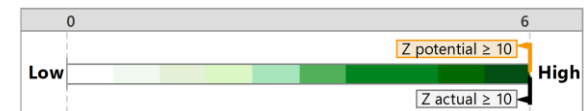
Normality Plot



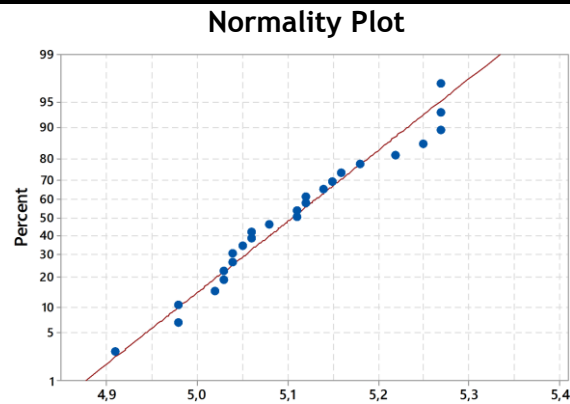
Actual Capability Histogram



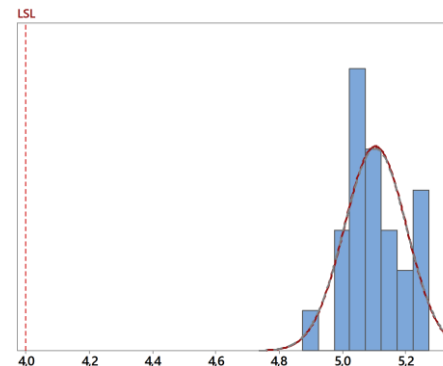
Total N 25  
 $C_p$  6.98  
 $C_{pk}$  4.73  
 P-value 0.393



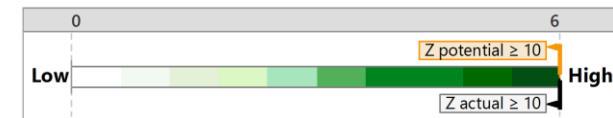
## Shrink-force



## Actual Capability Histogram



Total N	25
$C_p$	-
$C_{pk}$	3.71
P-value	0.384



Starting to analyze the results for *Sample* trial, which is the reference, it is possible to observe that the 3 presented capability graphics are in the target. Regarding to Process Potential Index ( $C_p$ ), Process Capability Index ( $C_{pk}$ ) and p-value, they presented values that shows that experimental trial is correctly adapted, as well the scale of how capable is the process, where shrinkage and shrink-force present high values.

On the other hand, the capability graphics for *PI Settings* trial show that results belong to the range between the target and the upper specification limit, which is not the intended. As previously said, it is preferable to be under the target than above. Considering the  $C_p$ ,  $C_{pk}$  and p-value, they also presented consistent values as also the how capable is the process graphics.

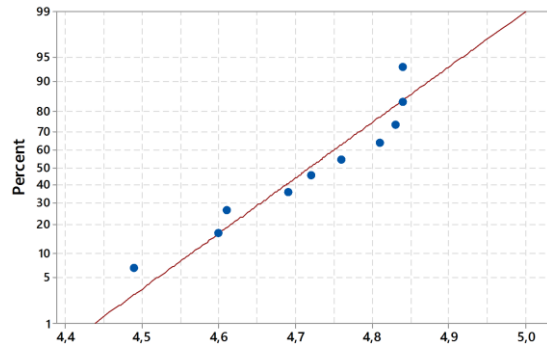
Regarding to *Production Settings* trial, which was previous concluded to be the best fit conditions, the results presented in capability graphics belong to the range between the target and the lower specification limit. The  $C_p$ ,  $C_{pk}$  and p-value show that trial is correctly adapted, as well the scale of how capable is the process, presenting all high values of potential.

Table 20. Summary table of statistical analysis for Nylon C.

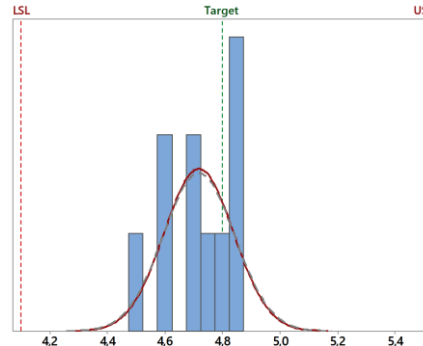
### Nylon C

#### Sample Shrinkage

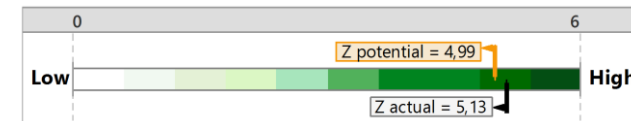
Normality Plot



Actual Capability Histogram

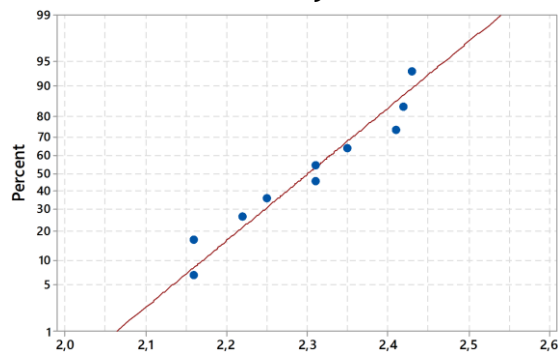


Total N 10  
 $C_p$  1.88  
 $C_{pk}$  1.66  
 P-value 0.297

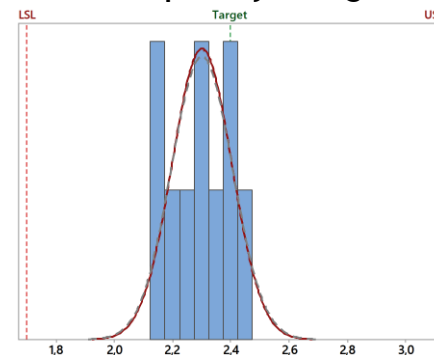


#### Residual

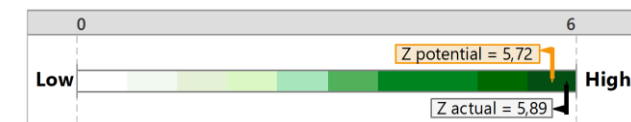
Normality Plot



Actual Capability Histogram

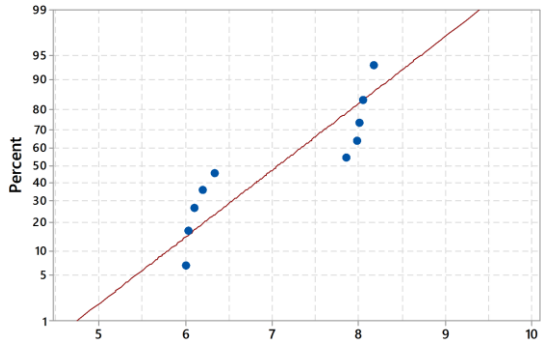


Total N 10  
 $C_p$  2.22  
 $C_{pk}$  1.91  
 P-value 0.492

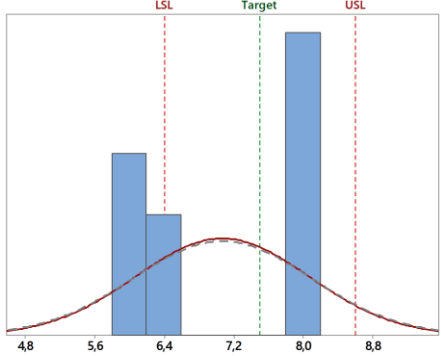


**Shrink-force**

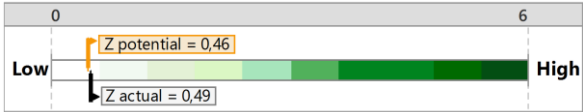
**Normality Plot**



**Actual Capability Histogram**



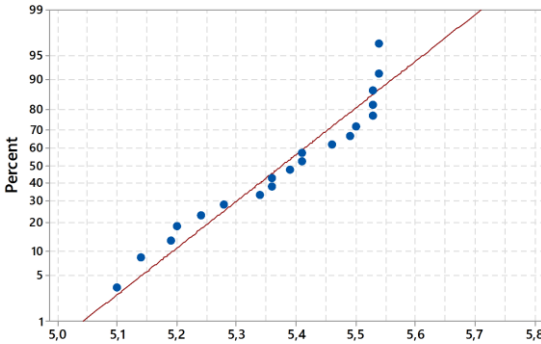
Total N 10  
 $C_p$  0.36  
 $C_{pk}$  0.22  
 P-value < 0.005



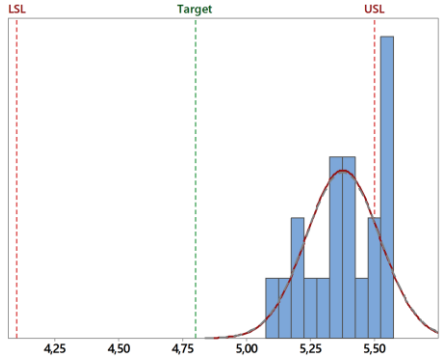
**PI Settings**

**Shrinkage**

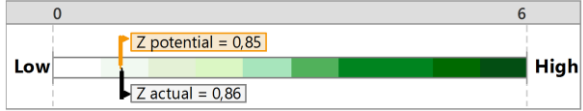
**Normality Plot**



**Actual Capability Histogram**

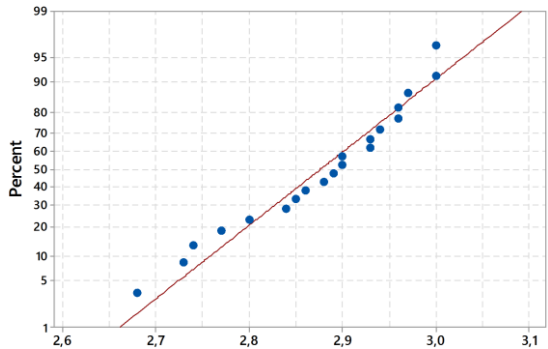


Total N 20  
 $C_p$  1.61  
 $C_{pk}$  0.28  
 P-value 0.116

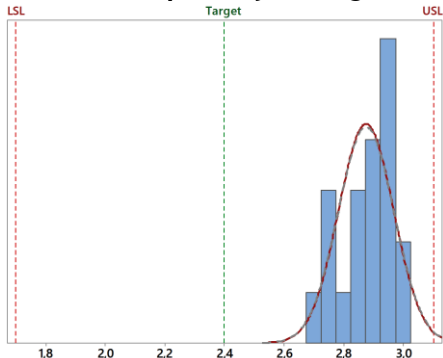


**Residual**

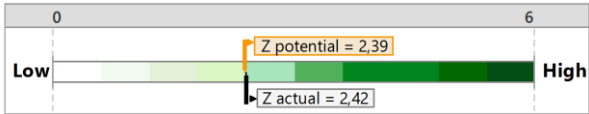
**Normality Plot**



**Actual Capability Histogram**

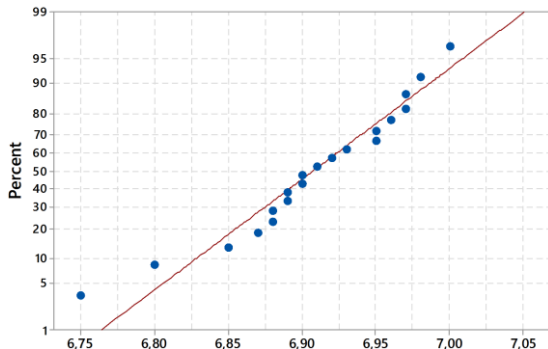


Total N 20  
 C<sub>p</sub> 2.49  
 C<sub>pk</sub> 0.80  
 P-value 0.326

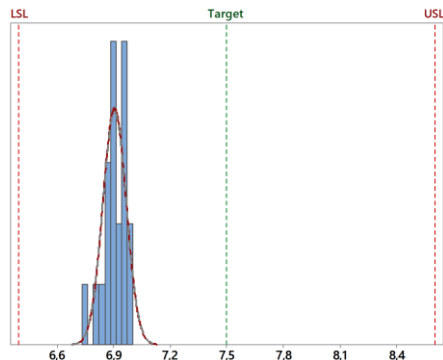


**Shrink-force**

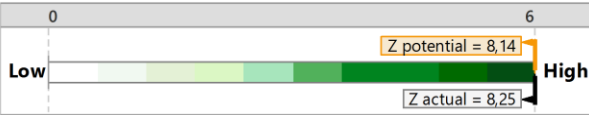
**Normality Plot**



**Actual Capability Histogram**



Total N 20  
 C<sub>p</sub> 5.88  
 C<sub>pk</sub> 2.71  
 P-value 0.378

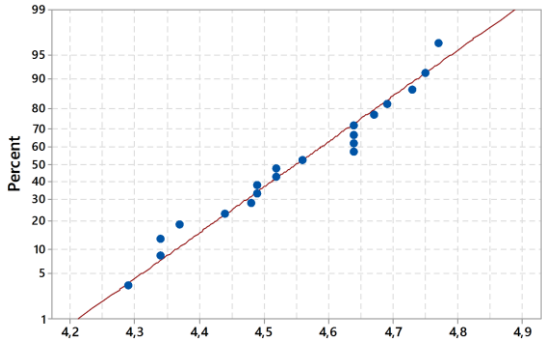




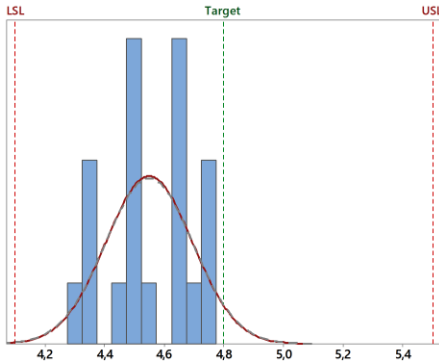
**Study A**

**Shrinkage**

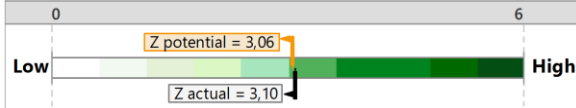
**Normality Plot**



**Actual Capability Histogram**

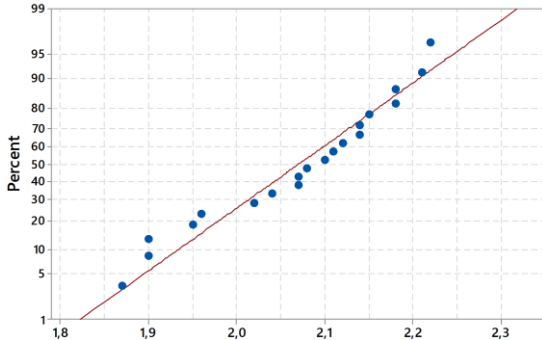


Total N 20  
 C<sub>p</sub> 1.58  
 C<sub>pk</sub> 1.02  
 P-value 0.386

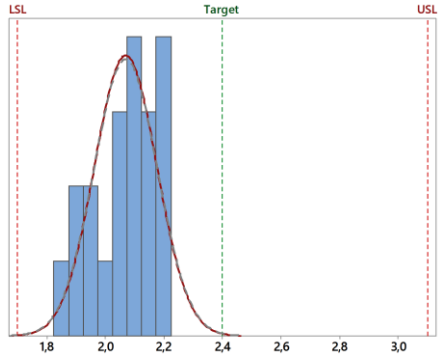


**Residual**

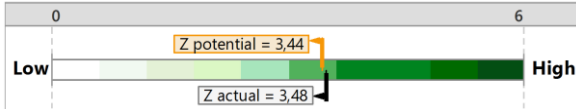
**Normality Plot**



**Actual Capability Histogram**

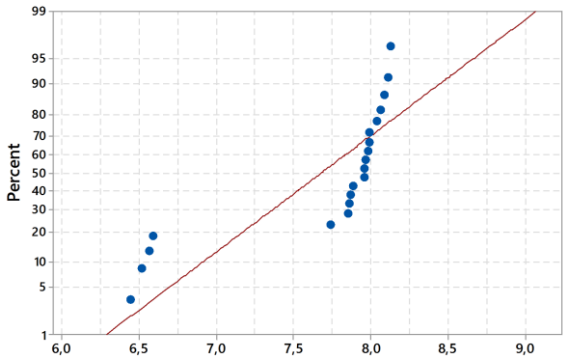


Total N 20  
 C<sub>p</sub> 2.16  
 C<sub>pk</sub> 1.15  
 P-value 0.232

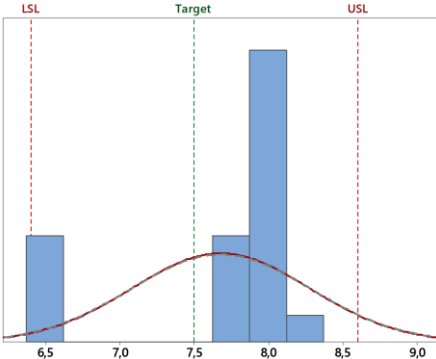


**Shrink-force**

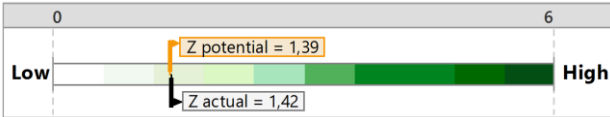
**Normality Plot**



**Actual Capability Histogram**



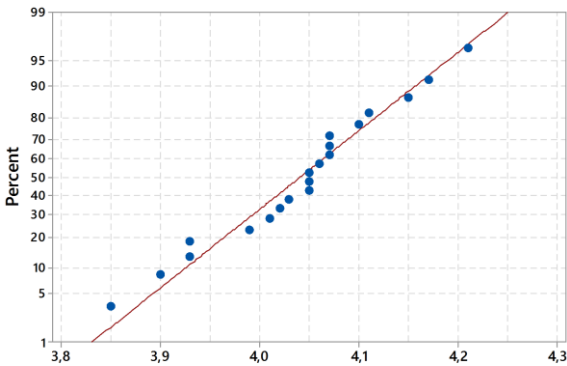
Total N 20  
 C<sub>p</sub> 0.61  
 C<sub>pk</sub> 0.51  
 P-value < 0.005



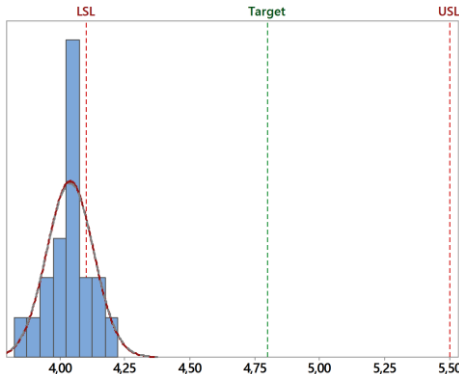
**Production Settings**

**Shrinkage**

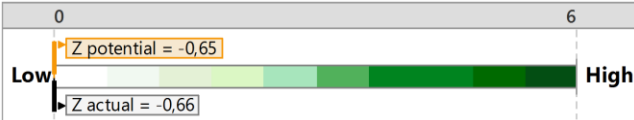
**Normality Plot**



**Actual Capability Histogram**

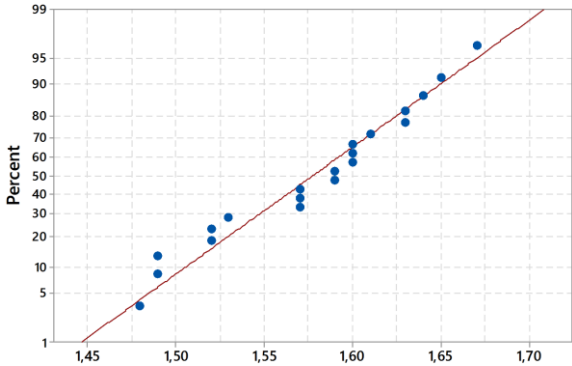


Total N 20  
 C<sub>p</sub> 2.56  
 C<sub>pk</sub> -0.22  
 P-value 0.442

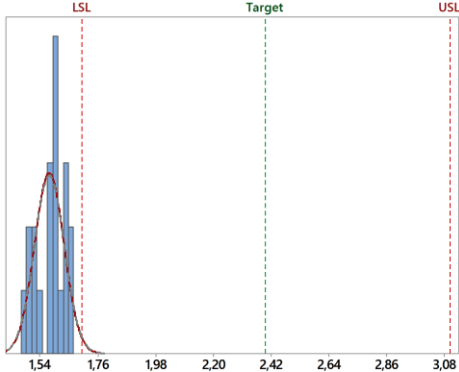


**Residual**

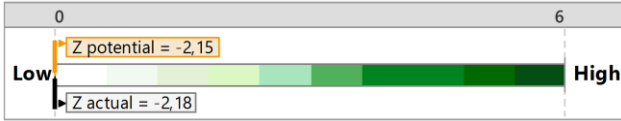
**Normality Plot**



**Actual Capability Histogram**

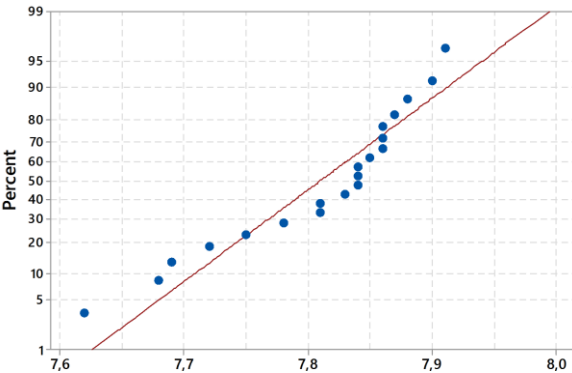


Total N 20  
 C<sub>p</sub> 4.10  
 C<sub>pk</sub> -0.72  
 P-value 0.306

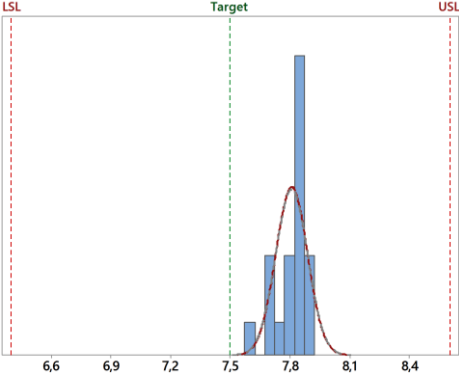


**Shrink-force**

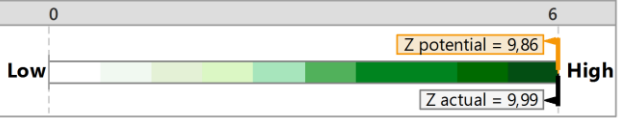
**Normality Plot**



**Actual Capability Histogram**



Total N 20  
 C<sub>p</sub> 4.58  
 C<sub>pk</sub> 3.29  
 P-value 0.017



Starting to analyze the results for *Sample* trial, which is the reference, it is possible to observe that the 3 presented capability graphics are in the target. Regarding to Process Potential Index ( $C_p$ ), Process Capability Index ( $C_{pk}$ ) and p-value, they presented values that shows that experimental trial is correctly adapted, as well the scale of how capable is the process, where shrinkage and shrink-force present high values.

On the other hand, the capability graphics for *PI Settings* trial show that results except shrink-force belong to the range between the target and the upper specification limit, which is not the intended. As previously said, it is preferable to be under the target than above. Considering the  $C_p$ ,  $C_{pk}$  and p-value, they also presented consistent values.

In *Study A* trial, which was previous concluded to be the best fit conditions, the results obtained in capability graphics belong to the range between the target and the lower specification limit. The  $C_p$ ,  $C_{pk}$  and p-value show that trial is correctly adapted, as well the scale of how capable is the process, presenting all middle values of potential.

Regarding to *Production Settings* trial, the results presented in capability graphics belong to the range between the target and the lower specification limit. However, when how capable is the process graphics are analyzed it presents really low values, not being reliable. The  $C_p$  has good values contrary to  $C_{pk}$  that presents negative ones.

## Annex 6 Simulation

### A.6.1 Materials

One of the indispensable conditions needed to set up in simulation are the materials, being them the air and the fabric material. The simulation is based on the dipping process of a Nylon fabric, more specifically Polyamide 6.6.

Starting with the air, it was necessary to define its properties. It was assumed that all of them was constant during the time of simulation except the density, since the temperature of the air along different zones of the oven's chamber is changing. According to this, a study to the different presented models was made to reach a conclusion about what fitting the best. The chosen values for the definition of this material is resumed in Table 21.

Table 21. Properties of air [26].

Property	Units	Model	Value
Density	kg/m <sup>3</sup>	Boussinesq	0.7005
Cp (Specific heat)	J/kg·K	Constant value	1006.4
Thermal Conductivity	w/m·K	Constant value	0.0242
Viscosity	kg/m·s	Constant value	1.7894×10 <sup>-5</sup>
Thermal Expansion Coefficient*	1/K	Constant value	1.97×10 <sup>-3</sup>

\*This parameter is directly dependent on the choice of the Boussinesq model.

Regarding to the fabric material, in the database of the ANSYS® Fluent did not exist Polyamide 6.6 properties. Thus, it was necessary to do some research to fill the values presented in Table 22.

Table 22. Properties of Polyamide 6.6 [27, 28].

Property	Units	Model	Value
Density	kg/m <sup>3</sup>	Constant value	1140
Cp (Specific heat)	J/kg·K	Constant value	1670
Thermal Conductivity	w/m·K	Constant value	0.25

#### A.6.1.1 What is the Boussinesq approximation?

The Boussinesq approximation, created by Valentin Joseph Boussinesq, is a popular method for solving non-isothermal flow, such as natural convection problems, without having to solve all the compressible formulations of the Navier-Stokes equations. This method is applied when density variations are slight and assuming this do not have effect on the flow field, except they give rise to buoyancy forces [29]. This model considers density as a constant value in all solved equations, excepting for the buoyancy term in the momentum equation like described in Equation (16) [30].

$$(\rho - \rho_0)g \approx \rho_0\beta(T - T_0)g \quad (16)$$

Where  $\rho_0$  is the density of the flow assumed constant,  $T_0$  is the operating temperature and  $\beta$  is the thermal expansion coefficient.

The Boussinesq approximation is valid when  $\beta(T - T_0) \ll 1$ .

It is important to keep in mind that this approximation cannot be used with species calculations, combustion and reactions.

## A.6.2 Mathematical Modelling

In order to know the regime of the simulation in ANSYS® Fluent, it was necessary to calculate the Reynolds Number,  $Re$ , according with the Equation (17).

$$Re = \frac{\rho v_s D}{\mu} \quad (17)$$

Where  $\rho$  is the air density,  $v_s$  the air velocity,  $D$  the diameter of the tuber and  $\mu$  the dynamic viscosity of the air, all at the operating temperature. At this particular case, once the channel where the air come from is a rectangular surface, the diameter calculation is based on Equation (18) [22].

$$D = \frac{2ab}{a + b} \quad (18)$$

Where  $a$  is the height of the open surface and  $b$  the length. After the calculation, the obtain value of  $Re$  will determine the regime flow according to:

- $Re < 1000$ : laminar
- $Re > 3000$ : turbulent
- $1000 < Re < 3000$ : transition

The operating temperature is 235 °C, which drives into a  $Re$  of 2486 for the maximum capacity of ventilation. Although the value is in the transition regime, it was assumed a turbulent one.

Previous studies have successfully used Reynolds Averaged Navier-Stokes (RANS) model to predict the air flow in baking ovens [20]. Thus, this model was applied to the studied textile oven, solved using the SIMPLE algorithm and Second Order Upwind equations used for all flow variables and solutions [23]. The Equations (19) and (20) are the continuity and momentum equations, respectively.

$$\frac{\partial \rho}{\partial t} = \frac{\partial}{\partial x_i} (\rho u_i) \quad (19)$$

$$\frac{\partial}{\partial t}(\rho u_i) + \frac{\partial}{\partial x_i}(\rho u_i u_j) = -\frac{\partial p}{\partial x_i} + \frac{\partial}{\partial x_j} \left[ \mu \left( \frac{\partial u_i}{\partial x_j} + \frac{\partial u_j}{\partial x_i} - \frac{2}{3} \delta_{ij} \frac{\partial u_l}{\partial x_l} \right) \right] + \rho g + \frac{\partial}{\partial x_i}(-\rho \overline{u'_i u'_j}) \quad (20)$$

Where  $\rho$  and  $u_i$  are the air density and velocity components in the coordinate direction  $x_i$  respectively,  $p$  is pressure and  $g$  is the acceleration due to gravity.

The last term of the Equation (19),  $\frac{\partial}{\partial x_i}(-\rho \overline{u'_i u'_j})$ , represents the turbulent stress that requires additional closure equations to be solved [21]. Turbulence is modelled using the realizable k- $\epsilon$  transport model, which is an industrial standard. The turbulence is described by two additional variables, being them  $k$  (turbulent kinetic energy) and  $\epsilon$  (turbulent dissipation) enabling the computation of the turbulent stress and the turbulent viscosity [21, 24]. The realizable k- $\epsilon$  transport model is an improvement of the standard k- $\epsilon$  model that can be useful for flows in complex geometries and consists in two equations of transport, Equations (21) and (22) [20, 21]. Equation (23) helps to define one of the variables presented in Equation (22).

$$\frac{\partial}{\partial t}(\rho k) + \frac{\partial}{\partial x_j}(\rho k u_j) = \frac{\partial}{\partial x_j} \left[ \left( \mu + \frac{\mu_t}{\sigma_k} \right) \frac{\partial k}{\partial x_j} \right] + G_k + G_b - \rho \epsilon - Y_M + S_k \quad (21)$$

$$\frac{\partial}{\partial t}(\rho \epsilon) + \frac{\partial}{\partial x_j}(\rho \epsilon u_j) = \frac{\partial}{\partial x_j} \left[ \left( \mu + \frac{\mu_t}{\sigma_\epsilon} \right) \frac{\partial \epsilon}{\partial x_j} \right] + \rho C_1 S \epsilon - \rho C_2 \frac{\epsilon^2}{k + \sqrt{\nu \epsilon}} + C_{1\epsilon} \frac{\epsilon}{k} C_{3\epsilon} G_b + S_\epsilon \quad (22)$$

Where,

$$C_1 = \max \left[ 0.43, \frac{\eta}{\eta + 5} \right], \eta = S \frac{k}{\epsilon}, S = \sqrt{2 S_{ij} S_{ij}} \quad (23)$$

In these equations,  $G_k$  and  $G_b$  represent the generation of turbulence kinetic energy due to the mean velocity gradients and due to buoyancy effect.  $Y_M$  represents the contribution of the fluctuating dilatation in compressible turbulence to the overall dissipation rate. The terms  $C_2$  and  $C_{1\epsilon}$  are constants,  $\sigma_k$  and  $\sigma_\epsilon$  are the turbulent Prandtl numbers for  $k$  and  $\epsilon$ , respectively which leads to the turbulent viscosity  $\mu_t$  and  $S_k$  and  $S_\epsilon$  are user-defined source terms [25]. The term  $\nu$  is the component of the flow velocity parallel to the gravitational vector and  $u$  is the component of the flow velocity perpendicular to the gravitational vector [20]. The negative terms represent the energy dissipation. More details about the realizable k- $\epsilon$  can be found in ANSYS Fluent Theory Guide (2013) [25].

Regarding to the energy analysis, the Equation (24) describes the energy equation.

$$\frac{\partial}{\partial t}(\rho C_p T) + \frac{\partial}{\partial x_i}(u_i \rho C_p T) = \frac{\partial}{\partial x_j} \left( \lambda \frac{\partial T}{\partial x_j} \right) \quad (24)$$

Where  $C_p$ ,  $T$  and  $\lambda$  are the specific heat capacity, temperature and thermal conductivity of the air, respectively.